NQO1-BIOACTIVATABLE DRUGS AT THE INTERFACE OF CANCER METABOLISM AND THE DNA DAMAGE RESPONSE

APPROVED BY SUPERVISORY COMMITTEE

First Name Last Name, credentials

David A. Boothman, Ph.D. (Mentor)

Sandeep Burma, Ph.D. (Chair)

Rolf Brekken, Ph.D.

Ralph DeBerardinis M.D.,Ph.D.

DEDICATION

For Rima, Ahaana, Banani, Gopendu, Nayan and Priti.

NQO1-BIOACTIVATABLE DRUGS AT THE INTERFACE OF CANCER METABOLISM AND THE DNA DAMAGE RESPONSE

by

GAURAB CHAKRABARTI

DISSERTATION

Presented to the Faculty of the Graduate School of Biomedical Sciences

The University of Texas Southwestern Medical Center at Dallas

In Partial Fulfillment of the Requirements

For the Degree of

DOCTOR OF PHILOSOPHY
The University of Texas Southwestern Medical Center at Dallas

Dallas, Texas

Degree Conferral May, 2017

ACKNOWLEDGEMENTS

The work described in this dissertation would not have been possible without the help of multiple people. I would first like to express my gratitude and appreciation to my mentor, Dr. David A. Boothman for his guidance and support and for providing me a scientific home to explore my creativity and curiosities for the past three years. Thank you for helping me sharpen my scientific skillset, for sharing your passion for science and for teaching me about the power of perseverance. This work would not have been possible were it not for the support from members of the Boothman laboratory. In particular, I would like to acknowledge Zachary Moore, Drs. Mariya Ilcheva, Molly Silvers, Farjana Fattah, Praveen Patadar, Julio Morales, Edward Motea and Xiumei Huang for their scientific insights, advice and friendship.

I would also like to thank my committee members Drs. Sandeep Burma, Rolf Brekken and Ralph DeBerardinis for their guidance and advice throughout my graduate training. I have been extremely fortunate to closely collaborate with members of Dr. Ralph DeBerardinis's laboratory and have learned a great deal from this team. I thank you for your critical insights and suggestions on my work.

Finally, I would like to express my appreciation for my friends and family members for their constant support and love. I would especially like to thank my amazing parents Gopendu and Banani, my in-laws Nayan and Priti, my niece and little-buddy Ahaana, and my best friend, teacher, intellectual Ping-Pong partner and wife, Rima.

NQO1-BIOACTIVATABLE DRUGS AT THE INTERFACE OF CANCER METABOLISM AND THE DNA DAMAGE RESPONSE

Publication No. _____

Gaurab Chakrabarti, Ph.D.

The University of Texas Southwestern Medical Center at Dallas, 2017

Supervising Professor: David Allen Boothman, PhD

Abstract

Increased levels of reactive oxygen species (ROS) have been observed in multiple cancer types, where they are crucial for tumor biology. Concomitantly, tumor cells also have enhanced expression of antioxidant pathway proteins to detoxify excess ROS. Thus, a challenge for anti-cancer therapeutics is to fine-tune this delicate balance from ROS protection, to ROS production while sparing normal tissue from toxicity. The phase II detoxification enzyme, NAD(P)H:quinone oxidoreductase-1, NQO1, is dramatically overexpressed in many solid tumor types, including pancreatic ductal adenocarcinoma (PDA)

and non-small cell lung cancer (NSCLC). The Boothman laboratory has demonstrated that NQO1 bioactivates a unique class of quinones, such as ß-lapachone (ß-lap) and deoxyniboqunine (DNQ), through a futile redox cycle to generate massive levels of superoxide radical to induce extensive DNA oxidative base damage, single strand breaks and poly(ADP-ribose) polymerase 1 (PARP1)-driven depletion of intracellular NAD^+. However, tumor cell NADPH and glutathione (GSH) biogenesis can attenuate the efficacy of this class of drugs by blunting the ROS formation produced from the futile redox cycle. Therefore, it is increasingly important to identify and target tumor specific antioxidant defenses to sensitize cancer cells, but not normal tissue, to NQO1 bioactivatable drugs. The data presented in the first half of this dissertation demonstrate that targeting glutamine dependent transamination reactions depletes antioxidant defenses in PDA and sensitizes tumors, but not normal tissue, to ß-lap-induced programmed necrosis *in vitro* and *in vivo*. Downstream of ROS formation, another mechanism by which tumors can attenuate ß-lap efficacy is through the repair of DNA lesions, specifically through base excision repair (BER). The latter half of this thesis focuses on inhibiting BER in combination with ß-lap as a mechanism to drive PARP1 hyperactivation and synergistic killing of NQO1-expressing PDA, but not associated normal tissue.

TABLE OF CONTENTS

TITLE FLY i

DEDICATION ii

TITLE PAGE iii

COPYRIGHT iv

ACKNOWLEDGEMENTS v

ABSTRACT vii

TABLE OF CONTENTS x

PRIOR PUBLICATIONS xvi

LIST OF FIGURES xviii

LIST OF TABLES xxii

LIST OF ABBREVIATIONS xxv

CHAPTER ONE: EXPANDING THE THERAPEUTIC WINDOW BY TARGETING CANCER-SPECIFIC NADPH BIOGENESIS PATHWAYS ……1

1.1 INTRODUCTION 2

1.2 NADPH BIOGENESIS PATHWAYS IN NORMAL *VS* CANCER CELLS 3

1.3 PREDICTING TUMOR-SPECIFIC NADPH-BIOGENESIS PROFILES FROM PUBLICALLY AVAILABLE DATASETS ……12

1.4 MODULATING NADPH-BIOGENESIS AS A MECHANISM TO POTENTIATE NQO1-BIOACTIVATBLE DRUGS…….....15

1.5 CONCLUSION ……...16

CHAPTER TWO: MATERIALS AND METHODS ……26

CHAPTER THREE: TARGETING GLUTAMINE TRANSAMINATION SENSITIZES PANCREATIC CANCER TO PARP1-DEPENDENT METABOLIC CATASTROPHE INDUCED BY ß-LAPACHONE 31

3.1 INTRODUCTION 32

3.2 RESULTS 35

3.3 DISCUSSION 42

CHAPTER FOUR: INHIBITING BASE EXCISION REPAIR SIGNALING SENSITIZES PANCREATIC CANCER TO PARP1-DEPENDENT METABOLIC CATASTROPHE INDUCED BY ß-LAPACHONE 59

4.1 INTRODUCTION 60

4.2 RESULTS 64

4.3 DISCUSSION 76

CHAPTER FIVE: CONCLUSIONS AND FUTURE DIRECTIONS 99

BIBLIOGRAPHY 101

PUBLICATIONS

1. **Chakrabarti G.**, Gerber, D.E., Boothman, D.A. (2015) "Expanding antitumor therapeutic windows by targeting cancer-specific NADPH biogenesis pathways." Clinical Pharmacology *in press*
2. **Chakrabarti G.,** Silvers M., Ilcheva M., Liu Y., Moore Z., Lou X., Gao J., Anderson G., Liu L., Burma S., DeBerardinis R.J., Gerson S., Boothman D.A. (2015) "Inhibiting base excision repair signaling sensitizes pancreatic cancer to PARP1-driven metabolic catastrophe induced by the NQO1 bioactivatable drug, ß-lapachone." Journal of Clinical Investigation *in review*
3. **Chakrabarti G.,** Moore Z., Luo X., Ilcheva M., Ali A., Padanad M., Zhou Y.Y., Xie Y., Burma S., Scaglioni P.P., Cantley L.C., Lyssiotis C.A., Kimmelman A.C., DeBerardinis R.J., Boothman D.A. (2015) "Targeting glutamine metabolism sensitizes pancreatic cancer to PARP1 driven metabolic catastrophe induced by ß-lapachone" Cancer Discovery *in review*
4. **Chakrabarti G.,** Padanand M., Zhou Y.Y., Xie Y., Scaglioni P.P., Boothman D.A. (2015) "Glutamine metabolism is regulated by mutant *KRAS* and is a predictive marker for response to radiation therapy in NSCLC." British Journal of Cancer *in preparation*
5. Moore Z., **Chakrabarti G.**, Luo, X., Ali, A., Hu, Z., Fattah, F. J., Vemireddy, R., DeBerardinis, R. J., Brekken, R. A., Boothman, D. A. (2015). "NAMPT inhibition sensitizes pancreatic adenocarcinoma cells to tumor-selective, PAR-independent

metabolic catastrophe and cell death induced by beta-lapachone." Cell Death Dis **6**: e1599.

6. Cao, L., Li, L. S., Spruell, C., Xiao, L., **Chakrabarti G.**, Bey, E. A., Reinicke, K. E., Srougi, M. C., Moore, Z., Dong, Y., Vo, P., Kabbani, W., Yang, C. R., Wang, X., Fattah, F., Morales, J. C., Motea, E. A., Bornmann, W. G., Yordy, J. S., Boothman, D. A. (2014). "Tumor-selective, futile redox cycle-induced bystander effects elicited by NQO1 bioactivatable radiosensitizing drugs in triple-negative breast cancers." Antioxid Redox Signal **21**(2): 237-250.
7. Buteau, A., Buteau, A., Seideman, C. A., Svatek, R. S., Youssef, R. F., **Chakrabarti, G**., Reed, G., Bhat, D., Lotan, Y. (2014). "What is evaluation of hematuria by primary care physicians? Use of electronic medical records to assess practice patterns with intermediate follow-up." Urol Oncol **32**(2): 128-134.

LIST OF FIGURES

Figure 1.1: NAD+ salvage pathway and oxidative pentose phosphate pathway 18

Figure 1.2: One-carbon serine catabolism pathway..... 19

Figure 1.3: Kras-reprogrammed glutamine metabolism 20

Figure 1.4: Agents targeting NADPH-biogenesis 21

Figure 1.5: Screen setup 22

Figure 1.6: Cancer specific NADPH-biogenesis screen 23

Figure 1.7: Cancer specific NADPH-biogenesis screen continued 24

Figure 1.8: Screen results for MTHFD2 in NSCLC patients 25

Figure 3.1: Inhibition of glutamine transamination sensitizes PDA to ß-lap 47

Figure 3.2: GLS1 inhibition by BPTES sensitizes PDA to ß-lap in an NQO1 dependent manner..... 49

Figure 3.3: GLS1 inhibition decreases antioxidant defenses and increases susceptibility to ß-lap-induced DNA damage..... 51

Figure 3.4: GLS1 inhibition sensitizes pancreatic cancer to ß-lap *in vivo*..... 53

Figure SF3.1: ß-Lap MOA and *GOT2:GLUD1* Kaplan-Meier Curve 55

Figure SF3.2: BPTES sensitivity and *KRAS*-reprogrammed glutamine pathway 56

Figure SF3.3: Combination treatment leads to increased ROS by depleting reduced glutathione..... 57

Figure SF3.4: CB-839 and ß-lap *in vivo* validation in MiaPaca2..... 58

Figure 4.1: NQO1:Catalase ratios are elevated in PDA tumor vs normal pancreatic tissue 82

Figure 4.2: OGG1 modulates cellular responses to ß-lap-induced DNA damage, PARP1 hyperactivation and lethality 83
Figure 4.3: XRCC1 depletion enhances efficacy of ß-lap by increasing DNA damage and repressing metabolic recovery 85
Figure 4.4: The AP site modification factor, Methoxyamine (MeOX), sensitizes cancer cells to ß-lap in an NQO1-dependent manner 87
Figure 4.5: MeOX sensitizes cells to ß-lap by potentiating DNA damage and PARP1 hyperactivation 89
Figure 4.6: MeOX enhances the lethality of ß-lap against subcutaneous human pancreatic xenografts to ß-lap *in vivo* 91
Figure SF4.1: OGG1 depletion makes MiaPaca2 cells partially resistant to ß-lap-induced cytotoxicity 93
Figure SF4.2: XRCC1 supplementary figure 94
Figure SF4.3: ROS levels in MiaPca2 with ß-lap ± 12 mM MeOX 95
Figure SF4.4: MeOX supplementary figure 96
Figure SF4.5: Animal Studies supplementary figure 97
Figure SF4.6: Model of BER and ß-lap induced oxidative damage 98

LIST OF ABBREVIATIONS

ADP – adenosine diphosphate

APE1 – AP Endonuclease 1

ATP – adenosine triphosphate

BER – base excision repair

DER – dose enhancement ratio

DSB – double-strand break

Gln – glutamine

GLS1 – mitochondrial glutaminase

GOT1 – cytoplasmic glutamic-oxaloacetic transaminase

GOT2 – mitochondrial glutamic-oxaloacetic transaminase

GSH – reduced glutathione

IDH – isocitrate dehydrogenase

IP – intraperitoneal

IV – intravenous

KRAS - Kirsten rat sarcoma viral oncogene homolog

MDH1 – cytoplasmic malate dehydrogenase

ME1 – cytoplasmic malic enzyme

MeOX – methoxyamine

MTHFD2 -- mitochondrial methylene tetrahydrofolate dehydrogenase

NAD – nicotine adenine dinucleotide

NADP -- nicotine adenine dinucleotide phosphate

NAMPT – nicotinamide phosphorylribosyltransferase

NQO1 – NAD(P)H :quinone oxidoreductase

NSCLC – non-small cell lung cancer

OGG1 – oxoguanine glycosylase

OS – overall survival

PARP1 – poly(ADP ribose) polymerase

PBS – phosphate buffered saline

PD – pharmacodynamics

PK – pharmacokinetics

ROS – reactive oxygen species

ß-Lap – ß-lapachone

SSB – singe-strand breaks

T/C – treated/control

XRCC1 -- X-ray repair cross-complementing protein 1

CHAPTER ONE

Introduction

EXPANDING ANTITUMOR THERAPEUTIC WINDOWS BY TARGETING CANCER-SPECIFIC NADPH BIOGENESIS PATHWAYS

Abstract

NAD(P)H biogenesis is an essential mechanism by which both normal and cancer cells maintain redox balance. While antitumor approaches to treat cancers through elevated reactive oxygen species (ROS) are not new ideas, depleting specific NAD(P)H biogenesis pathways that control recovery and repair pathways are novel viable approaches for cancer therapy. However, to elicit efficacious therapies exploiting NAD(P)H biogenic pathways, it is crucial to understand and specifically define the roles of NAD(P)H biogenesis pathways used by cancer cells for survival or recovery from cell stress. It is equally important to select NAD(P)H biogenic pathways that are expendable or not utilized in normal tissue to avoid unwanted toxicity. Here, we address recent literature that demonstrates specific tumor-selective NADPH-biogenesis pathways that can be exploited using agents that target specific cancer cell pathways normally not utilized in normal cells. Defining NAD(P)H-biogenesis profiles of specific cancer types should enable novel strategies to exploit these therapeutic windows for increased efficacy against recalcitrant neoplastic disease, such as pancreatic cancers. Accomplishing the goal of using ROS as a weapon against cancer cells will also require agents, such as NQO1 bioactive drugs, that selectively induce ROS in cancer cells,

but not normal tissue. This chapter will focus on tumor-specific NADPH-biogenesis pathways, methods to predict such pathways in different cancer types and a discussion of ROS-inducing anti-cancer agents, with an emphasis on NQO1-bioactivatable drugs.

1.1 Introduction

Reduced nicotinamide adenine dinucleotide phosphate (NADPH) is a necessary cofactor for anabolic reactions, such as lipid and nucleic acid synthesis. Additionally, NADPH provides reducing power to oxidation-reduction reactions necessary for protecting cancer cells against the build-up of reactive oxygen species (ROS) produced during rapid cellular proliferation (Schumacker 2006).

While increased ROS in cancer cells may be an important initiating event in carcinogenesis, excessive levels of ROS can be toxic and lead to cell death by causing irreversible damage to DNA, lipids and proteins (Behrend, Henderson, and Zwacka 2003, Wu 2006, Schumacker 2006). Many chemotherapeutic agents act by inducing excessive ROS damage in cancer cells, but lack the ability to differentiate between normal and tumor tissue, leading to a narrow therapeutic window (Trachootham, Alexandre, and Huang 2009, Gorrini, Harris, and Mak 2013). In addition, some cancers in advanced stages may have become resistant to intrinsic oxidative stress and can upregulate canonical antioxidant defenses to protect against ROS inducing agents. Reduced glutathione (GSH) and thioredoxin (TRX) are essential ROS scavenging molecules in cancer and in normal cells (Fruehauf and Meyskens 2007). GSH and TRX are necessary for peroxidases, thioreductases and peroxiredoxins to detoxify ROS. GSH and TRX rely on continuous reduction from NADPH to sustain their

function as ROS scavengers (Fruehauf and Meyskens 2007). Therefore, strategies to inhibit NADPH biogenesis may dramatically alter the ROS scavenging abilities of cancer cells and sensitize them to oxidative damage. However, to achieve therapeutic selectivity, NADPH must be modulated through tumor-specific NADPH-biogenesis pathways that are necessary for cancer cells, but expendable in normal cells. To this end, this review attempts to characterize cancer-selective alterations in NADPH-biogenesis, define potential therapies that exploit these pathways to sensitize cancer to ROS damage and provide a method to predict cancer-specific NADPH-biogenesis profiles. We will not focus on pharmacological modulation of *de novo* glutathione and/or thioredoxin pathways, as these topics have been comprehensively reviewed elsewhere (Balendiran, Dabur, and Fraser 2004, Traverso et al. 2013, Mahmood et al. 2013).

1.2 NADPH Biogenesis Pathways in Normal *vs* Cancer Cells

1.2.1 Oxidative Pentose Phosphate Pathway

A key mechanism of NADPH generation in normal cells is through the oxidative arm of the pentose phosphate pathway (PPP). The PPP consists of two phases: the oxidative phase and the non-oxidative phase. The non-oxidative phase produces ribose from glucose, while the oxidative phase generates two NADPH molecules for every glucose entering the pathway (**F**ig. 1.1) (Kruger and von Schaewen 2003). NADPH produced from the oxidative PPP is essential for protection against radical damage arising from mitochondrial respiration, ionizing radiation, and various xenobiotic agents (Nathan and Ding 2010). In this pathway, glucose 6-phosphate dehydrogenase (G6PD) and 6-phosphogluconate dehydrogenase

(6PGD) reduce $NADP^+$ to NADPH while oxidizing glucose-6-phosphate (G6P) and carboxylating 6-phosphogluconate (6PG), respectively (Fig. 1.1) (Tian et al. 1998, Patra and Hay 2014).

Pyruvate kinase (PK) is an essential glycolytic enzyme for conversion of phosphoenol pyruvate (PEP) to pyruvate (Fig. 1.1). The M2 isoform of PK (PKM2) is found in many cancer cells and self-renewing cells, but is expressed in an inactive state in normal adult tissues (Zwerschke et al. 1999). In many human cancers, PKM2 can be inactivated by ROS, which diverts glycolytic flux back into the oxidative PPP to generate NADPH and detoxify ROS (Fig. 1.1) (Anastasiou et al. 2011). After ROS stress, PKM2 is essential in cancer, but not normal, cells to maintain cell viability via redox scavenging, providing a potential therapeutic window for ROS-inducing agents (Anastasiou et al. 2011). PKM2 overexpression ensures that rapidly proliferating cancer cells create enough NADPH to match oxidative metabolism-generating ATP production, protecting the cell from attack by oxidative damage (Schneider et al. 2002), (Cerwenka et al. 1999) and (Nathan and Ding 2010).

The tumor suppressor, p53, can also regulate flux into the oxidative PPP. During genotoxic stress, p53 induces TIGAR (TP53-induced glycolysis and apoptosis regulator), which encodes a protein that degrades fructose-2,6-bisphosphate (Fig. 1.1) (Bensaad et al. 2006). Low fructose-2,6-bisphosphate levels inhibit the activity of phosphofructokinase 1 (PFK1), a rate-limiting enzyme in glycolysis that leads to shuttling of earlier glycolytic metabolites into the oxidative PPP to generate NADPH. Overexpression of TIGAR was observed in colon, breast and glioblastoma cancers (Cheung et al. 2013, Sinha et al. 2013,

Won et al. 2012). Consistent with the enzyme's role in redox balance, TIGAR knockdown dramatically sensitized glioma cells to ionizing radiation (Pena-Rico et al. 2011).

In cancers that overexpress PKM2, activating PKM2 with ML202, ML203, or other PKM2 activators will block inhibition of PKM2 from ROS-inducing agents and decrease flux of glucose through the oxidative PPP, thereby attenuating production of NADPH during oxidative damage, thereby sensitizing cancer cells. In contrast, normal cells that have inactive PKM2 are not sensitized to ROS-inducing agents (Walsh et al. 2010, Anastasiou et al. 2012, Anastasiou et al. 2011). Alternatively, the FDA-approved G6PD inhibitor, 6-anicotinamide (6-AN), may be utilized in cancers with PKM2 or TIGAR overexpression, thus directly inhibiting NADPH production via the oxidative PPP pathway, sensitizing these cancers to ROS-inducing agents (Fig. 1.1) (Belfi et al. 1999). The utility of this latter strategy needs to be empirically determined as G6PD is also a major NADPH source in normal cells as well.

1.2.2 Serine Catabolism

Serine-driven, one-carbon metabolism has recently been shown to be a major source of NADPH in dividing cells (Fan et al. 2014). Serine is metabolized in the cytoplasm or mitochondria to methylene-tetrahydrofolate (methylene-THF) by serine hydroxymethyltransferase (SHMT) 1 or 2 (cytoplasmic and mitochondrial, respectively), which then forms 10-formyl-THF via methylenetetrahydrofolate dehydrogenase (MTHFD) 1 or 2 (cytoplasmic and mitochondrial, respectively). Flux through MTHFD generates NADPH in the cytoplasm or mitochondria. 10-formyl-THF is essential for purine biogenesis and

MTHFD's most important function was thought to solely facilitate purine biosynthesis. However, the NADPH generated from this reaction is an integral source of cellular reducing power in dividing cells (Fig. 1.2) (Fan et al. 2014).

Recently, it was reported that this serine catabolism pathway can regulate mitochondrial redox control during hypoxia in Myc-driven cancers (Ye et al. 2014). Specifically, it was shown that SHMT2 was essential in maintaining mitochondrial NADPH and reduced glutathione levels during hypoxia. SHMT2 expression was transcriptionally regulated by coordinate activity of Myc and HIF-1α. Indeed, knockdown of SHMT2 in neuroblastoma cell lines significantly decreased growth *in vitro* under hypoxic conditions, and in a xenograft model of neuroblastoma (Fig. 1.2) (Ye et al. 2014). Additionally, the authors demonstrated that high SHMT2 levels correlated with a poorer prognostic outcome in neuroblastoma patients, providing a clinical context for targeting this pathway. While SHMT2 is a source of NADPH in normal dividing cells, inhibiting SHMT2 in normal cells should not significantly alter NADPH biogenesis, since normal cells have robust compensatory mechanisms for redox balance, unlike cancer cells (Fan et al. 2014).

In Myc-driven neuroblastoma, inhibiting SHMT2 or MTHFD2 would decrease NADPH biogenesis derived from one-carbon serine catabolism. While there are currently no known specific inhibitors of SHMT2 or MTHFD2, targeting production of serine's obligate reaction partner, THF, may offer a strategy to decrease NADPH production from serine catabolism in a tumor-selective manner. For example, inhibiting dihydrofolate reductase (DHFR) with the anti-folate, methotrexate, will decrease THF production, thereby decreasing flux through SHMT2 and MTHFD2, and attenuating NADPH levels specifically in cancer

cells with elevated SHMT2 expression (Fig. 1.2). Indeed, methotrexate exposure leads to cytostasis in overactive inflammatory cells seen in autoimmune diseases by decreasing GSH production, presumably due to decreased NADPH biogenesis (Phillips, Woollard, and Griffiths 2003, Sung et al. 2000). Alternatively, the new-generation anti-folate, pemetrexed, can also attenuate NADPH production from THF/serine catabolism by inhibiting both thymidylate synthase (TS) and DHFR, enzymes essential in THF synthesis (Fig. 1.2) (Adjei 2004). Utilizing anti-folate drugs in SHMT2 overexpressing cancers in combination with ROS-inducing agents may provide a therapeutic window for these agents.

1.2.3 Malic Enzymes

Another source of cellular NADPH is the NADP-dependent family of malic enzymes. This family of enzymes catalyzes the oxidative decarboxylation of malate to generate CO_2 and pyruvate, while reducing NAD^+ or $NADP^+$ to NADH or NADPH in the process (Fig. 1.3) (Baggetto 1992). Three isoforms have been identified in mammalian systems: cytosolic $NADP^+$ -dependent (ME1), mitochondrial $NAD(P)^+$-dependent (ME2), and mitochondrial $NADP^+$ -dependent malic enzyme (ME3) (Pongratz et al. 2007).

A recent report demonstrated the requisite of the cytosolic malic enzyme (ME1) in utilizing glutamine as an upstream metabolite to generate NADPH and to maintain redox balance in KRAS-mutated pancreatic ductal adenocarcinomas (PDAC), but not normal pancreatic tissue (Fig. 1.3) (Son et al. 2013). The canonical metabolism of glutamine generates αKG via the upstream activity of glutamate dehydrogenase (GLUD1) to drive

anapleurosis and replenish the TCA cycle (DeBerardinis et al. 2008). However, in KRAS-mutated PDAC, glutamine flux is primarily driven through mitochondrial aspartate transaminase (GOT2) to generate mitochondrial αKG and aspartate from glutamate and oxaloacetate (OAA). This aspartate is shuttled to the cytoplasm and then acted on by cytosolic aspartate transaminase (GOT1) and is converted back to OAA (Fig. 1.3). OAA is then converted to malate by malate-dehydrogenase 1 (MDH1) and then to pyruvate and NADPH by ME1 (Fig. 1.3). Depletion of ME1 in these PDAC cancer cells suppressed cell-line growth and tumor growth *in vivo* by ROS accumulation from loss of NADPH (Son et al. 2013). Furthermore, inhibition of these enzymes in normal pancreatic cells did not significantly alter NADPH concentrations. Intriguingly, KRAS mutated PDAC were shown to dramatically decrease glucose flux into the oxidative PPP, suggesting this non-canonical glutamine pathway is compensated for decreased NADPH production from the oxidative PPP (Ying et al. 2012). In PDAC with activating KRAS mutations (which is ~90% of all PDAC), inhibiting ME1 would decrease the utilization of glutamine for NADPH production sensitizing cells to oxidative damage. While there are currently no known ME1 inhibitors, inhibiting the upstream utilization of glutamine via glutaminase 1 (GLS1) with BPTES, Compound 968, CB-839 or other GLS1 inhibitors would sensitize KRAS-mutated PDAC to ROS inducing agents in a tumor specific manner (Fig 1.3) (Elhammali et al. 2014, Shukla et al. 2012, Gross et al. 2014).

A recent report demonstrated that a subset of lung tumors overexpress ME2 relative to normal lung tissue. A similar overexpression of ME2 was observed in melanoma vs. normal skin, suggesting an important role for ME2 in these cancer types (Ren et al. 2014).

Indeed, when ME2 was knocked down in the A549 lung cancer cell line, the cellular NADPH/$NADP^+$ decreased 3-fold compared to non-targeting control, indicative of a pro-oxidant state in the absence of ME2.

It was recently shown that ME1 and ME2 are negatively regulated by wild-type p53, and that the absence of a functional p53 led to a dramatic upregulation of ME1/2 expression (Jiang et al. 2013). Consistent with this finding, the authors demonstrated that ME1/2 were essential for NADPH maintenance in the absence of 9unctional p53 (Jiang et al. 2013). In the context of cancer, this is an important observation as p53 is a commonly mutated tumor suppressor and loss of its function may lead to a cancer cell-specific mechanism of NADPH/-biogenesis via ME1/2 de-repression.

1.2.4 Isocitrate Dehydrogenases

NADPH production can also be driven by the conversion of isocitrate to α-ketoglutarate (αKG) by the $NADP^+$-dependent cytosolic isocitrate dehydrogenase 1 (IDH1) and mitochondrial isocitrate dehydrogenase (IDH2) (Nekrutenko et al. 1998) and (Leonardi et al. 2012). While NADPH generation has well known roles in reduction of ROS, αKG also detoxifies ROS, such as by scavenging H_2O_2 through non-enzymatic decarboxylation to form water and succinate (Mailloux et al. 2009, Fedotcheva, Sokolov, and Kondrashova 2006).

IDH1 and IDH2 are mutated in approximately 80% of cases of adult glioma and secondary glioblastoma, and in 30% of cases of acute myeloid leukemia (AML) (Mardis et al. 2009, Ichimura et al. 2009). It was originally believed that these mutants led to enzymatic loss of function through dominant-negative inhibition of wild-type IDH 1 and IDH2 (Balss et

al. 2008, Ichimura et al. 2009) (Parsons et al. 2008). However, it is now believed that IDH1 and IDH2 mutants confer these enzymes the ability to convert αKG to the novel oncometabolite, 2-hydroxyglutarate (2-HG) (Ward et al. 2010).

This change causes mutated IDH1 and IDH2 enzymes to consume NADPH instead of producing NADPH, altering the cellular redox balance and leading to a pro-oxidant state in the cancer cell (Bleeker et al. 2010, Atai et al. 2011). Additionally, overexpression of the IDH1 mutant protein in glioma cell lines sensitizes these cells to the ROS-inducing effects of ionizing radiation (Li et al. 2013).

Glioma patients with $IDH1^{R132}$ mutations have prolonged survival compared to patients with wild-type IDH1 (Balss et al. 2008, Yan et al. 2009, Bleeker et al. 2010). A hypothesis for this observation could be that IDH1 mutants are defective in generating protective concentrations of NADPH to maintain reduced glutathione and thus are more sensitive to oxidative damage. Thus, glioma or AML patients with the R132 mutation might benefit from ROS inducing agents early in the course of treatment.

1.2.5 NAMPT

NADPH generation can be driven through the NAD^+ salvage pathway via nicotinamide phosphoribosyltransferase (NAMPT), which catalyzes the transfer of the phosphoribosyl group from 5-phosphoribosyl-1-pyrophosphate to nicotinamide, forming nicotinamide mononucleotide (NMN), and pyrophosphate (Fig. 1.1) (Garten et al. 2009). NAD^+ generation can then be coupled with NAD+ kinase (NADK) activity to generate

$NADP^+$ that can then be reduced to NADPH through the enzymes discussed above (Fig. 1.1) (Ying 2008).

Increased NAMPT expression has been reported in colorectal, non-small cell lung (NSCL), prostate and pancreatic cancer (Wang et al. 2011, Srivastava, Khurana, and Sugadev 2012, Hufton et al. 1999, Bi et al. 2011, Chini et al. 2014). In these contexts, NAMPT has been shown to be an important source of reducing equivalents for redox balance within the cancer cell (Wang et al. 2011). In fact, knockdown of NAMPT sensitized prostate and head and neck cancer cell lines to the ROS induction from ionizing radiation (Cerna et al. 2012, Wang et al. 2011, Kato et al. 2010, Okumura et al. 2012).

NAMPT inhibitors are undergoing clinical trials as a single agent therapy, but recent results have not been promising (von Heideman et al. 2010). The NAMPT inhibitors, FK866 and GMX1778, may have the greatest efficacy when combined with ROS-inducing agents that take advantage of the pro-oxidant state of NAMPT inhibited tumors. Indeed, pre-clinical studies have validated this strategy utilizing GMX1778 to sensitize breast cancer against the ROS production from ionizing radiation therapy, FK866 to sensitize prostate cancer against H_2O_2 and FK866 to sensitize neuroblastoma against cisplatin (Cerna et al. 2012, Wang et al. 2011, Travelli et al. 2011). To enhance the selectivity of these NAMPT inhibitors, NQO1 bioactivatable drugs can be used in combination resulting in a specific antitumor activity in cancer cells overexpressing NADPH:quinone oxidoreductase 1 (NQO1) (Moore et al. 2015), such as in pancreatic, Non-Small Cell Lung, breast, prostate and head and neck cancers.

1.3 Predicting tumor-specific NAD(P)H-biogenesis profiles from publically available datasets

Known NAD(P)H-biogenesis pathways can be useful when combined with publically available cancer gene expression and patient outcomes data to generate hypotheses for tumor-specific NADPH biogenesis profiles.

Here, we present a conservative set of criteria for determining candidate genes (Fig. 1.5):

1. Determine if genes of interest are significantly up-regulated in patient tumor tissue vs associated normal tissue in two or more independent datasets for the cancer type in question. Only genes with *p-value*$< 1x10^{-4}$ in each dataset will be considered for further analyses.
2. Of the up-regulated genes found in #1, determine which genes significantly predict poor outcomes in patients after radiation treatment.
3. Of the candidates from #2, determine if genes in the same NADPH-biogenesis pathway as the candidate gene are coordinately up-regulated. Only positive correlation values of 0.5 and above will be considered for further analysis.
4. Determine if common oncogenic drivers of the tumor type in question drive genes from #3.

Utilizing these criteria, we attempted to assess the NADPH-biogenesis profile of NSCLC. Using the Oncomine webtool (www.oncomine.com) we first determined which NADPH-biogenesis related genes were overexpressed in NSCLC tissue vs associated normal tissue from patient samples. To ensure robustness of our results, a gene was only considered a potential hit if it was found to be up-regulated in two or more datasets with a p-value $<1x10^{-4}$ in each dataset. This narrowed our initial list of 10 genes down to 4 potential genes (Fig. 1.6 and 1.7A). Next, to determine if our potential targets were clinically relevant in the context of ROS-inducing therapy, we used the KMPLOT software and stratified NSCLC patients into high and low expressers of our genes of interest and compared overall survival outcomes between these groups after radiation therapy (Fig. 1.7A and 1.8C) (Gyorffy et al. 2013).

From this analysis, we selected genes whose high expression in NSCLC patients led to significantly decreased survival after radiation therapy, suggesting that these genes may confer tumor protection from radiation-induced ROS, presumably through enhanced NADPH biogenesis (Diehn et al. 2009). Using this cutoff, we were able to narrow down our gene list to PKM2, which regulates NADPH biogenesis via the oxidative PPP, and MTHFD2, which generates NADPH from serine catabolism (Fig. 1.7B). We next wanted to determine if these genes were coordinately up-regulated with other enzymes in their respective NADPH biogenesis pathways. Utilizing the R2 Genomics Analysis platform's (r2.amc.nl) co-expression analysis feature in NSCLC patient samples, we found that G6PD was coordinately up-regulated with PKM2 in patient samples with a correlation value of 0.26 and

that TS and SHMT2 were co-expressed with MTHFD2 with correlation values of 0.63 and 0.64, respectively (Fig. 1.7B and 1.8D). Given that we defined our correlation cutoff at 0.5 and above, we considered MTHFD2 as our top candidate for NSCLC (Fig. 1.7B and 1.8D).

Next, we wanted to determine if mutant-KRAS, the most common oncogenic driver in NSCLC (Roberts and Stinchcombe 2013), might regulate MTHFD2, as this might give us insight into regulatory mechanisms of MTHFD2 and additional therapeutic targets. For this we utilized publically available gene expression datasets from the NCBI Gene Expression Omnibus (GEO). To determine if mutant-KRAS regulates MTHFD2, we analyzed mRNA expression-profiling data from a transgenic mouse model of NSCLC expressing doxycycline-inducible $KRAS^{G12D}$ in the respiratory epithelium (GSE40606) (Fisher et al. 2001). When fed doxycycline, the mice develop lung tumors that are dependent on constitutive $KRAS^{G12D}$ expression. Within 48 h of doxycycline withdrawal, $KRAS^{G12D}$ expression was extinguished and whole-genome gene expression analyses of lung tumors were performed. Expression levels of MTHFD2 were significantly up-regulated when $KRAS^{G12D}$ was induced *vs* 48 h after KRAS extinction with doxycycline withdrawal, indicating a positive regulatory role for mutant-KRAS in MTHDF2 expression (Fig. 1.7C and 1.8E).

If this hypothesis is validated through RNAi and redox balance studies, this may suggest that utilization of serine catabolism inhibitors such as methotrexate or pemetrexed may provide an effective therapeutic strategy to target NADPH-biogenesis specifically in KRAS-mutated NSCLC. This analysis also reveals that more than one NADPH-biogenesis pathway may also be regulating NADPH as observed from the PKM2 data. However,

validation experiments will need to be conducted to determine which pathway predominates in NSCLC.

1.4 Modulating NAD(P)H-biogenesis as a mechanism to potentiate NQO1-bioactivatble drugs

To exploit these metabolic vulnerabilities with ROS-inducing agents in a tumor specific manner, we believe that NQO1-bioactivatable drugs represent an ideal class of agents to combine with the aforementioned inhibitors. NQO1 is an inducible phase II detoxifying enzyme overexpressed in breast, lung, pancreatic and colon cancers and is capable of reducing quinones by forming stable hydroquinones of the parent quinone(Cao et al. 2014, Awadallah et al. 2008). ß-lapachone (ß-lap, in clinical trials as ARQ761), IB-DNQ and other NQO1-bioactivatable drugs are unique quinones that are metabolized by NQO1 into an unstable hydroquinone that spontaneously oxidizes back to the parental compound, generating a futile redox cycle in which one mole of ß-lap generates ~120 moles of superoxide within two minutes, consuming >60 moles of NAD(P)H (Bey et al. 2013a, Pink, Wuerzberger-Davis, et al. 2000). The superoxide ($O_2^{\cdot-}$) radicals formed are quickly metabolized by superoxide dismutase (SOD) into hydrogen peroxide (H_2O_2) (Tagliarino et al. 2001, Bey et al. 2013a). This H_2O_2 pool leads to extensive oxidative DNA damage that hyperactivates poly(ADP-ribosyl) polymerase 1 (PARP1) resulting in a dramatic loss of the intracellular NAD^+/ATP pools, leading to DNA repair inhibition (Bentle et al. 2007, Boothman, Greer, and Pardee 1987, Boothman, Trask, and Pardee 1989) and caspase-independent apoptosis (Bey et al. 2013a). Cancer cells with >100 units of NQO1 enzyme

activity are sensitive to ß-lap toxicity, while normal tissues that lack, or express low levels of, NQO1 are spared (Li et al. 2011). While this class of drugs represents an attractive anti-tumor strategy, dose-limiting methemaglobinemia caused by non-specific ROS generation at high ß-lap doses may limit the efficacy of ß-lap in monotherapy (L. P. Hartner LR 2007). Strategies for increasing cancer cell cytotoxicity while maintaining NQO1 specificity could greatly enhance the feasibility of ß-lap for use in solid cancers that overexpress NQO1. In this context, tumor specific NADPH pathways limit the efficacy of this class of drugs by producing anti-oxidants that can suppress ROS generation from NQO1-treated cells. To this end, we believe that combining ß-lap with agents targeting cancer-specific NADPH pathways that are under clinical investigation, such as FK866, CB-839, 6-AN, pemetrexed and methotrexate, may expand the therapeutic window for this class of drugs in the clinic.

1.5 Part 1 Conclusion

Rapidly proliferating cells, such as cancer cells, require NADPH for macromolecular biosynthesis and redox balance. However, given this dual role, when cellular NADPH demand is high, as in proliferation, minor alterations in NADPH production for lipid and nucleotide biosynthesis threaten the maintenance of cellular redox balance (Vander Heiden, Cantley, and Thompson 2009). Thus, cancer cells need to tightly regulate NADPH biogenesis to protect against oxidative damage. To sustain protective levels of NADPH, cancer cells rely on various NADPH biogenesis pathways such as the oxidative PPP, serine catabolism, glutamine metabolism and NAD^+ salvage pathways (Fig. 1.1,1.2, 1.3). Strategies to inhibit NADPH biogenesis may dramatically alter the ROS scavenging abilities of cancer

cells and sensitize them to oxidative damage. However, to achieve therapeutic selectivity, NADPH must be modulated through tumor specific NADPH-biogenesis pathways that are necessary for cancer cells but are expendable in normal cells. Thus, by rigorously studying these unique pathways in the context of a specific cancer, we will be able to create novel therapeutic strategies that exploit the ROS balances of tumor tissue while sparing normal tissue in the process. Here we have summarized the current understanding of known cancer-specific NADPH-biogenesis pathways, drugs to specifically target these pathways, and an example of using publically available databases to predict cancer-type specific NADPH-biogenesis genes. It is our belief that studying these pathways and comprehensively profiling tumors based on this understanding will be an essential step forward in designing cancer-specific ROS combination therapies, such as the use of NQO1-bioactivatable drugs.

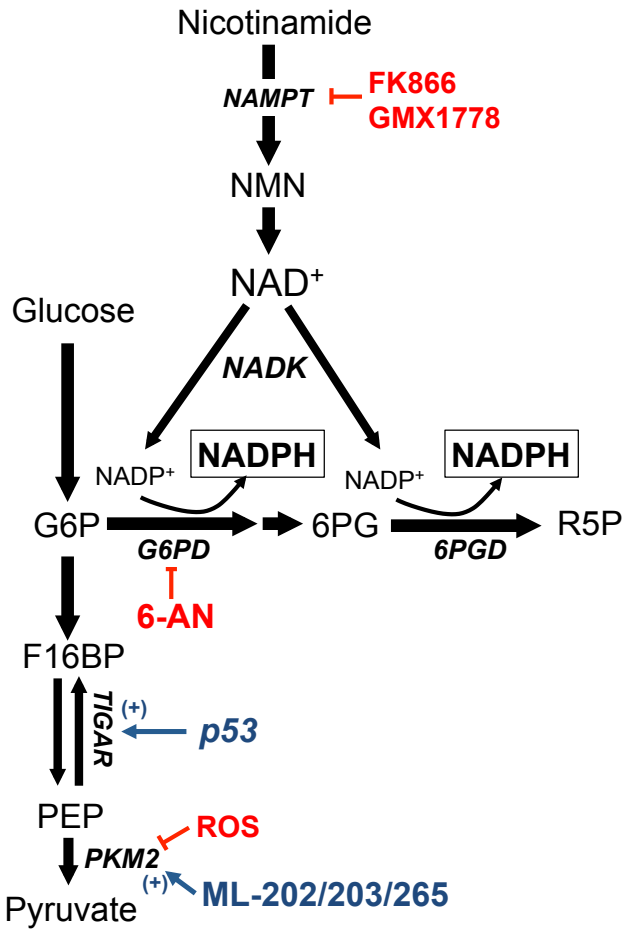

Figure 1.1 NAD+ salvage pathway and oxidative pentose phosphate pathway

Oxidative PPP highlighting usage of glucose to generate NADPH via glucose-6-phosphate dehydrogenase (G6PD) and 6-phosphogluconate dehydrogenase (6PGD). G6PD is inhibited by the FDA approved, 6-aminoactinomide (6-AN). NADP+ is generated through the NAD+ salvage pathway in which nicotinamide is converted to nicotinamide mononucleotide (NMN) via NAMPT, which is eventually converted to NADP+ by NAD+ -kinase (NADK). FK866 and GMX1778 can inhibit NAMPT to block the production of NADP+ and therefore NADPH. In the face of ROS stress, p53 positively regulates TP53-induced glycolysis and apoptosis regulator (TIGAR) to shunt glycolytic flux into the oxidative PPP. Pyruvate kinase 2 (PKM2), which is overexpressed in many cancers, is inhibited in the presence of ROS, allowing glycolytic flux to be shuttled into the oxidative PPP for NADPH generation. The small molecule compounds ML-202/203/265 can positively modulate PKM2, thereby decreasing glycolytic flux into the oxidative PPP and blunting NADPH-biogenesis in the face of ROS.

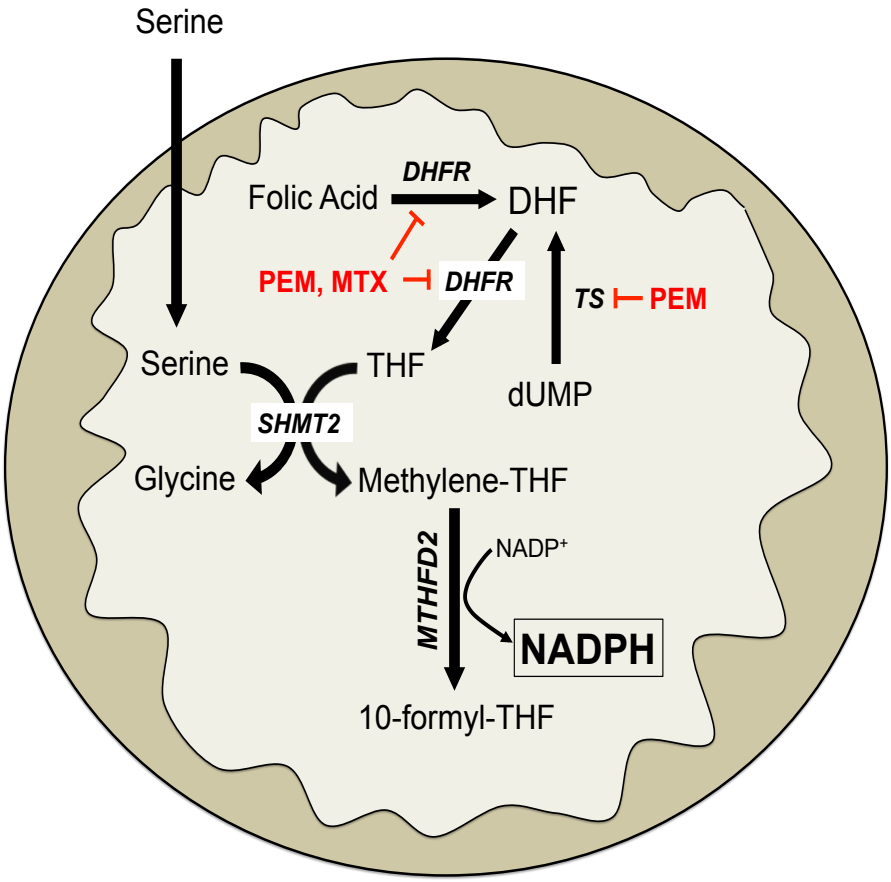

Figure 1.2 One-carbon serine catabolism pathway

Mitochondrial one-carbon serine metabolism pathway highlighting production of NADPH from serine and folic acid through mitochondrial methylene tetrahydrofolate dehydrogenase (MTHFD2). Tetrahydrofolate (THF) is produced from dihydrofolate (DHF) via folic acid through the enzyme dihydrofolate reductase (DHFR), which is inhibited by both pemetrexed (PEM) and methotrexate (MTX). Additionally DHF can be generated from deoxyuridine monophosphate (dUMP) via thymidylate synthase (TS), which is also inhibited by PEM.

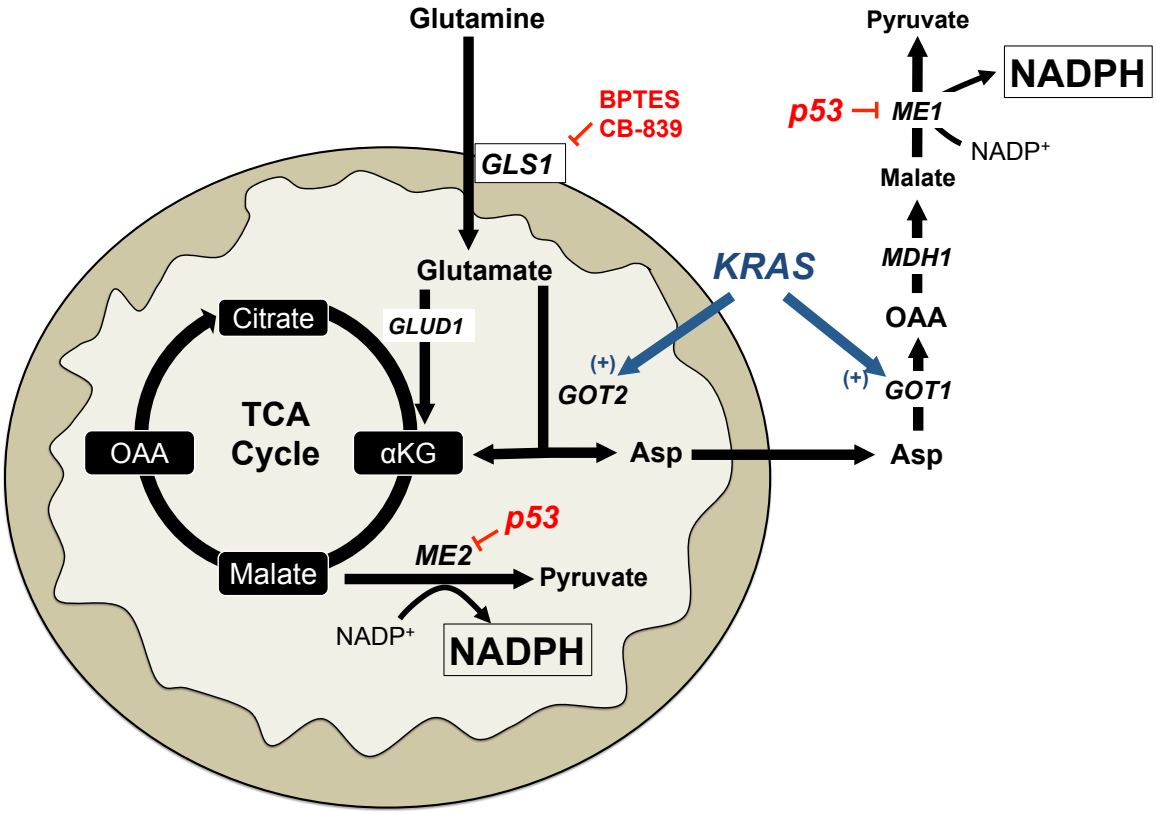

Figure 1.3 Kras-reprogrammed glutamine metabolism

In KRAS-mutant pancreatic cancer, mitochondrial glutamine flux is reprogrammed to predominantly flux through mitochondrial aspartate transaminase (GOT2) instead of the canonical glutamate dehydrogenase 1 (GLUD1). The aspartate (Asp) produced from this reaction is shuttled to the cytoplasm to eventually produce pyruvate and NADPH from malate via cytosolic malic enzyme (ME1). TCA cycle derived malate can also produce NADPH from mitochondrial malic enzyme (ME2). Wild-type p53 inhibits both ME1 and ME2. BPTES and CB-839 are non-competitive small molecule inhibitors of mitochondrial glutaminase 1 (GLS1). G6P = glucose-6-phosphate; 6PG = 6-phosphogluconate; R5P = ribulose-5-phosphate F16BP = fructose-1,6-bisphosphate; PEP = phosophoenolpyruvate; GLS1 = glutaminase 1; MDH1 = malate dehydrogenase 1; GOT1 = cytosolic aspartate transaminase.

Agent	*NADPH Pathway Targeted*	*Specificity*	*Status*	*Ref*
6-anicotinamide (6-AN)	Oxidative PPP via glucose-6-phosphate dehydrogenase (G6PD) inhibition	Cancers with TIGAR overexpression: colon, breast or glioblastoma	Approved	(25)
ML202, ML203, ML265	Oxidative PPP via PKM2 activation	Cancers with PKM2 overexpression: multiple cancers	Preclinical	(23,24)
BPTES, CB-839, Compound 968, Zaprinast	ME1 via GLS1 inhibition	KRAS mutant PDAC	CB-839 in Phase I	(36-38)
FK866, GMX1778	$NADP^+$ salvage pathway via NAMPT inhibition	Cancers with NAMPT overexpression; multiple cancers	Phase II	(59-61)
Pemetrexed, Methotrexate	One carbon serine-catabolism via TS and DHFR inhibition	SHMT2 or MTHFD2 overexpressing cancers, Neuroblastoma	Approved	(81)

Figure 1.4 Agents targeting NADPH-biogenesis

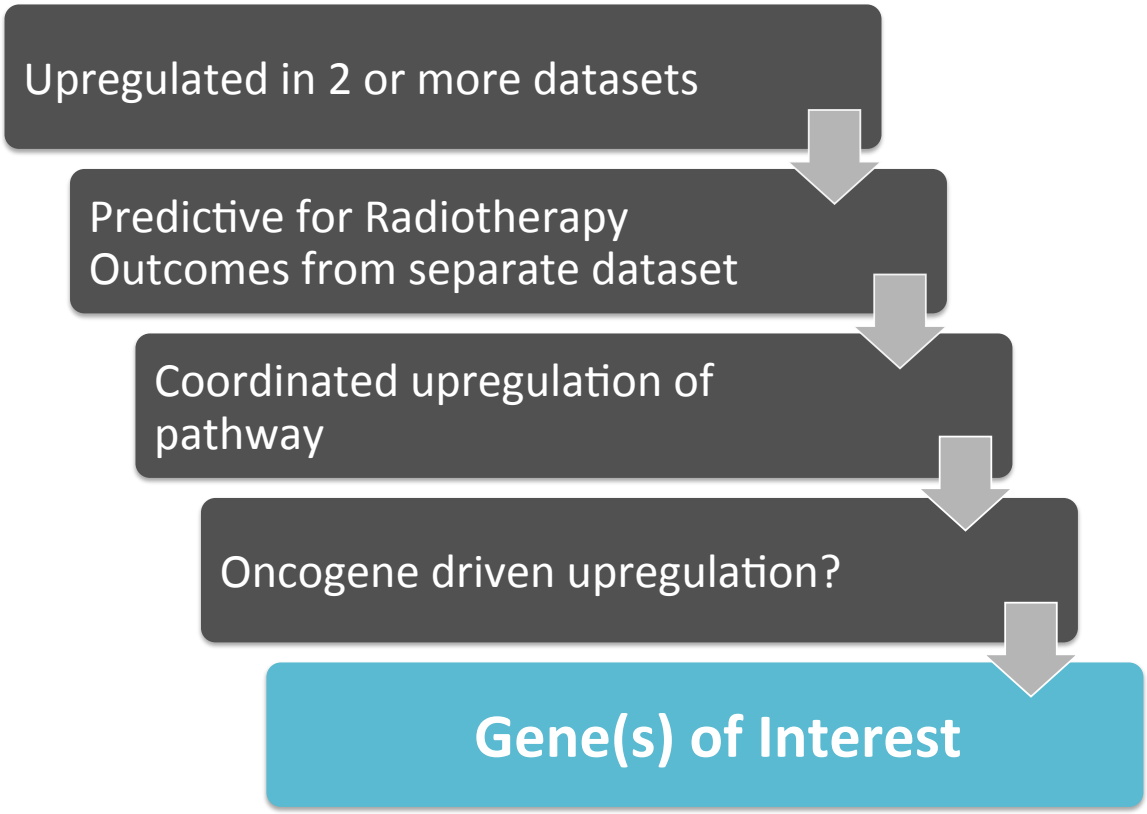

Figure 1.5 Screen Setup

NADPH-biogenesis related gene	Significantly upregulated in 2 or more datasets?	Number of Significant Datasets/Total # of Datasets
G6PD	no	0/3
PKM2	yes	3/3
TIGAR	no	0/0
SHMT2	yes	3/3
MTHFD2	yes	2/3
ME1	no	0/3
ME2	no	0/3
IDH1	no	1/3
IDH2	yes	3/3
NAMPT	no	0/3

Figure 1.6 Cancer specific NADPH-biogenesis screen

Overexpression status of NADPH-biogenesis genes of interest assessed using Oncomine in NSCLC patients. Datasets used are described (Landi et al. 2008, Hou et al. 2010, Talbot et al. 2005).

A

NADPH-biogenesis related gene	Do high expressers have significantly poorer prognosis after radiotherapy?	# of probes significant/ # of available probes
PKM2	yes	1/1
SHMT2	no	0/4
MTHFD2	yes	1/1
IDH2	no	0/2

B

NADPH-biogenesis related gene	Coordinate upregulation of NADPH pathway related genes	Correlation
PKM2	G6PD	0.26
MTHFD2	TS, SHMT2	0.63, 0.64

C

Oncogene	MTHFD2 Regulation	Specimen
KRAS	Upregulated	KRAS inducible NSCLC mouse model

Figure 1.7 Cancer specific NADPH-biogenesis screen continued

(A) Prognosis after radiation therapy in NSCLC patients. Dataset used is described (Gyorffy et al. 2013) (B) Correlation of genes of interest with upstream NADPH-biogenesis pathway members (C) Mutant KRAS-dependence of MTHFD2 in mouse model of NSCLC.

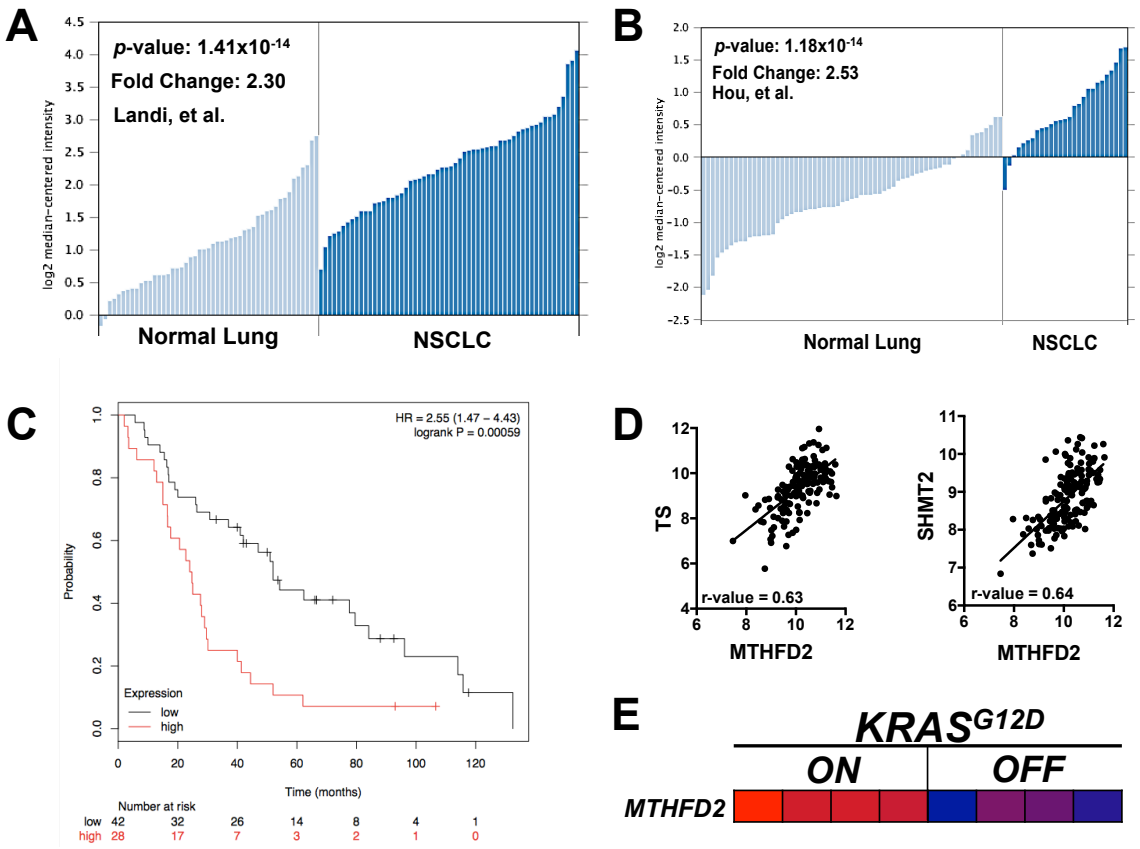

Figure 1.8 Screen results for MTHFD2 in NSCLC patients

CHAPTER TWO

MATERIALS AND METHODS

2.1 AP-site detection

AP sites measured by aldehyde reactive probe. AP site assay was done with aldehyde reactive probe reagent (Dojindo Molecular Technologies, Inc., Gaithersburg, MD) as previously described (20). Briefly, DNA (15 μg) extracted from cells with or without drug treatment was incubated with 1 mmol/L aldehyde reactive probe at 37°C for 10 min. After precipitation with 100% ethanol, DNA was washed and resuspended in Tris-EDTA buffer [10 mmol/L Tris-HCl, 1 mmol/L EDTA (pH 7.2)]. DNA was heat denatured at 100°C for 5 min, quickly chilled on ice, and mixed with an equal amount of ammonium acetate (2 mol/L). The ssDNA was then immobilized on a BAS-85 NC membrane (Schleicher & Schuell, Dassel, Germany) using a vacuum filter device (Schleicher & Schuell). The NC membrane was incubated with streptavidin-conjugated horseradish peroxidase (BioGenix, San Ramon, CA) at room temperature for 30 min. After NC membrane was rinsed with washing buffer containing NaCl (0.26 M), EDTA (1 mmol/L), Tris-HCl (20 mmol/L), and Tween 20 (1%), aldehyde reactive probe-AP sites were visualized with enhanced chemiluminescence reagents (Amersham).

2.2 Chemicals and Reagents

We synthesized and purified ß-lap and prepared a stock solution at 50 mM in DMSO. Methoxyamine, dicoumarol, rucaparib and BAPTA-AM were purchased from Sigma-Aldrich (St Louis, MO).

Cell Culture

Cell lines were obtained from ATCC. They were grown in DMEM (Life Technologies, Carlsbad, CA) containing 10% FBS (Fisher Scientific, Waltham, MA) in a 37° incubator with 5% CO_2. Cells were tested monthly to confirm absence of mycoplasma contamination. Lipofectamine RNAiMAX (Life Technologies) was used for siRNA transfections. Cells were transfected with one of two siRNAs purchased from Sigma-Aldrich to target OGG1 (OGG1 #1: SASI_Hs02_00340191, OGG1 #2: SASI_Hs02_00340192), or a non-targeting control siRNA). After 48 h of incubation with RNAiMax and siRNA in OptiMEM (Life Technologies), cells were detached with trypsin/EDTA (Life Technologies) and seeded for treatment assays or lysed for analysis of knockdown efficiency. For combination drug treatments, cells were co-treated with ß-lap and 12 mM MeOX for 2 h in complete media. Two h after treatment, the drug-containing media was removed and replaced with fresh media.

Clonogenicity

After ß-lap, MeOX, or combination treatment at 60% confluency, cells were trypsinized, counted with a Coulter Counter, and diluted in single cell suspension. Cells were then seeded at 100, 500, or 1000 cells per plate on 60mm plates and allowed to proliferate for seven days.

Plates were washed in PBS and cells were fixed and dyed with methanol/crystal violet. Colonies of fifty or more cells with normal appearance were counted and results were normalized to the colonies formed without drug treatment.

Nucleotide Assays

CellTiter-Glo (Promega, Madison, WI) was used for cell viability assays (24 h after treatment) and ATP assays (at indicated time points during or after ß-lap treatment) NAD/NADH-Glo assay was also purchased from Promega. CellROX

Green was obtained from Life Technologies. Unless otherwise noted, all raw luminescent values for treatment conditions were normalized to the signal from untreated cells (T/C). Standard curves were generated to ensure linearity.

Immunoblotting

Cells were lysed in ice-cold RIPA with protease and phosphatase inhibitors (Santa Cruz, Dallas, TX). Whole-cell extracts were prepared by centrifugation at 14,000 x g for 15 min. to remove insoluble components. Protein concentration was determined by BCA assay (Thermo Scientific, Waltham, MA) and loading volume was normalized. Extracts were run on 8% or 4-20% (Bio-Rad, Hercules, CA) gradient acrylamide SDS-PAGE gels and transferred to PVDF membrane. Primary antibodies for protein detection included: phospho-H2A.X (JBW301, Millipore, Billerica, MA), PARP1 (F-2, Santa Cruz), PAR (Trevigen, Gaithersburg, MD), Actin (C-2, Santa Cruz), XRCC1 (mouse monoclonal, Abcam, Cambridge, UK), small subunit calpain (EPR3324, Abcam). Primary hybridization was

carried out in Sigma casein blocking buffer at 4° overnight. Secondary HRP conjugated antibodies were incubated for 1 h at room temperature, followed by detection with SuperSignal West Pico (Thermo Scientific). Bands were quantified by mean intensity in ImageJ and normalized to the actin band intensity to control for loading variation.

Glucose consumption and lactate production

Cells were co-treated with ß-lap and methoxyamine for 2 h in complete media. After co-treatment, media was replaced with low glucose, phenol free DMEM (Invitrogen) with 5% FBS and collected at indicated times for analysis with a BioProfile Automated Analyzer (Nova Biomedical, MA).

Flow Cytometry

For TUNEL analysis, cells were co-treated with ß-lap and MeOX for 2 h. Drug-containing media was removed and cells were incubated in fresh complete media for 48 h. Cells were trypsinized, and both adherent and floating cells were collected and washed in 1% BSA in PBS. After fixing cells in 70% ethanol, cells were washed and resuspended in BSA/PBS buffer containing propidium iodine and saponin. Cells were analyzed on a FACSAria (BD Biosciences, San Jose, CA) and cell cycle distribution was calculated in FlowJo.

Mouse tumor studies

Nu/Nu nude mice were obtained commercially (Harlan). Subcutaneous tumors were generated by injecting 2×10^6 MiaPaca2 cells subcutaneously in 50 μL PBS/Matrigel into 6-week-old Nu/Nu mice. Tumors were measured at the indicated times with digital calipers (Fisher Scientific), and tumor volumes were calculated (length × width^2 × 0.5). Treatment was initiated when the subcutaneous tumors reached an average size of 100 mm^3. Mice were treated with MeOX by IP, ARQ761 by IV (retro-orbital) or both or with vehicle (HPßCD; 1:9, v/v; Sigma-Aldrich) as control. The treatment regimen consisted of a total of 5 doses of drug given every other day. Mice bearing subcutaneous tumors were treated with 150 mg/kg MeOX and/or 25 mg/kg ARQ761. Mice bearing subcutaneous tumors were sacrificed when tumors reached 2,000 mm^3. Mice were weighed 3 times per week during the drug-treatment period and afterward. All animal studies were performed under protocols approved by the Institutional Animal Care and Use Committee of UT Southwestern Medical Center.

Statistics

Unless otherwise noted, graphs are plotted as mean with error bars denoting standard deviation. Curve fitting and calculation of IC50 values, ANOVA, and two-tailed Student t-tests for statistical significance with Holm/Sidak multiple comparison correction were performed in GraphPad Prism 6.

CHAPTER THREE

TARGETING GLUTAMINE METABOLISM SENSITIZES PANCREATIC CANCER TO PARP1-DEPENDENT METABOLIC CATASTROPHE INDUCED BY ß-LAPACHONE

Abstract

Activating mutations in *KRAS*, which occur in 95% of pancreatic ductal adenocarcinoma (PDA), have been shown to activate a glutamine-dependent pathway of cytosolic NADPH production for redox homeostasis. Enzymes required for this pathway (*GLS1, GOT1 and GOT2*) are highly upregulated in PDA with a high *GOT:GLUD1* ratio being a predictor of poor survival in PDA patients. Although inhibiting this pathway with *GLS1* inhibitors is an emerging therapeutic strategy, such approaches alone will be cytostatic, provide a narrow therapeutic window and lack durable benefit in controlling advanced disease. Here, we report that reducing NADPH pools by genetically or pharmacologically (BPTES or CB-839) inhibiting glutamine metabolism in mutant-*KRAS* PDA sensitizes tumors to high levels of reactive oxygen species (ROS) from the futile redox cycling of the *NQO1* bioactivatable drug, ß-lapachone (ß-lap, clinical form ARQ761). This results in extensive DNA damage and rapid PARP1-mediated NAD^+ consumption in *NQO1* overexpressing PDA tumors, but not in *NQO1* deficient associated normal pancreatic tissue. This treatment strategy simultaneously decreases tumor anti-oxidant defenses and induces supra-physiological ROS formation,

lowering required doses of both agents *in vitro* and *in vivo*. The non-overlapping specificities of *GLS1* inhibitors and ß-lap for PDA tumors afford high tumor-selectivity, while sparing normal tissue.

3.1 Introduction

Pancreatic ductal adenocarcinoma (PDA) is a recalcitrant cancer in which patients have <6% 5-year survival rates. Mortality from this disease is predicted to be the second leading cause of cancer-related death by 2020 (Hidalgo 2010). PDAs are highly resistant to conventional chemotherapies (Hidalgo 2010), and activating mutations in *KRAS* are present in >95% of all cases (Bryant et al. 2014). An emerging therapeutic approach is to target PDA's altered metabolism (Bryant et al. 2014, Kong et al. 2013, Lyssiotis et al. 2013, Kamphorst et al. 2015). PDA cells generate the bulk of the ribose used for *de novo* nucleotide biosynthesis through the non-oxidative arm of the pentose phosphate pathway (Ying et al. 2012). This *KRAS*-driven reprogramming of glucose metabolism bypasses the NADPH-generating oxidative arm. To compensate for this decoupling, PDAs utilize glutamine through *GLS1* (mitochondrial glutaminase), *GOT2* (mitochondrial glutamic-oxaloacetic transaminase 2) and *GOT1* (cytoplasmic glutamic-oxaloacetic transaminase 1) to support cellular redox balance (NADPH and GSH biogenesis) in the face of rapid proliferation and growth (S3.2B) (Bryant et al. 2014, Son et al. 2013, Shanware et al. 2011). This is in contrast to the metabolism of glutamine through *GLUD1* (glutamate dehydrogenase 1) to supply a carbon backbone for the TCA cycle. In an attempt to leverage increased tumor-cell reliance on glutamine, small molecule inhibitors of GLS1 were developed (e.g., BPTES, CB-839, Compound 968)

(Shukla et al. 2012, Gross et al. 2014, Stalnecker et al. 2015). GLS1 catalyzes the conversion of glutamine to glutamate, the substrate for GOT2 and a necessary metabolite for NADPH/GSH biogenesis in PDA (Son et al. 2013). Importantly, inhibitors of GLS1 have relatively minor effects on tumor growth in preclinical cancer models, are cytostatic, drive compensatory metabolic resistance pathways in the tumor and may result in systemic toxicities (Emadi et al. 2014, Zhdanov et al. 2014, Le et al. 2012, Seltzer et al. 2010, Cheng et al. 2011).

To increase the specificity and efficacy of GLS1 inhibition in PDA, we combined BPTES or CB-839 with ß-lapachone (ß-lap), a targeted cancer therapeutic that causes tumor-selective reactive oxygen species (ROS) formation in an NADPH:quinone oxidoreductase 1 (NQO1)-specific manner (Bey et al. 2007). ß-Lap is a substrate for two-electron oxidoreduction by NQO1, a Phase II quinone-detoxifying enzyme. The resulting hydroquinone form of ß-lap is highly unstable and spontaneously reacts with oxygen to revert back to the parent compound, generating two moles of superoxide per mole NAD(P)H used in the process (Bey et al. 2007).

This results in a futile cycle that occurs rapidly in NQO1-overexpressing cells, resulting in massive ROS formation, oxidative DNA damage and single-strand DNA breaks resulting from H_2O_2 generated from the futile redox cycle. In an attempt to repair this damage, PARP1 becomes hyperactivated, generating extensive free branched poly(ADP ribose) (PAR) polymer levels. Hyperactivated PARP1 substantially depletes intracellular pools of NAD^+

and adenosine triphosphate (ATP), thereby inhibiting subsequent repair of ß-lap-induced DNA lesions. NQO1 is highly expressed in many types of cancer, and the therapeutic window provided by NQO1 bioactivation of ß-lap has advanced its use to phase I and Ib clinical trials (ARQ761) (L. P. Hartner LR 2007). Elevated NQO1 expression (≥10-fold) has been identified in ~90% of patient tissue from pancreatic ductal adenocarcinoma (PDA), making pancreatic cancer an especially appealing target for therapy using NQO1 bioactivatable drugs, such as ß-lap (Awadallah et al. 2008, Bey et al. 2007, Lyn-Cook et al. 2006, Lewis et al. 2005).

Unfortunately, dose-limiting methemoglobinemia caused by nonspecific ROS generation at high ß-lap doses somewhat limits the efficacy of ß-lap as monotherapy (L. P. Hartner LR 2007). Strategies for increasing cancer cell cytotoxicity, while maintaining NQO1-specificity could further enhance efficacy of ß-lap for therapy against PDAs.

ß-Lap and GLS1 inhibition have distinct, but highly complementary mechanisms of action. ß-Lap induces tumor-selective ROS generation specifically in PDA cells that express high levels of NQO1. GLS1 inhibition primes PDA cancer cells for cell death by lowering anti-oxidant pools derived from glutamine, sensitizing the cell to ROS damage. Here, we show using an *in vivo* pre-clinical model of PDA that the increased dependence of PDA cells on glutamine is specifically targeted by exposure to both drugs. Use of ß-lap with GLS1 inhibitors results in synergistic NQO1- and PARP1-dependent cancer cell death, allowing use of lower doses and shorter treatment times for both agents.

3.2 Results

Inhibiting glutamine metabolism sensitizes PDA to ß-lap.

Genes necessary for glutamine metabolism, *GLS1, GOT1/2,* and *ME1* were significantly upregulated in PDA compared to 17 other cancers in addition to *NQO1* (Fig. 3.1A) (Son et al. 2013). This was apparent in both cell lines and tumor samples. However, *GLUD1* was not upregulated in PDA relative to other cancer types (Fig. 3.1A). Additionally, glutamine metabolic enzymes, *NQO1,* and *GLUD1* were found to be significantly upregulated in PDA relative to normal pancreatic tissue (Fig. 3.1A). To determine the clinical relevance associated with the PDA glutamine metabolic pathway relative to other enzymes in glutamine metabolism, we evaluated the association of individual gene expression levels with overall survival in the data set that contained clinical follow-up information (Zhang et al. 2012). Kaplan-Meier analysis did not show a significant difference in outcome when patients were separated into high and low expression levels of the respective genes of interest (data not shown). However, when *GOT1* and *GOT2* were normalized to *GLUD1* expression, we found that a high *GOT1:GLUD1* or *GOT2:GLUD1* ratio was significantly associated with poor outcome (Fig. 13.B and SF3.1B). These data suggest that gene expression of transamination enzymes are generally elevated in PDA and have prognostic and functional significance relative to expression of *GLUD1*.

Given the reliance of glutamine metabolism for redox balance in PDA, we hypothesized that glutamine deprivation of *NQO1*-overexpressing PDA cells would sensitize them to

subsequent ß-lap exposure by lowering the cell's anti-oxidant defenses, thereby increasing *NQO1*-induced ROS damage. MiaPaca2 cells were grown in Gln-free or Gln-containing (2 mM) media for 16 h, then exposed to ß-lap for 2 h. Short-term Gln deprivation did not significantly alter clonogenic survival on its own (Fig. 3.1C), but did sensitize MiaPaca2 cells to ß-lap, at normally sub-lethal and higher doses of the drug (Fig. 3.1C). To confirm these results, we repeated this experiment in 5 other PDA cell lines: ASPC1, MPanc96, HPAFII, SW1990 and DAN-G (Fig. 1D-H). Additionally, we demonstrated that the observed cytotoxicity was NQO1-dependent, as addition of the potent NQO1 inhibitor, dicoumarol (DIC), spared cells from lethality (Cao et al. 2014, Bey et al. 2013a, Bey et al. 2013b).

Next, RNAi-mediated knockdown of glutamine metabolism enzymes (Fig. 3.1I) revealed that knockdown of genes associated with glutamine transamination, *GLS1, GOT1* and *ME1* dramatically sensitized MiaPaca2 and ASPC1 PDA cell lines to ß-lap relative to the non-targeting control (siScr) (Fig. 3.1J,K). Intriguingly, knockdown of *GLUD1*, had no effect on ß-lap sensitivity (Fig. 3.1K). Sensitization of ß-lap-treated MiaPaca2 cells by *GLS1* knockdown was rescued by replenishing metabolic substrates for glutamine transamination: oxaloacetate (OAA), the product of GOT1 or cell-permeable dimethyl malate the substrate for ME1 (Fig. 3.1L,M). These data indicate that PDA cells have an increased reliance on glutamine in the presence of ß-lap-induced ROS stress.

GLS1 inhibition by BPTES sensitizes PDA to ß-lap in an NQO1-dependent manner.

To pharmacologically mimic ß-lap sensitization to transamination inhibition, MiaPaca2 cells were treated with a sublethal dose of the mitochondrial GLS1 inhibitor, BPTES (500 nM, 48 h Fig. 3.2A), and then exposed to various doses of ß-lap (μM, 2 h), ± DIC (Fig. 3.2B). While BPTES delayed growth of MiaPaca2 cells at nanomolar concentrations with 72 h treatment, 48 h pretreatment had no effect on cell viability (SF3.2A). BPTES pretreatment in combination with ß-lap significantly reduced clonogenic survival vs ß-lap alone, while addition of DIC spared the lethality (Fig. 3.2B). To confirm that our results were due to transamination inhibition and not a general inhibition of all cellular glutamine metabolism, we pre-treated MiaPaca2 cells with epigallocatechin gallate (EGCG), an inhibitor of GLUD1 (Choo et al. 2010) for 48 h and then exposed them to ß-lap. Consistent with our RNAi studies (Fig. 3.1K), we found that GLUD1 inhibition by EGCG had no effect on ß-lap sensitivity (Fig. 3.2C). Furthermore, normal human IMR-90 embryonic lung fibroblasts, which have low *NQO1* levels (Bey et al. 2013b) were not affected by ß-lap, with or without BPTES treatments (Fig. 3.2D). Replenishing the NADPH-producing transamination pathway with the addition of OAA or dimethyl-malate rescued BPTES-dependent hypersensitivity to ß-lap in MiaPaca2, ASPC1 and HPAFII PDA cells (Fig. 3.2E).

Given recent literature that suggests mutant *KRAS* reprograms glutamine metabolism to drive transamination (Fig. SF3.2B) (Bryant et al. 2014, Son et al. 2013), we wanted to determine if other mutant *KRAS* cancer types were sensitive to this pharmacological combination strategy. BPTES pretreatment sensitized a variety of *NQO1*-expressing, *KRAS* mutant cancer cell lines to ß-lap, including lung, triple-negative breast, and additional pancreatic cancer cell lines.

NQO1-deficient *KRAS* mutant lines remained resistant to ß-lap, whether or not BPTES was added (Fig. 3.2F). However, pretreatment with 500nM BPTES for 48 h did not increase the sensitivities of ß-lap-responsive *NQO1*-expressing, *KRAS* wild-type lung, breast and pancreatic cancer cell lines, consistent with reported literature (Saqcena et al. 2014, Son et al. 2013)

GLS1 inhibition attenuates antioxidant defenses and increases susceptibility to ß-lap-induced DNA damage.

We observed a dose-dependent increase in NADP+/NADPH ratios, a proxy for the cell's oxidative state, in MiaPaca2 cells exposed to ß-lap alone, reaching 4-fold higher levels *versus* baseline NADP+/NADPH ratios found in untreated cells (Fig. 3.3A). BPTES pretreatment (500 nM, 48 h) significantly lowered reduced-glutathione (GSH) levels >2-fold in MiaPaca2 cells compared to DMSO vehicle alone (SF3.3A). With BPTES pretreatment, we noted a 7-fold increase in NADP+/NADPH ratios in ß-lap-exposed cells *vs* baseline level in untreated MiaPaca2 cells (Fig. 3.3A), an ~2-fold higher level than in cells exposed to ß-lap alone. Extracellular H_2O_2 production was dramatically increased after BPTES + ß-lap treatment in a time- and dose-dependent manner (Fig. 3.3B, SF3.3B). We observed a decrease in the minimum time to death for ß-lap-induced lethality in MiaPaca2 with BPTES pretreatment in line with H_2O_2 productions kinetics (Fig. 3.3C). The antioxidant reduced diethyl-ester GSH dramatically rescued clonogenic survival of ß-lap-exposed MiaPaca2,

ASPC1, HPAFII and MPanc96 cells after 48 h pre-treatment with BPTES + 2 h ß-lap (Fig. 3.3D). Pre-treatment with BPTES followed by exposure to ß-lap synergistically increased total DNA lesions in ASPC1 assessed using alkaline comet assay immediately after 2 h treatment and DNA double strand break formation in MiaPaca2 cells as monitored by 53BP1 foci formation 24 h after treatment (Fig. 3.3E,F,G). Pre-treatment with BPTES followed by treatment with ß-lap dramatically increased PARP1 hyperactivation noted by concomitant NAD^+ depletion and PAR formation, which was blocked with the addition of the PARP1 inhibitor, Rucaparib (AG014699), in MiaPaca2 cells compared to either treatment alone (Fig. 3.3H,I). These data indicate that PDA cells become reliant on glutamine to supply the transamination pathway as a mechanism to generate NADPH and glutathione, protect cells from ß-lap-induced DNA damage, and prevent PARP1-driven metabolic catastrophe.

GLS1 inhibition sensitizes pancreatic cancer to ß-lap *in vivo*.

To determine whether pharmacologic inhibition of GLS1 in combination with ß-lap would lead to synergistic inhibition of PDA tumor growth *in vivo*, we utilized the clinical formulation of ß-lap (ARQ761), HPßCD-ß-lap, and the orally available GLS1 inhibitor, CB-839, manufactured by Calithera Biosciences. Both of these compounds are in separate PhaseI/II clinical trials for a variety of cancer types (NCT01502800, NCT02071862, NCT02071888 and NCT02071927) (Gross et al. 2014). We switched from BPTES to CB-839 due to BPTES's poor metabolic stability and low solubility *in vivo*, problems that have been overcome with CB-839 (Gross et al. 2014). We confirmed that CB-839 pre-treatment also sensitized PDA cell lines *in vitro* to ß-lap similar to BPTES in the MiaPaca2 and ASPC1

lines (Fig. 4.4A). We generated subcutaneous tumors from human MiaPaca2 cells injected into the right hind limb in Nu/Nu female athymic mice and allowed the tumors to grow to a volume of 100 mm^3 before beginning treatment. Mice were sacrificed when tumor volumes reached 1,000 mm^3.

Animals received either vehicle (HPßCD) or CB-839 (200 mg/kg) by oral gavage twice a day for 10 days, with or without a sub-efficacious dose of ß-lap (25 mg/kg) administrated intravenously (IV) every other day (Fig. 4.4B, arrows) (Li et al. 2011). After only one regimen of treatment (10 days), we found that animals treated with CB-839 + ß-lap displayed significantly delayed tumor growth compared to either agent alone through day 60. Importantly, we noted that neither CB-839 (200mg/kg) nor ß-lap (25 mg/kg) administered alone significantly altered tumor growth (Fig. 4.4B). Additionally, combination treatment did not decrease mouse weights when compared to vehicle treated mice (Fig. SF4.4A).

Mice were sacrificed when their original body weight dropped by one third, tumor volume exceeded 1000 mm^3 or when tumors began to ulcerate or impede normal motion as per IACUC policies. Kaplan-Meier curves showed a significant antitumor effect of the drug combination (Fig. 4.4C). Treatment with a sub-efficacious dose of ß-lap (25 mg/kg) resulted in a median survival of 49 days, while the vehicle-treated group displayed a median survival time of 39.5 days (Fig. 4.4C). Treatment with a sub-efficacious dose of CB-839 resulted in a median survival time of 42 days. Treatment with ß-lap + CB-839 resulted in a median

survival of 64 days, significantly extending median survival by 24.5 days compared to the vehicle treated group (Fig. 4.4C).

Importantly, to ensure that the anti-tumor efficacy we observed was due to on-target effects of both drugs and by the same mechanism of action observed *in vitro*, we analyzed the pharmacodynamics profile of each agent alone and in combination. Briefly, MiaPaca2 tumor-bearing mice received either vehicle (HPßCD) alone or 200 mg/kg CB-839 by oral gavage twice a day for 4 days, with or without a single sub-efficacious dose of ß-lap at 25 mg/kg IV on day 4. After the last dose of CB-839 and 30 min after ß-lap injection, mice were sacrificed and tumor tissue was harvested. Tumor glutamate levels were measured from multiple animals for each treatment condition (Fig. SF4.4C). CB-839 and CB-839 + ß-lap treated mice displayed significantly lower overall tumor glutamate levels when compared to vehicle or ß-lap alone treatments, consistent with GLS1 inhibition *in vivo* (Fig. SF4.4C).

We then immunoblotted tumor tissue lysates for poly(ADP-ribose) (PAR) polymer formation as a proxy for PARP1 hyperactivity and gH2AX to assess DNA double strand breaks (DSBs) (Li et al. 2011) (Fig. 4.4D). Consistent with our results *in vitro*, we found that animals treated with the combination of ß-lap + CB-839 displayed dramatically increased PAR and gH2AX formation relative to all other groups (Fig. 4.4D). Additionally, we harvested surrounding pancreas and liver ("Normal Tissue" in Fig. 4.4D) from the combination-treated mice and found no change in PAR formation or gH2AX formation, consistent with a lack of response to ß-lap in NQO1-deficient, normal tissues (Cao et al. 2014, Li et al. 2011).

Next, to determine the redox status of tumors after treatment, we measured the GSH:GSSG ratio of tumor lysate after vehicle alone or CB-839, with or without 30 min ß-lap treatment (Fig. 4.4E). Interestingly, we found that the GSH:GSSG ratio was significantly decreased in CB-839 or ß-lap-treated mice (Fig. 4.4E). Moreover, the combination treatment resulted in an even greater decrease in the oxidized glutathione, monitored by the GSH:GSSG ratio (Fig. 4.4E). Taking our pharmacodynamics observations and anti-tumor studies together, these data demonstrate that modulating glutamine transamination in PDA *in vivo* results in a significantly decreased anti-oxidant defense state that specifically sensitizes NQO1-expressing tumors, but not associated normal tissue, to ROS-induction from ß-lap, leading to DNA damage, PARP1 hyperactivation and tumor-selective death.

Discussion

Tumor cells display unique metabolic alterations that impact the biological behavior of the tumor and have therapeutic implications (Hanahan and Weinberg 2011, Cheong et al. 2012). A well-documented example of such an alteration is the increased utilization of glutamine in a variety of human tumors, including lung, prostate lymphoma and PDA (Brunelli et al. 2014, Fendt et al. 2013, Son et al. 2013, Le et al. 2012). Glutamine has pleiotropic roles in the cell that include the regulation of autophagy, signal transduction, anabolic growth and redox balance (Shanware et al. 2011). In particular, pancreatic cancers, 95% of which are mutant *KRAS* (Sousa and Kimmelman 2014b, Bryant et al. 2014, Sousa and Kimmelman 2014a, Collins and Pasca di Magliano 2013, Wang et al. 2013, Roberts and Stinchcombe

2013), utilize glutamine through a *KRAS*-dependent, transamination pathway driven by *GOT1* and *GOT2* instead of the pathway catalyzed by *GLUD1* (Son et al. 2013). This transamination pathway is necessary to maintain redox balance in PDA via NADPH/GSH biogenesis (SF3.2C) (Bryant et al. 2014, Son et al. 2013, Shanware et al. 2011). While this understanding provides insight into PDA metabolism, how to most appropriately target this metabolic vulnerability remains to be determined. Targeting this pathway alone may be cytostatic, drive compensatory metabolic resistance pathways in the tumor and/or result in systemic toxicities.

Genes involved in the transamination pathway (*GLS1, GOT1/2, ME1*) and *NQO1*, but not *GLUD1*, are highly expressed in PDA relative to other cancers, and overexpression of these genes is a major feature in the transition from normal cells to tumor. Clinical PDA cases expressing a high *GOT1:GLUD1* or *GOT2:GLUD1* ratio in the tumor have the worst outcome. Here, we found that genetic or pharmacological inhibition of this pathway, sensitizes PDA to the NQO1 bioactivatable drug, ß-lap. Addition of ß-lap to short-term BPTES treatment resulted in enhanced tumor-cell specificity and efficacy in PDA cell lines, not typically found with BPTES treatment alone. Consistent with prior reports of differential usage of glutamine in mutant *KRAS* vs wild-type *KRAS* cancers (Elhammali et al. 2014, Saqcena et al. 2014, Son et al. 2013, Kong et al. 2013), we found that mutant *KRAS*, but not wild-type *KRAS* PDA, lung and breast cancer cell lines were sensitized to ß-lap upon pre-treatment with BPTES. These data suggest that mutant *KRAS* cancers other than PDA may

also rely on glutamine to supply the transamination pathway to maintain redox balance, but future studies to elucidate this mechanism will be needed.

48 h pre-treatment with BPTES followed by 2 h treatment with ß-lap resulted in elevated DNA lesions, more extensive NAD^+/ATP loss mediated by PARP1, and metabolic catastrophe. Mechanistically, addition of BPTES to NQO1-overexpressing cancer cells decreased NADPH/GSH anti-oxidant defenses against the ß-lap-induced ROS burst leading to enhanced DNA damage and NAD+/ ATP depletion in a near-identical manner to the caspase-independent, μ-calpain-mediated cell death pathway induced by lethal doses of ß-lap alone (Moore et al. 2015). For our *in vivo* studies, we utilized the GLS1 inhibitor CB-839, as this compound has far greater solubility and stability in animals than BPTES (Gross et al. 2014). A single regimen of CB-839+ß-lap in tumor bearing mice resulted in durable tumor regression and significantly improved survival compared to animals treated with either agent alone. Pharmacodynamics analysis revealed that the mechanism of synergy with combination treatment was consistent with *in vitro* results.

When considering the ROS burst generated from NQO1-bioactivatable drugs, as evidenced by ß-lap's H_2O_2 production profile, cells require an equally robust antioxidant response to suppress the build-up of ROS. Thus, one can imagine that a competition between the rates of engagement of the antioxidant machinery and the production of ROS determines the fate of cancer cells within a tumor following NQO1-bioactivatable drug treatment. Notably, we previously reported that catalase (an essential enzyme for the detoxification of $2H_2O_2$ to

$2H_2O + O_2$) expression was significantly down-regulated in tumor tissue vs normal tissue, and that the NQO1:catalase ratio is markedly increased in tumor tissue vs normal tissue and the addition of PEGylated-catalase significantly protected breast cancer cell lines from ß-lap-induced lethality (Bey et al. 2013a). To maintain redox balance, PDA may utilize glutamine metabolism to compensate for this decrease in catalase. By suppressing this pathway in PDA, the pool of available antioxidants is dramatically diminished, shifting the cellular redox balance to a pro-oxidant state.

Novel therapies are desperately needed for patients with PDA. By combining *GLS1* inhibition (e.g., CB-839) and NQO1 bioactivatable drugs (e.g., β-lap, ARQ761) we exploit the reliance of PDA on glutamine for redox balance, as well as the tumor-selective overexpression of NQO1 through the use of agents that are bioactivated to induce cell death. Combination treatment with GLS1 inhibitors+ß-lap addresses issues associated with either agent alone. This combination is expected to enhance efficacy at well-tolerated doses of these drugs. We noted that CB-839+ß-lap combination treated animals did not display increased cytotoxicity in normal pancreatic and liver tissue based on the lack of PAR and DNA damage formation that was present in the tumor tissue after combination treatment. Thus, elevated *NQO1* expression is still required to achieve cell death. Furthermore, the ß-lap and CB-839 doses used in our studies are relevant to those achievable in patients (NCT01502800, NCT02071862, NCT02071888 and NCT02071927) (Savage et al. 2008, Gross et al. 2014). These findings illustrate a rational combination strategy to target PDA dependence on

glutamine by *GLS1* inhibition in combination with an NQO1-bioactivatable drug and we hope to further study this strategy in a clinical context.

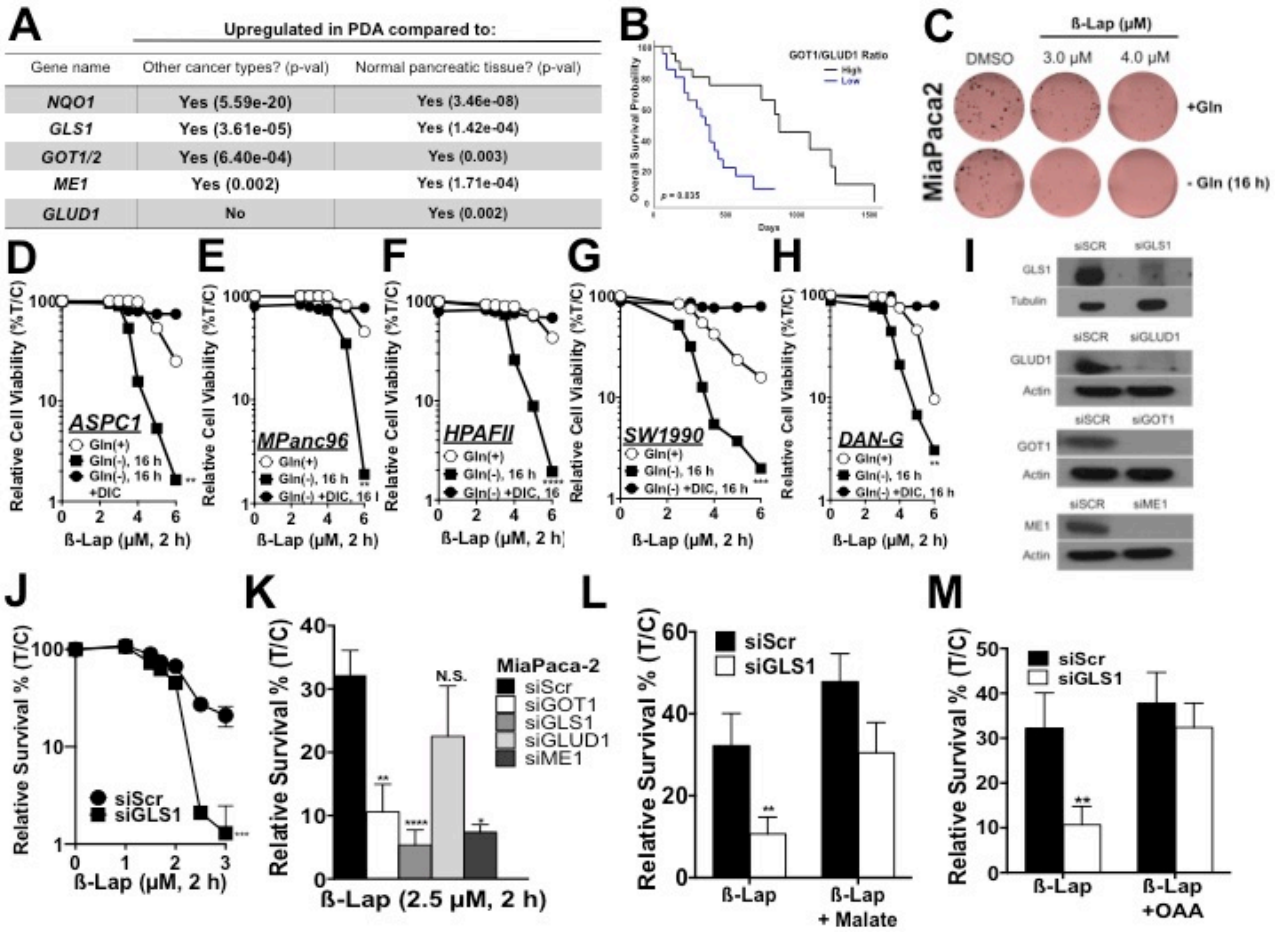

Figure 3.1. ß-Lap inhibits glycolytic and mitochondrial capacity in an NQO1-dependent manner (A) *NQO1,* transamination enzymes and *GLUD1* expression assessed in PDA vs 17 other cancers and PDA vs normal pancreatic tissue **(B)** Kaplan Meier survival curve of 45 PDA patients grouped according to high vs low *GOT1:GLUD1* expression **(C)** MiaPaca2 cells were plated in complete media and allowed to adhere overnight, then depleted of glutamine for 16 hours, followed by treatment with ß-lap for 2 hours. This was followed by addition of fresh media containing 2mM glutamine and 10mM glucose for 8 days. Plating efficiency with MiaPaca2 was 16% and colony formation after glutamine deprivation did not

significantly alter final colony number, though these colonies did appear smaller, they did have >50 cells per colony. **(D-H)** Repeat of the glutamine deprivation experiments in ASPC1, MPanc96, HPAFII, SW1990, and DAN-G PDA cell lines **(I)** *GLS1*, *ME1*, *GOT1* and *GLUD1* were knocked down in MiaPaca2 cell lines for 48 h using siRNA in OptiMEM with Lipofectamine RNAiMAX. Knockdown was assessed by western blot in MiaPaca2 cells with tubulin and actin as a loading control **(J) (K)** *GLS1, GOT1, GLS1, GLUD1,* and *ME1* MiaPaca2 knockdown cells were treated with 2.5 μM ß-lap for 2 h. Relative survival represents means of CellTiter-Glo survival assay 48 h after treatment, percentage treated/control (T/C), ±SE from sextuplicate samples. **(L, M)** GLS1 was knocked down in MiaPaca2 as described, but either 3mM oxaloacetate (OAA) or 3mM dimethyl malate was added for 24 h followed by a 2 h treatment with 2.5μM ß-lap. Relative survival represents means of CellTiter-Glo survival assay 48 h after treatment, percentage treated/control (T/C), ±SE from sextuplicate samples. Data represent clonogenic survival assays in sextuplicate per dose of ß-lap. All results were compared using ANOVA unless otherwise stated. As indicated, *$p<0.05$; ***$p<0.001$; ****$p<0.0001$.

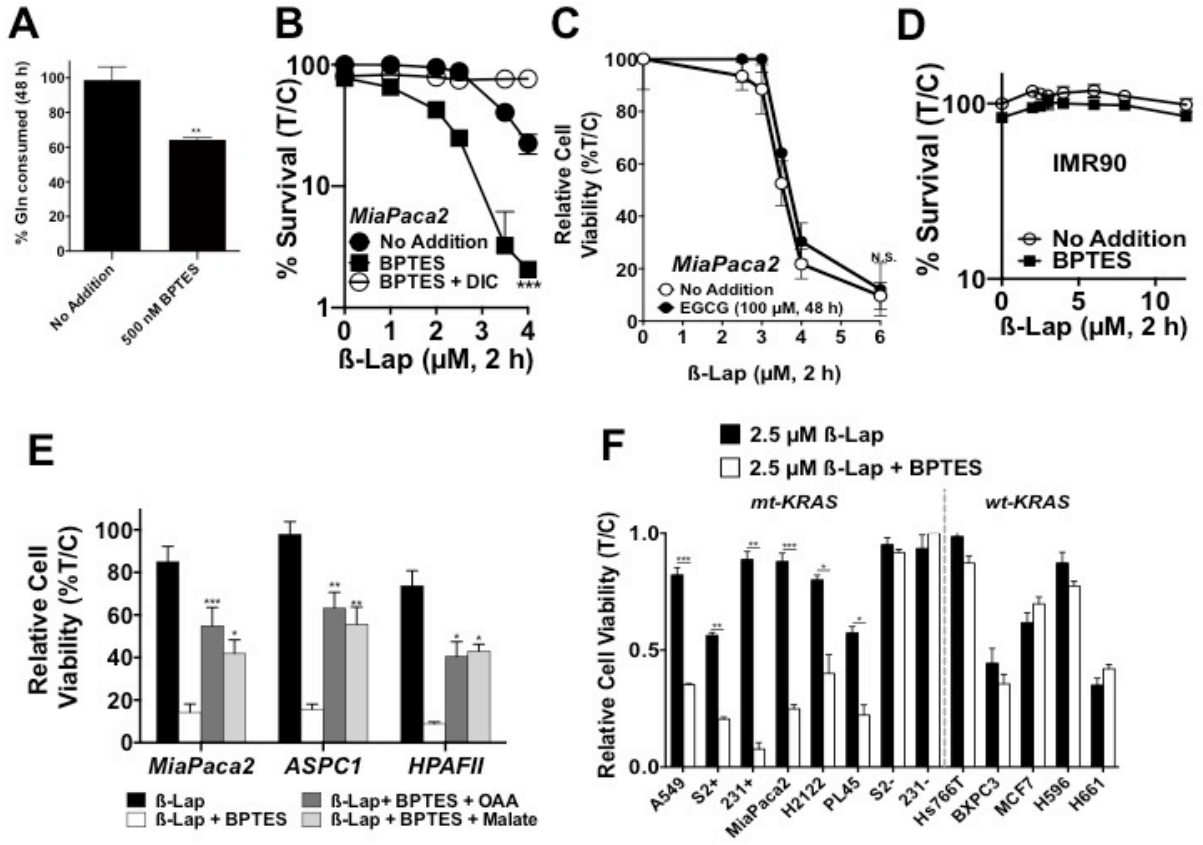

Figure 3.2. GLS1 inhibition by BPTES sensitizes PDA to ß-lap in an NQO1-dependent manner (A) Glutamine consumption was measured in MiaPaca2 cells treated ±500nM BPTES for 48 h in complete media using the Nova Bioprofile analyzer and normalized to cell number. **(B)** Clonogenic survival assay of MiaPaca2 pretreated with ± 500nM BPTES for 48 hours followed by the addition of ß-lap ±50µM DIC for 2 h. Data represent survival means ±SE from quadruplicate samples. **(C)** MiaPaca2 cells treated with 100µM of the GLUD1 inhibitor, EGCG, for 48 h followed by 2 h ß-lap dose response. Relative cell viability represents mean of CellTiter-Glo survival assay 48 h after ß-lap treatment, percentage treated/control (T/C), ±SE from sextuplicate samples. **(D)** Normal lung fibroblast

cell line, IMR90, pre-treated with ±500nM BPTES for 48 hours followed by 2 hours of ß-lap treatment. **(E)** MiaPaca2, ASPC1 and HPAFII PDA cell lines were pre-treated with ± 500nM BPTES for 48 h followed by the addition of either 3mM oxaloacetate (OAA) or 3mM dimethyl malate for last 24 h followed by a 2 h treatment with 2.5μM ß-lap. Relative cell viability represents means of CellTiter-Glo survival assay 48 h after treatment, percentage treated/control (T/C), ±SE from sextuplicate samples. **(F)** Various cancer cell lines pretreated with ± 500nM BPTES (sublethal) for 48 h followed by the addition of 2.5 μM ß-lap for 2 h; Mutant *KRAS* lines: A549 non-small cell lung (NSCL), PL45 PDA, S2-013-NQO1 expressing (S2+) PDA, MDA-MB-231-NQO1 expressing (231+) triple negative breast, H2122 NSCL, S2-013-NQO1 deficient (S2-) PDA and MDA-MB-231-NQO1 deficient (231-) triple negative breast cancer cells. Wild-type *KRAS*, lines: Hs766T PDA, BxPC3 PDA, MCF7 breast, as well as *NQO1*+ H596 NSCL and H661 NSCL cancer cell lines.

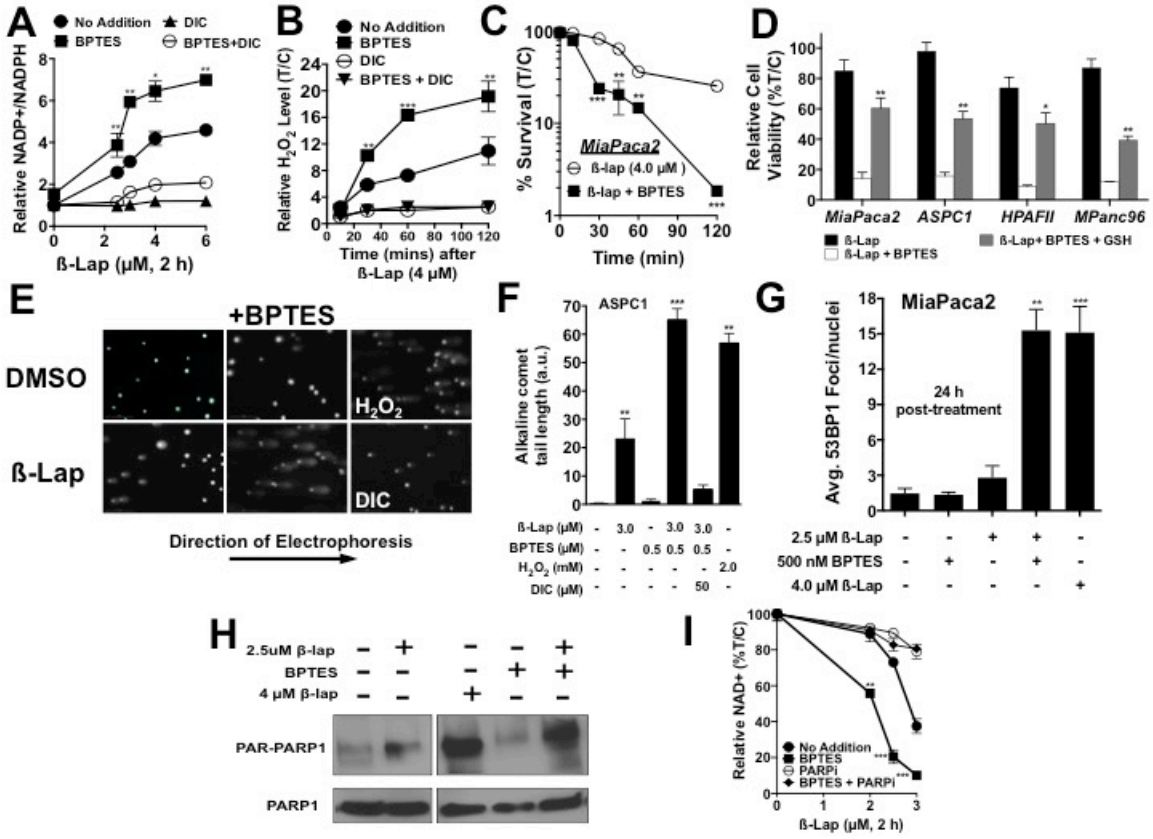

Figure 3.3. *GLS1* inhibition decreases antioxidant defenses and increases susceptibility to ß-lap-induced DNA damage. (A) Relative NADP+ to NADPH ratio was determined using the Promega NADPH-Glo luminescence assay. MiaPaca2 cells were pretreated with ßPTES for 48 hours at 500nM, and then treated with ß-lap for 2 h in a 96 well plate. NADP+ and NADPH levels were measured immediately after 2 h treatment (statistical significance was calculated with a two-tailed Student's t-test at every dose). **(B)** Relative extracellular H_2O_2 was measured through luminescence assay from the media of 4µM ß-lap ± DIC, ± BPTES treated MiaPaca2 over a time-frame of 120 minutes, ±SE from sextuplicate samples. **(C)** Clonogenic survival of MiaPaca2 pretreated with ± 500nM BPTES for 48 hours followed

by the addition of ß-lap for various incubation times. Data represent survival means ±SE from quadruplicate samples. **(D)** MiaPaca2, ASPC1, HPAFII and MPanc96 pretreated with ± 500nM BPTES and ± GSH reduced ethyl ester for 48 h followed by the addition of ß-lap for 2 h. **(E,F)** Alkaline comet assay of ASPC1 PDA cell lines pre-treated with ±500 nM followed by 2 h of ß-lap. **(G)** Average 53BP1 foci 24 h after treatment conditions in MiaPaca2. **(H)** Western blot for PAR formation with indicated treatment after 15 min. of ß-lap exposure. **(I)** Relative NAD+ levels ±BPTES with various doses of ß-lap after 2 h of treatment. All results were compared using Student's t-tests as indicated. *$*p<0.05; **p<0.01; ***p<.001$*.

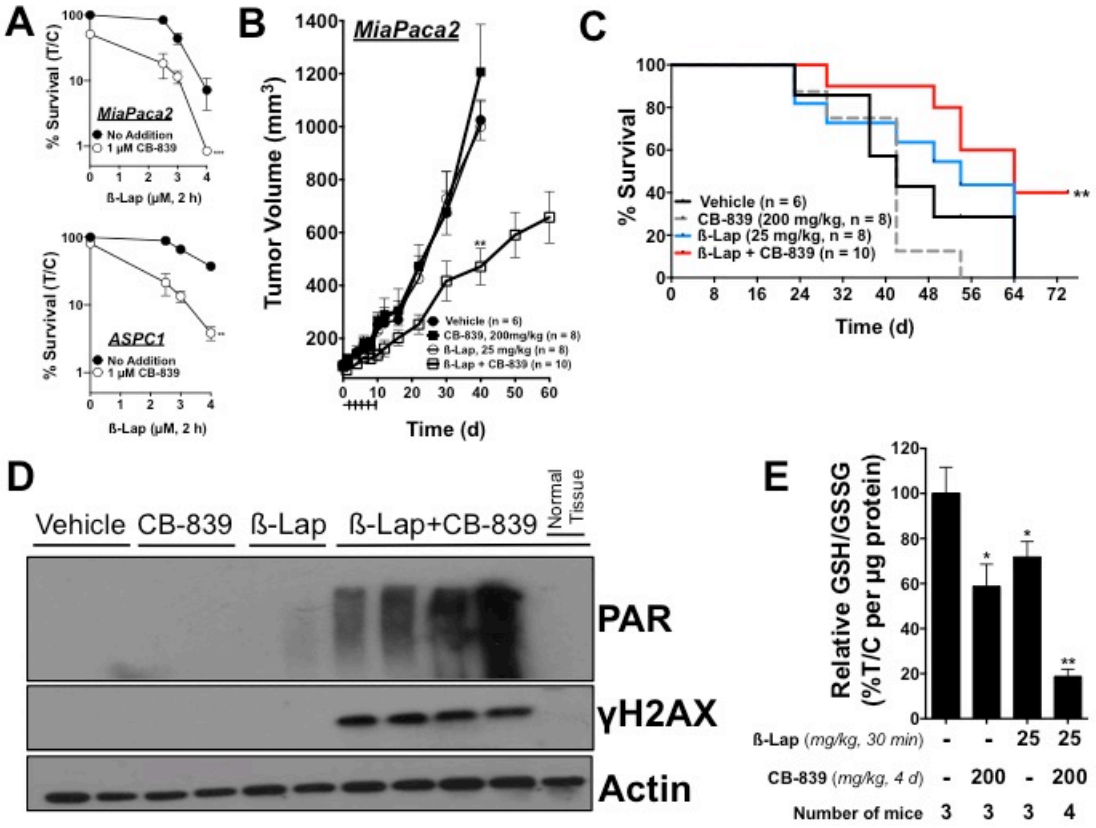

Figure 3.4. *GLS1* inhibition sensitizes pancreatic cancer to ß-lap *in vivo*

(A) Clonogenic survival of MiaPaca2 and ASPC1 cells pre-treated with 1 μM CB-839 for 48 h followed by 2 h of ß-lap dose response. **(B)** Subcutaneous tumors grown from MiaPaca2 cells in nude mice were allowed to reach a volume of 100 mm^3, after which mice were treated every other day with vehicle (HPßCD, n = 6), sub-efficacious dose of CB-839 (oral gavage, 200 mg/kg, n= 8), sub-efficacious dose of ß-lap (IV, 25 mg/kg, n= 8) or sub-efficacious doses of CB-839 in combination with ß-lap (n = 10) for a total of 5 doses (arrows). Tumor growth was monitored until tumors reached 1,000 mm^3. Error bars, SEM. **(C)** Survival of tumor–bearing mice represented as a Kaplan–Meier plot. Mice were sacrificed when tumors reached 1,000 mm^3. **(D)** Western blot quantification of PAR and

yH2AX from a set of tumors harvested 30 min after treatment with ß-lap ± CB-839, n = 3 tumors per group, same doses as above. Error bars, SEM. **(E)** Relative GSH/GSSG ratio in treated groups normalized to μg of tumor protein. All results were compared using Student's t-tests as indicated. **p<0.05; **p<0.01; ***p<.001*.

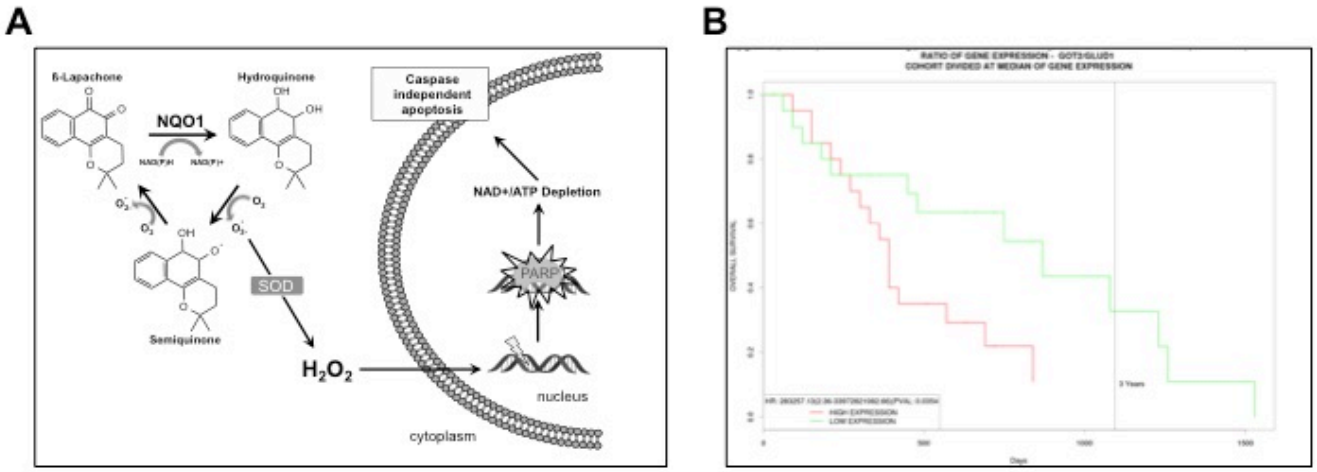

Figure SF3.1. **ß-Lap MOA and *GOT2:GLUD1* Kaplan-Meier Curve . (A)** ß-lap mechanism of action. **(B)** *GOT2:GLUD1* Kaplan-Meier curve, n = 45 patients

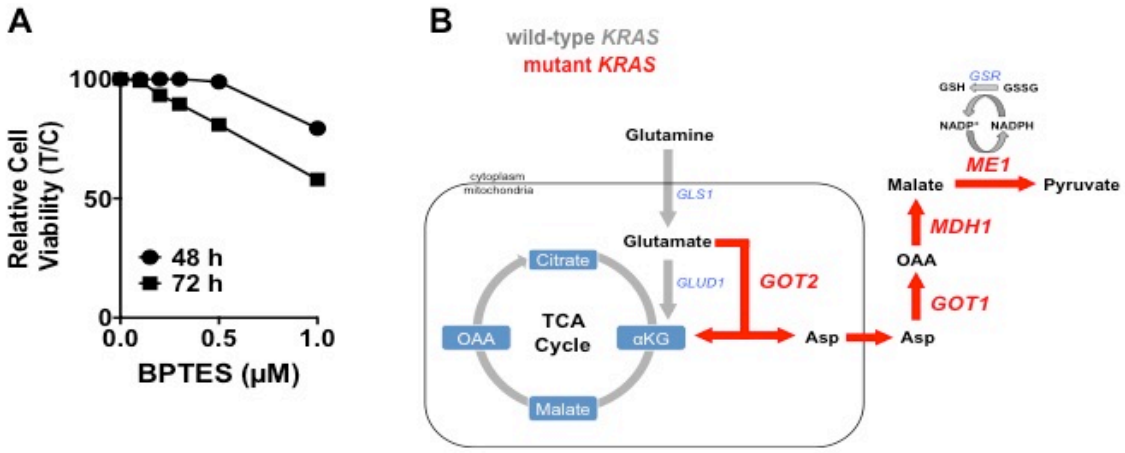

Figure S3.2. BPTES sensitivity and *KRAS*-reprogrammed glutamine pathway. (A) Sensitivity of MiaPaca2 cells, as monitored by loss of ATP, to short-term (48 h) or long-term (96 h) BPTES treatments. **(B)** Proposed model of *KRAS*-reprogrammed glutamine metabolism in PDA, via flux through GOT2 *vs.* GLUD1.

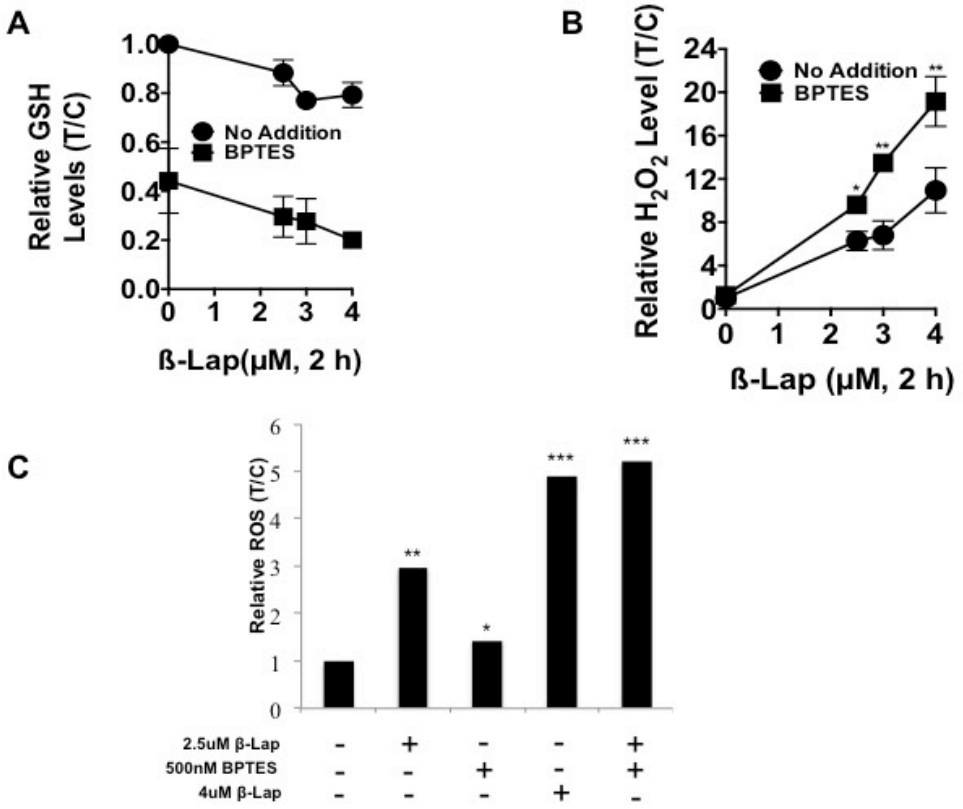

Figure SF3.3. Combination treatment leads to increased ROS by depleting reduced glutathione (A) Relative GSH levels ±500nM BPTES pre-treatment followed by ß-lap treatment. **(B)** Relative H_2O_2 production with ±500nM BPTES pre-treatment followed by ß-lap treatment **(C)** CellROX quantification of total ROS at 15min of ±4µM ß-lap ±DIC, ±BPTES (48 h pre-treatment).

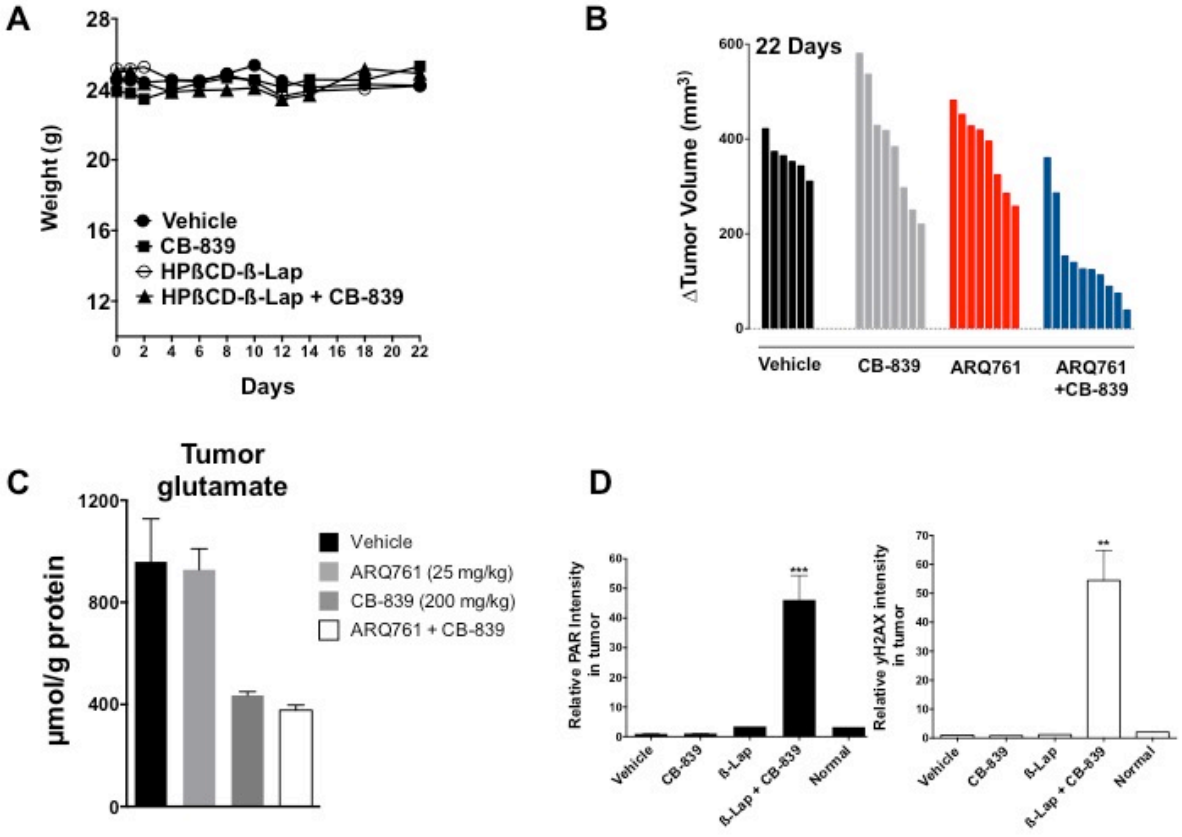

Figure S3.4 CB-839 and ß-lap *in vivo* validation in MiaPaca2 (A) Mouse weights during treatment with ß-lap (IV, 25 mg/kg), CB-839 (IP, 200 mg/kg) or vehicle treatment. **(B)** Change in tumor volumes per animal at day 22 compared to day 1. **(C)** Tumor glutamate levels, n = 3 mice per group. **(D)** Quantification of relative PAR and yH2AX from tumor tissue lysate.

CHAPTER FOUR

INHIBITING BASE EXCISION REPAIR SIGNALING SENSITIZES PANCREATIC CANCER TO PARP1-DRIVEN METABOLIC CATASTROPHE INDUCED BY THE NQO1 BIOACTIVATABLE DRUG, TO ß-LAPACHONE

Abstract

DNA repair inhibitors, including agents that inhibit base excision repair (BER), lack tumor-selectivity and are plagued by normal tissue toxicity. Here, we use the NAD(P)H:Quinone Oxidoreductase 1 (NQO1) bioactivatable drug, ß-lapachone (ß-lap, in clinical form ARQ761), to provide tumor-selectivity and enhanced synergistic efficacy with BER inhibition. ß-Lap undergoes NQO1-dependent futile redox cycling, generating massive hydrogen peroxide (H_2O_2) levels and oxidative DNA lesions selectively in cancer cells. This results in the hyperactivation of poly(ADP-ribose) polymerase 1 (PARP1), leading to rapid intracellular NAD^+/ATP depletion and selective antitumor activity through programmed necrosis. Inhibiting BER by genetically depleting XRCC1, or using the AP-site-modifying drug, methoxyamine (MeOX), in combination with ß-lap led to dramatic increases in PARP1 hyperactivation and synergistic killing of NQO1-expressing pancreatic ductal adenocarcinomas (PDAs). In contrast, depleting the BER sensing enzyme, OGG1 glycosylase, dramatically spared cells from ß-lap-induced lethality and blunted PARP1

hyperactivation. Combined treatment of MeOX + ß-lap increased DNA base lesions, inciting dramatic PARP1 hyperactivation-related NAD^+/ATP losses with dramatic suppression of glycolysis. MeOX + ß-lap treatments potently sensitized a broad range of NQO1-expressing cancers, including PDA, breast, lung and head and neck cancer cells. In MiaPaca2-derived xenografts, MeOX + ß-lap sensitized tumors, delaying tumor volume growth, enhanced PARP1 hyperactivation in tumor tissue, and improved survival of mice. Synergy was beneficial to each agent, affording tumor selectivity to DNA repair (BER) inhibition, while reducing normal tissue cytotoxicity for ß-lap (ARQ761).

4.1 Introduction

Pancreatic ductal adenocarcinoma (PDA) will be the second leading cause of cancer-related deaths in the US by 2020, with a current 5-year survival rate of <6% (2013). The majority of chemotherapies approved for the therapy of PDA include DNA-damaging agents (ionizing radiation, cisplatin, irinotecan) or antimetabolites that inhibit DNA synthesis (5-fluorouracil, gemcitabine) (Maginn et al. 2014, Cao, Le, and Yang 2013). These agents have very narrow therapeutic windows, with tumor selectivity based solely on DNA synthesis rates, and are consequently highly toxic to patients. They are often used in combination with one another, but despite the selected regimen, dismal response rates and a lack of continuous therapeutic efficacy remain a fundamental characteristic of PDA. There is a desperate need to identify new therapeutic targets and strategies to specifically target PDA, while sparing normal tissue.

Novel NQO1 bioactivatable drugs represent a promising new strategy for the treatment of PDAs. NAD(P)H:quinone oxidoreductase 1 (NQO1, EC1.6.99.2), was previously reported to be elevated, at levels ranging up to 100-fold, in PDA above that of associated normal pancreas tissue (Li et al. 2011, Lewis et al. 2005, Awadallah et al. 2008, Lyn-Cook et al. 2006). NQO1 is an inducible phase II detoxifying enzyme capable of detoxifying quinones by forming stable hydroquinones, which are then conjugated with glutathione by glutathione S transferase and excreted from the cell (Glen et al. 1997). For most quinones, this reaction avoids toxic one-electron oxidoreductions in normal cells. However, in recent years our laboratory discovered novel quinones that undergo futile redox cycling by NQO1. The NQO1 bioactivatable drug, ß-lapachone (ß-lap, in clinical form, ARQ761), is metabolized by NQO1 to form an unstable hydroquinone that spontaneously oxidizes back to the parent compound in two one-electron oxidations using two separate oxygen molecules. This reaction generates a futile redox cycle in which one mole of ß-lap generates ~120 moles of superoxide within two minutes and consumes ~60 moles of NAD(P)H (Bey et al. 2013a, Pink, Wuerzberger-Davis, et al. 2000). Superoxide ($O_2^{\cdot-}$) radicals are quickly metabolized by superoxide dismutase (SOD) into hydrogen peroxide (H_2O_2) (Tagliarino et al. 2001, Bey et al. 2013a). Elevated, cell membrane-permeable H_2O_2 pools, in turn, lead to extensive oxidative DNA lesions that 'hyperactivates' poly(ADP-ribosyl) polymerase 1 (PARP1), generating extensive free branched poly(ADP-ribose) (PAR) polymers that deplete intracellular NAD+ and ATP levels, thereby inhibiting subsequent repair of ß-lap-induced DNA lesions (Bentle et al. 2007, Boothman, Greer, and Pardee 1987, Boothman, Trask, and Pardee 1989). ß-Lap-exposed, NQO1+ cancer cells die by a unique caspase-independent

programmed necrosis pathway termed NAD^+-Keresis (Bey et al. 2013a, Moore et al. 2015). Few drugs mechanistically act to induce PARP1-mediated programmed necrosis in a tumor-specific manner at clinically relevant doses (Huang et al. 2013). Most agents known to stimulate PARP1-mediated programmed necrosis (e.g., >5 mM MNNG or >200 μM hydrogen peroxide) (Zong et al. 2004, Yu et al. 2002) do so at supra-lethal, clinically non-achievable doses. In contrast, ß-lap stimulates PARP1 hyperactivation at clinically achievable doses (L. P. Hartner LR 2007). Cancer cells with >100 units of NQO1 enzyme activity are sensitive to ß-lap, while normal tissues that lack, or express low levels of, NQO1 are spared (Li et al. 2011).

We previously demonstrated that a lethal dose of ß-lap (~4 μM) creates a significant level of DNA lesions in NQO1-expressing cancer cells immediately after drug exposure (Bentle et al. 2007). However, when cells were analyzed by neutral comet assays, DNA double strand breaks (DSBs) were not detected. In contrast, alkaline comet assays revealed that the majority of DNA lesions immediately created in NQO1+ cancers after exposure to ß-lap were DNA base lesions and single strand breaks (SSBs) (Bentle et al. 2007). Since PARP1 can bind to DNA lesions and SSBs (Prasad et al. 2014, Campalans et al. 2013, Khodyreva et al. 2010), upstream base excision repair (BER) processes represent possible resistance mechanisms that could be targeted to improve NQO1 bioactivatable drugs, such as ß-lap. Such a strategy may lower the dose-limiting Methemaglobinemia caused by NQO1 bioactivatable drugs, while improving the DNA damage-specificity of DNA repair inhibitors.

BER is responsible for removing and repairing non-helix distorting base lesions in the genome. Unlike nucleotide excision repair (NER), which repairs helix-distorting lesions, BER is essential for removing oxidatively damaged bases that can lead to genomic mutations through base mispairing or replicative DNA breaks (Krokan and Bjoras 2013). Bases in DNA can be damaged by a variety of mechanisms including oxidation, deamination and alkylation. One of the most common base lesions resulting from ROS exposure is the oxidation of the 8th carbon of guanine, forming 8-oxoguanine (8-oxo-G) (Bruner, Norman, and Verdine 2000). 8-Oxo-G formation can result in the mismatched pairing of guanine to adenine, causing G:C to G:A transversions, thus compromising a cell's genomic integrity leading to a pro-oncogenic environment. However, cells have evolved the 8-oxoguanine DNA N-glycosylase 1 (OGG1) as a dedicated repair enzyme to detect and cleave 8-oxo-G from the DNA backbone. Once 8-oxo-G lesions are excised by OGG1, as well as by other albeit less avid DNA N-glycosylases, apurinic/apyrimidinic (AP)-sites are generated. PARP1 can bind to AP sites, which in turn, stimulates its poly(ADP ribose) polymerase activity generating free poly-ADP polymers (PAR) using NAD^+ as a substrate. AP-sites can also be substrates for AP endonuclease (APE1) or AP lyase, and these enzymatic activities can generate SSBs in the DNA backbone (El-Khamisy et al. 2003, Campalans et al. 2013, Prasad et al. 2014, Khodyreva et al. 2010, Krokan and Bjoras 2013, Boiteux and Guillet 2004, Izumi et al. 2003), which are also substrates for PARP1. Through PARylation of downstream proteins, PARP1 recruits the BER scaffolding protein, XRCC1, to facilitate the interaction of BER complex proteins at the damaged site. Along with auto-PARylation or PARP1, this action

acts to facilitate dissociation of PARP1 from the damaged site, allowing DNA repair to commence (Campalans et al. 2013, Almeida and Sobol 2007, Horton et al. 2013).

Here, we show that the expression profile of NQO1 and Catalase levels offers an optimal therapeutic window for use of NQO1 bioactivatable drug, and in combination with a BER inhibitor synergistic antitumor responses result. The massive pools of H_2O_2 generated from NQO1-dependent ß-lap futile redox cycling and the concomitant lowered levels of Catalase in PDA tumors, leads to the induction of oxidative DNA lesions, including extensive 8-oxo-G formation. Extensive base damage signals BER machinery and can attenuate PARP1 hyperactivation and ultimately ß-lap-induced cytotoxicity. Indeed, we show the roles of both OGG1 and XRCC1 in modulating PARP1 hyperactivation and ß-lap efficacy. Therapeutically, we demonstrated that addition of the AP site-modifying drug and BER small molecule inhibitor, methoxyamine (MeOX), to ß-lap can greatly potentiate antitumor efficacy and survival of PDA xenograft-containing mice (Liu and Gerson 2004). The drug combination is beneficial to both agents, with ß-lap affording tumor-selectivity to MeOX, and MeOX lowering the efficacious dose of ß-lap required for antitumor activity and survival of PDA-bearing mice.

4.2 Results

Tumor versus normal tissue NQO1:Catalase expression ratios offer an exploitable therapeutic window for pancreatic cancer.

Analyses of mRNA expression data from 59 PDA patient tumor and directly matched associated normal tissue showed that NQO1 mRNA levels were elevated 5- to >100-fold (**Figs. 4.1A,C,F**), consistent with prior observations (Awadallah et al. 2008). Importantly, however, we also found that Catalase mRNA levels were significantly lower in PDA *vs* associated normal pancreatic tissue, with NQO1:Catalase ratios significantly elevated in PDA (**Figs. 4.1B,D,G**). In contrast, associated normal tissue expressed relatively elevated catalase levels with concomitantly low levels of NQO1. Catalase is an important upstream resistance mechanism against NQO1 bioactivatable drugs, such as ß-lapachone (ß-lap), given the massive levels of H_2O_2 generated from NQO1-mediated futile redox cycling (Bey et al. 2013a). Thus, NQO1:Catalase ratios in tumor *vs* normal tissue offer a significant therapeutic window that can be exploited using NQO1 bioactivatable drugs, such as ß-lap. This is particularly true for protection of normal tissue where the lack of NQO1 means extremely low level futile redox cycling will occur, while elevated Catalase levels will offer protection.

ß-Lap-induced 8-oxo-Guanine requires OGG1 for PARP1 detection and subsequent hyperactivation.

Prior data from our laboratory demonstrated that a 30-60 min exposure to ß-lap (4 μM) could kill NQO1+-overexpressing cancer cells, including MiaPaCa2, through a PARP1 hyperactivation mechanism regardless of p53, oncogenic driver, or cell cycle status (Bentle et al. 2006, Moore et al. 2015, Bey et al. 2007, Huang et al. 2013, Bey et al. 2013b, Li et al. 2011). Thus, understanding events within this ‘minimum time to death’ period are essential for developing novel ways to improve the drug’s therapeutic potential. Since NQO1 and

Catalase were the only two enzymes that could potentiate (Pink, Planchon, et al. 2000) or partially block (Bey et al. 2013a) ß-lap lethality, respectively, we examined the roles of ROS (H_2O_2)-induced 8-oxo-G formation and removal by Ogg1, and subsequent DNA lesion detection by PARP1 (**Fig. 4.2A**). Total ROS formation during the first 30 min of ß-lap treatment in NQO1-expressing MiaPaca2 PDA cells was monitored using CellROX Green dye (Li et al. 2011). Flow cytometry analyses revealed NQO1-dependent, dose-dependent ROS formation in MiaPaca2 cells treated with 4 μM ß-lap that was essentially equivalent to high dose H_2O_2 (1 mM, 30 mins) (**Fig. 4.2B**). Importantly, we showed that cells treated with ß-lap (4 μM, a lethal dose in MiaPaca2 cells) displayed a short-term burst in the oxygen consumption rate (OCR), indicative of superoxide radical formation after mitochondrial inhibition with rotenone and oligomycin (**Fig. 4.2C**), consistent with an NQO1-dependent mechanism of O_2 utilization and ROS formation in the cytoplasm where NQO1 is located intracellularly. This is consistent with prior data from our lab showing the cytoplasmic localization of NQO1 and subsequent initial ROS formation inside the cell (Tagliarino et al. 2003, Tagliarino et al. 2001). Addition of the noncompetitive NQO1 inhibitor, dicoumarol (DIC), abolished ROS formation and the OCR spike in MiaPaca2 cells in response to 4 μM ß-lap (**Figs. 4.2B,C**). Quantification of 8-Oxo-G formation demonstrated dose- and NQO1-dependency (**Fig. 4.2D**), mirroring relative ROS levels (**Fig. 4.2B**). We then silenced expression of the 8-Oxo-G repair enzyme, OGG1 DNA N-glycosylase, using specific siRNAs and confirming knockdown via Western blotting in MiaPaca2 and ASPC1 PDA cells (**insets, Figs. 4.2E,F**). Since OGG1 detects and cleaves 8-Oxo-G moieties from the DNA backbone to generate APE1- or AP lyase-susceptible AP-sites that, in turn, are detected, and

bound, by PARP1 (Prasad et al. 2014), we wanted to determine if OGG1 loss reduced ß-lap-induced PARP1 hyperactivity, NAD+/ATP loss and lethality; Total intracellular ATP levels were measured 2 h after ß-lap treatment as a proxy for PARP1 hyperactivity, and the PARP1 inhibitor, Rucaparib, was used to prevent PARP1 activity (Gartner, Burger, and Lorusso 2010). Indeed, depletion of OGG1 significantly rescued severe PARP1 hyperactivation-mediated ATP loss in ß-lap-exposed MiaPaca2 or ASPC1 PDA cells (**Fig. 4.2E**). Consistently, clonogenic survival assays also revealed that OGG1 depletion rescued cells from ß-lap-induced cytotoxicity at doses consistent with the ATP depletion data (**SF1A**).

XRCC1 depletion enhances the efficacy of ß-Lap by increasing DNA damage and repressing metabolic recovery.

To further elucidate the role of BER in ß-lap-induced lethality, we stably knocked down the critical BER scaffolding protein, X-ray cross complementing 1 (XRCC1) protein in MiaPaca2 cells. XRCC1 acts as an integral node to mediate BER complex signaling at the site ofa DNA lesion, typically an AP site or SSB (El-Khamisy et al. 2003). We generated several stable shXRCC1 clones varying in XRCC1 expression (shXRCC1#1-8) (**inset, Fig. 4.3A**). When MiaPaca2 clones were ranked by relative XRCC1 expression (using actin for normalization), stable loss of relative XRCC1 expression strongly correlated with hypersensitivity to ß-lap relative to non-targeted control cells (**Fig. 4.3A**). XRCC1-depleted cells did not display altered baseline growth characteristics compared to parental or shRNA-NS control cells. Utilizing stable shXRCC1 clone #8, whose levels were depleted >90% by Western blotting (**inset, Fig. 4.3A**), we showed significant hypersensitivity to ß-lap in a

dose-dependent manner (**Fig. 4.3B**). Interestingly, loss of XRCC1 dramatically increased DSB formation as measured by gH2AX foci after ~15 min of exposure to ß-lap. DSBs were formed in a dose-dependent manner compared to similarly treated stable shScr MiaPaca2 cells (**Fig. 4.3C**). Furthermore, stable XRCC1 depletion dramatically sensitized cells to ß-lap-induced NAD^+ and ATP losses (**Figs. 4.3D, SF2A**), where losses of intracellular NAD^+ and ATP pools were surrogates for PARP1 hyperactivation (Li et al. 2011, Moore et al. 2015). These data strongly suggested that loss of XRCC1 promoted ß-lap-induced PARP1 hyperactivation, consistent with known kinetics and interactions of XRCC1 and PARP1 at DNA lesion sites, where XRCC1 aids in the disassociation of PARP1 from damaged sites and attenuates further PARylation allowing other BER factors access for DNA repair (SF6) (Campalans et al. 2013, El-Khamisy et al. 2003). Interestingly, loss of XRCC1 decreased metabolic recovery after PARP1 hyperactivation during ß-lap treatment, as indicated by significant decreased ATP recovery over a 4 h period and decreased lactate accumulation (an indicator of glycolytic activity) over a 6 h period after a 2 h treatment with ß-lap (**Figs. 4.3E,F**). These data suggest that initial NAD+ depletion via hyperactivated PARP1 led to intracellular metabolic catastrophe from which cells were unable to recover.

While there are currently no known XRCC1 inhibitors we wondered whether XRCC1 expression was decreased in PDA tissue compared to associated normal pancreatic tissue in patient samples, as this would provide a strategy to exploit a specific cancer vulnerability and further increase the tumor selectivity of ß-lap in PDA tissue through the mechanism described above. We compared XRCC1 mRNA expression levels in matched PDA tissue

and associated normal pancreatic tissue isolated from 45 PDA patients (Zhang et al. 2012) and discovered that XRCC1 expression was significantly elevated in PDA tissue relative to associated normal pancreatic tissue. These data suggested that PDA may demonstrate a robust BER response to ß-lap exposures compared to associated normal tissue (SF2B). While the significance of XRCC1 elevations in PDAs are not known, we reasoned that pharmacological inhibition of BER in PDA, instead of segregating PDA patients based on XRCC1 expression, would be the most practical strategy to enhance the tumor specificity and efficacy of ß-lap.

The AP site modification factor, Methoxyamine (MeOX), sensitizes cancer cells to ß-lap in an NQO1-dependent manner

MeOX covalently binds to aldehydes exposed within AP sites and the subsequent modified MeOX-AP site prevents access of BER complexes to the damage (Yan et al. 2007, Guerreiro et al. 2013, Montaldi and Sakamoto-Hojo 2013, Fishel et al. 2007, Liu and Gerson 2004). Increased levels and prolonged half-lives of AP sites result. However, it is not known how these sites are repaired or whether these sites would promote or prevent PARP1 binding. MiaPaca-2 and genetically matched SUIT2-NQO1-deficient and SUIT2-NQO1-proficient metastatic pancreatic cancer cells were treated with various doses of ß-lap (μM. 2 h), ± 12 mM MeOX, and with or without dicoumarol (DIC) for 2 h (**Figs. 4.4A,B**). Cells were washed and assessed for survival by colony forming ability assays (Li et al. 2011). The combination treatment of MeOX + ß-lap led to significant synergistic lethality compared to ß-lap alone, but only in NQO1-expressing cells (**Fig. 4.4B**). The lethality of ß-lap alone (not

shown) or the combination of MeOX + ß-lap were rescued by inhibiting NQO1 using DIC (Figs. 4A,B). MeOX alone (12 mM, 2 h) did not affect cell viability, plating efficiency or overall survival (Fig. 4A). A sublethal dose of ß-lap (2.5 μM, 2 h) in combination with a nontoxic dose of MeOX (12 mM) led to a dramatic increase in %TUNEL+ cells compared to lethal doses of ß-lap alone (4 μM, 2 h) or H_2O_2 (1 mM, 30 mins). The synergistic effect was NQO1-dependent, since DIC addition completely blocked lethality of ß-lap alone, or the combination of ß-lap + MeOX (**Fig. 4.4C**). To confirm that MeOX was hitting its target within the cell, we monitored AP site formation using a reactive aldehyde probe that competes with MeOX for AP site aldehyde binding. In this assay, modified MeOX-AP sites are not detected by the probe. Indeed, MeOX co-treatment blocked detection of AP-sites by the probe generated from ß-lap treatment in NQO1+ MiaPaca2 cells, consistent with the published function of MeOX, (**Fig. 4.4D**) (Montaldi and Sakamoto-Hojo 2013, Liu and Gerson 2004, Liu, Nakatsuru, and Gerson 2002). In contrast, exposure to ß-lap alone generated over 5-fold increases in AP sites within a 90 min period (**Fig. 4.4D**).

We then examined a broad range of NQO1-expressing vs genetically matched NQO1-deficient cancer cell lines for survival following treatment with ß-lap ± 12 mM MeOX (**Fig. 4.4, Table 4.1**) Complete dose-response analyses revealed a consistent LD_{50} dose enhancement ratio (DER) of $\geq$1.67 when NQO1+ breast, non-small cell lung, or head and neck cancer cell lines cells were exposed to an LD_{50} of ß-lap (ranging from 1.8-3.0 μM. 2 h, depending on cell line) in combination with MeOX (12 mM, 2 h); DER values were calculated as the LD50 ratio of cells exposed to ß-lap alone divided by cells treated with ß-

lap + MeOX (**Fig. 4.4, Table 4.1**). For each cell line, lethality caused by ß-lap alone or in combination with MeOX was prevented by dicoumarol addition (not shown). In contrast, genetically matched NQO1-deficient cells remain nonresponsive to either ß-lap alone or ß-lap + MeOx and DER value calculations were not applicable (NA) (**Fig. 4.4, Table 4.1**).

Methoxyamine potentiates ß-lap-induced PARP1-hyperactivation and downstream DSB formation

Using gH2AX as a proxy for DSB formation, we found that treatment with the combination of a sublethal dose of ß-lap (2.5 μM, 2 h) + a nontoxic MeOX dose (12 mM) significantly increased gH2AX formation at 15 and 30 min compared to ß-lap (2.5 μM, 2 h) or MeOX (12 mM, 2 h) alone exposures (**Fig. 4.5A**). At 30 min, the combination was more efficient at inducing DSBs than either a lethal dose of ß-lap (4 μM, 2 h) or a supralethal dose of H_2O_2 (1 mM, 15 min) alone. Using 53BP1 foci as an additional marker for DSB formation, we noted that DSB repair was severely impaired in cells exposed to ß-lap (2.5 μM) + MeOX (12 mM) for 2 h *versus* a sublethal dose of ß-lap (2.5 μM) alone, which caused significant damage after 2 h of treatment, but DSB repair occurred to basal levels within 9 h. It is significant that the combination of a sublethal ß-lap dose + nontoxic dose of MeOX caused DSB formation equivalent to a lethal dose of ß-lap (4 μM, 2 h), and that both treatments caused DSBs that were not repairable over a 24-h time-course (**Fig. 4.5B**). In contrast, although cells treated with a sublethal dose of ß-lap (2.5 μM) or a nontoxic MeOX dose (12 mM, 2 h) alone exhibited significant DSBs, these exposed cells were able to resolve their DSBs within 3 h post-treatment (**Fig 4.5B**). Since it was possible that MeOX addition could enhance ROS

formation from the ß-lap-induced futile redox cycle, thereby explaining the synergistic effects noted, ROS levels were measured in cells using the CellROX dye. These analyses revealed that there was no significant difference in ROS formation in cells exposed to ß-lap alone *vs* ROS levels formed in ß-lap + MeOX-treated MiaPaca2 cells (**SF3**).

We previously reported that ß-lap-induced lethality was driven by the dramatic loss of NAD^+ pools as a consequence PARP1 hyperactivation in a broad range of NQO1-expressing cancer cell lines (Bey et al. 2007, Moore et al. 2015). To determine the effect of MeOX on ß-lap-induced DNA threshold levels for PARP1 hyperactivation, we assessed changes in relative NAD^+ and ATP pools after various doses of ß-lap (μM, 2 h), in the presence or absence of an otherwise nontoxic dose of MeOX (12 mM, 2 h). MeOX addition dramatically decreased NAD^+/ATP pools in MiaPaca2 cells in a dose-dependent manner up to 2 μM ß-lap and within 2 h co-treatment compared to ß-lap alone (**Figs. 4.5C and SF4A**). Assessment of PAR polymer formation after 20 min of treatment with various doses of ß-lap ± MeOX revealed that PAR formation increased at significantly lower doses of ß-lap when MeOX was added compared to ß-lap exposure alone (**Fig. 4.5C**). Importantly, addition of a PARP1 inhibitor (e.g., Rucaparib) significantly blocked PAR formation after either ß-lap alone or the combination therapy (**Fig. 4.5D**). These data strongly suggest that the addition of MeOX lowered the threshold of DNA damage created by ß-lap for PARP1 hyperactivation (**Figs. 4.5D and SF4E**). Importantly, metabolic recovery in the form of ATP pool increases after damage was blunted after co-treatment with ß-lap + MeOX versus ß-lap alone (**SF4B,C**). Since endoplasmic reticulum released calcium ($Ca+2^{ER}$) is required for PARP1

hyperactivation after ß-lap treatment (Bentle et al. 2006, Tagliarino et al. 2001, Moore et al. 2015), we noted significant sparing of ß-lap-induced lethality after addition of BAPTA-AM, which chelates intracellular Ca^{2+ER}. Colony formation assays showed that pre-loading cells with BAPTA-AM (5 μM, 2 h) rescued cells from ß-lap-induced lethality, with or without MeOX co-treatment (**Fig. 4.5E**). Consistent with a role of PARP1 hyperactivation in ß-lap-induced NAD+ loss (**Fig. 4.5C**), addition of the PARP1 inhibitor, Rucaparib, also significantly attenuated suppression of glucose utilization in ß-lap-treated MiaPaca2 cells, regardless of MeOX addition (**Fig 4.5F**). Indeed, Rucaparib addition restored glucose utilization to all ß-lap-treated cells (SF4E). Note that the combination of a sublethal ß-lap dose (2.5 μM, 2 h) + a nontoxic dose of MeOX (12 mM, 2 h) was far superior than ß-lap alone in suppressing glucose utilization in MiaPaca2 cells (**Fig. 4.5F**). MeOX alone treatments had no effect on glucose utilization compared to untreated cells (not shown). Overall, these data strongly suggest that chemical modulation of AP-sites by MeOX increases the ability of PARP1 to exhaust NAD+ pools in NQO1+ cancer cell after ß-lap treatment. Once NAD^+ levels are exhausted, and enzyme-inactive PAR-PARP1 is formed, BER cannot function properly to repair SSBs induced by ß-lap. While PARP1 protects ß-lap-induced AP sites and SSBs early after exposure, once PARP1 activity is exhausted through NAD+ loss and PAR-PARP1 PARylation, the resulting SSBs are converted to DSBs in a delayed, but efficient manner. Indeed, delayed yH2AX and 53BP1 DSB foci induction normally seen with sublethal doses of ß-lap (2.5 μM, 2 h) alone appeared more rapidly in MiaPaca2 cells exposed to ß-lap + MeOX (**Fig. 4.5A**) and the DSBs created were not repaired.

MeOX + ß-lap provides synergistic antitumor activity against human pancreatic cancer xenografts *in vivo*

To determine if BER inhibition by MeOX would result in increased antitumor sensitization and tumor regression *in vivo*, we generated subcutaneous xenografts in female Nu/Nu-athymic mice and treated these animals with one regimen of the drugs. This model was chosen since optimal ß-lap treatment regimenare typically minimally efficacious against subcutaneous xenografts at doses that are significantly lower than the MTD of 40 mg/kg HPßCD-ß-lap, i.v. alone (Cao et al. 2014). Once MiaPaca2 xenografts were ~100 mm^3, animals were treated every other day for 10 days with a total of five injections of: (a) sub-efficacious HPßCD-ß-lap (intravenous (i.v.) 25 mg/kg); (b) intraperitoneal (i.p.) doses of MeOX (150 mg/kg); (c) a combination of ß-lap + MeOX at these doses and routes of administration; or (d) vehicle (HPßCD) alone as described (Li et al. 2011). Mice were sacrificed when tumor volumes reached 1,000 mm^3. The combination treatment (MeOX + ß-lap) significantly delayed tumor growth relative to either treatment alone, but caused no significant decrease in mouse weights over time when compared to other treatment conditions (**Figs. 4.6A,B and SF5A**). Importantly, there was no significant increase in dose-limiting methemaglobinemia in the combination, which is the key toxicity noted in ARQ761 preclinically and clinically (D. Gerber et al. 2014). During and well after treatment (up to day 12), we noted significant tumor regression in 5 of 8 mice following MeOX + ß-lap, where regression was not noted after any of the other treatments (**Figs. 4.6A,B**). Note that none of the other treatments (ß-lap or MeOX alone) caused significant antitumor responses alone

(**Figs. 4.6A,B**). For target validation, tumors were harvested 30 min after the treatment conditions above and analyzed for PAR-PARP1 (PAR) and yH2AX formation as pharmacodynamic (PD) markers of efficacy as described previously (Li et al. 2011, Dong et al. 2010, Huang et al. 2013) (**Fig. 4.6C**). Consistent with our results *in vitro*, PAR formation increased ~150-fold after exposure to the combination of a sub-efficacious dose of HPßCD-ß-lap + MeOX compared to vehicle alone, and two-fold above HPßCD-ß-lap alone. Importantly, DSB formation (monitored by gH2AX levels) were dramatically elevated (>10-fold) in tumors from mice receiving MeOX + HPßCD-ß-lap (**Figs. 4.6C, SF5B**) compared to HPßCD-ß-lap alone.

Combined treatment of sub-efficacious doses of HPßCD-ß-lap + MeOX significantly prolonged the survival of tumor-bearing mice (**Fig. 4.6D**). Mice were sacrificed when body weight dropped by one third of their original values due to tumor-associated cachexia, and when tumor volume exceeded 1000 mm^3, or when tumors were ulcerated or impeded normal motion as per IACUC policies. Treatment with sub-efficacious doses of HPßCD-ß-lap (25 mg/kg) or MeOX (150 mg/kg) alone resulted in no significant difference in overall survival compared to vehicle (HPßCD) alone groups, with a median survival of ~47 days (**Fig. 4.6D**). In contrast, the combined HPßCD-ß-lap + MeOX treatment group had a median survival time of 75 days, which was 35 days longer than the median survival of vehicle (HPßCD) alone, or MeOX (150 mM) alone or HPßCD-ß-lap (25 mg/kg) alone. Taken together, our observations indicate that use of a nontoxic dose of MeOX in combination with a sub-efficacious dose of ß-lap (HPßCD-ß-lap) in NQO1-expressing tumors results in increased PARP1

hyperactivation, significantly elevated DSB formation, tumor growth delay and regression is some animals, and extended survival compared to agents alone. Indeed, ~37% (3 of 8) of MiaPaca2-bearing xenograft mice exposed to HPßCD-ß-lap + MeOX exhibited apparent cures of their tumors (**Fig. 4.6D**).

4.3 Discussion

There is a desperate need for new efficacious therapeutic strategies to treat recalcitrant PDAs. The standard-of-care for PDA consists of a series of DNA damaging agents (e.g., gemcitabine, Nab-paclitaxel) that lack tumor selectivity, have narrow therapeutic windows, and quickly become ineffective due to intrinsic or acquired drug resistance (Maginn et al. 2014). The NQO1/catalase ratios demonstrated in Fig. 4.1 revealed a dramatic potential therapeutic window that can be exploited by NQO1 bioactivatable drugs, such as ARQ761 (ß-lapachone), currently in clinical trials (NCT01502800). The high NQO1/Catalase ratios in pancreatic cancers strongly suggest that NQO1-overexpressing PDA cancer cells will respond to NQO1 bioactivatable drugs by producing extremely elevated levels of ROS and supra-lethal doses of H_2O_2. Reasons for elevated levels of NQO1 remain unknown. Numerous reports suggest that NQO1 elevation is a by-product of Nrf2 overexpression in cancer cells due to increased oxidative stress and inflammation and that NQO1 suppresses ROS formation and promotes tumor progression by activating NF-κB signaling through p53 inhibition (Thapa et al. 2014, Choi et al. 2007, Lyn-Cook et al. 2006, Ahn et al. 2006). Lowered catalase expression may indicate elevated 8-oxo-G levels, which promotes genomic instability.

Concomitant low expression of Catalase should make PDA tumors selectively sensitive to NQO1 bioactivatable drugs, with a lack of significant resistance mechanisms. Even if particular PDA tumors express significant Catalase levels, the NQO1-mediated futile redox cycle that generates H_2O_2 can easily swamp endogenous Catalase activities (Cao et al. 2014, Bey et al. 2013a). In contrast, the low NQO1 expression and elevated catalase levels in most normal tissue, particularly in associated normal pancreas and liver, offer significant protection from NQO1 bioactivatable drugs, as noted in ß-lap treatment mice (Fig. 4.6). However, current NQO1 bioactivatable drugs cause significant NQO1-independent, dose-limiting methemaglobinemia in red blood cells that somewhat restricts use of specific regimen, limiting efficacy (Blanco et al. 2010, D. Gerber et al. 2014). Strategies, such as using specific DNA repair inhibitors, to lower the efficacious doses of NQO1 bioactivatable drugs, thereby significantly reducing risk of methemaglobinemia, are needed. Data presented here offer 'proof of principle' in achieving superior efficacy of NQO1 bioactivatable drugs against recalcitrant NQO1-overexpressing PDA, as well as most other solid cancers.

DNA repair inhibitors have been under development for over 40 years, and all developed drugs commonly lack tumor-selectivity, even when combined with focused ionizing radiation (IR) therapy. DNA damaging agents that specifically target selectively chosen cancers are desperately needed. Our data strongly suggest that NQO1 bioactivatable drugs enable tumor-selective use of DNA repair inhibitors, such as MeOX. We demonstrated that combination therapy with sublethal doses of ß-lap and a nontoxic dose of MeOX synergistically enhanced

cytotoxicity in PDA, NSCLC, breast and head/neck cancers (Fig. 4.4 and Table 4.1). The observed synergy was NQO1-dependent as NQO1-deficient cell lines, or addition of dicoumarol (DIC), to NQO1-expressing cell lines spared cells from ß-lap-induced lethality, including the synergistic lethality brought about by exposing cells to MeOX + ß-lap. Mechanistically, the observed synergistic response with ß-lap + MeOX was driven by enhanced ß-lap-induced PARP1 hyperactivation due to the prolongation of AP sites modified by MeOX (Fig. 4.5). These findings strongly suggest that modification of AP-sites by MeOX increases the ability of PARP1 to exhaust NAD^+ pools after ß-lap treatment. Once NAD^+ levels are exhausted, PARP1 cannot function properly to repair SSBs induced by ß-lap, resulting in their rapid conversion to DSBs, as indicated by the dramatic increase in gH2AX and 53BP1 foci formation. Ongoing studies are proceeding in our lab to understand whether PARP1 binds with high avidity to MeOX-modified versus unmodified AP sites, and what other cofactors (e.g., released intracellular Ca^{+2}_{ER}) are needed mechanistically for PARP1 hyperactivation.

The combination treatment developed here using ß-lap + MeOX addresses issues associated with both agents alone, most importantly offering broad tumor type-selectivity to MeOX and eliminating dose-limiting methemaglobinemia caused by higher ß-lap doses otherwise required for efficacy. The antitumor efficacy data presented offer ‘proof of principle’ that the combination enhances efficacy at well-tolerated doses of ß-lap and at completely nontoxic doses of MeOX. Furthermore, the ß-lap + MeOX doses used in our animal studies are relevant to those achievable in patients (Savage et al. 2008, P. Caimi 2014). A major

advantage of ß-lap + MeOX-induced NAD^+-Keresis is the lack of resistance mechanisms available to cancers to overcome this combination therapy. Metabolically depleting cancer cells of NAD^+/ATP results in the irreversible loss of glycolytic (Moore et al. 2015) and Kreb's cycle function (*unpublished data*). This treatment strategy will be pursued in further preclinical studies to optimize potential clinical utility, and to further elucidate the pathways and mechanisms of NAD^+-Keresis (Moore et al. 2015).

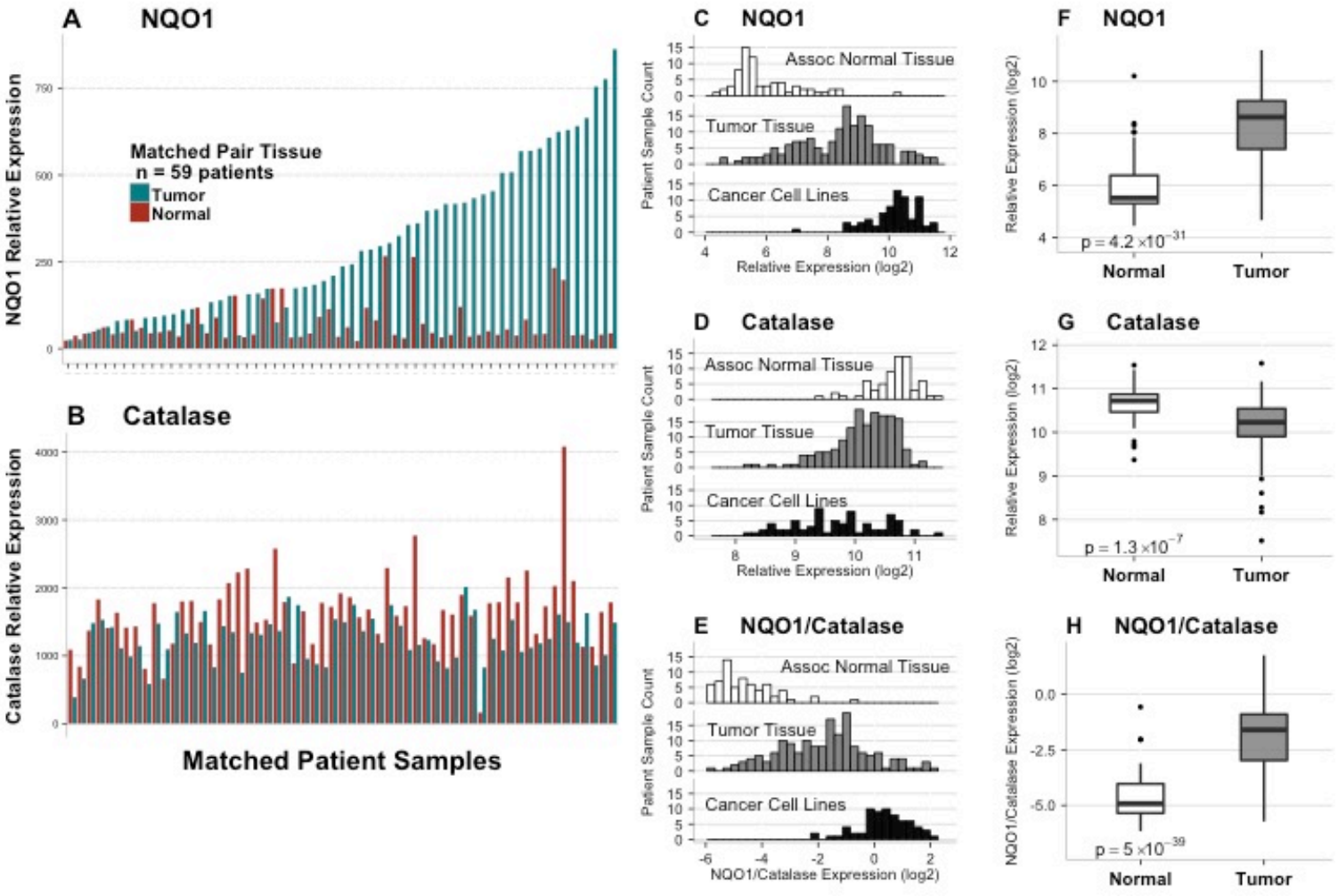

Figure 4.1. **NQO1:Catalase ratios are elevated in PDA tumor vs normal pancreatic tissue. (A,B)** NQO1 and Catalase log2 mRNA expression in matched PDA tumor *versus* normal pancreatic tissue from 59 patient samples. **(C-H)** NQO1, catalase and NQO1:Catalase ratio expression evaluated in 462 PDA tumor versus normal pancreatic tissue. NQO1 levels in a cohort of 22 PDA cancer cell lines are also shown for comparison to primary PDA tumors. Note that NQO1 levels are much higher in PDA cancer cell lines compared to primary PDA tumors.

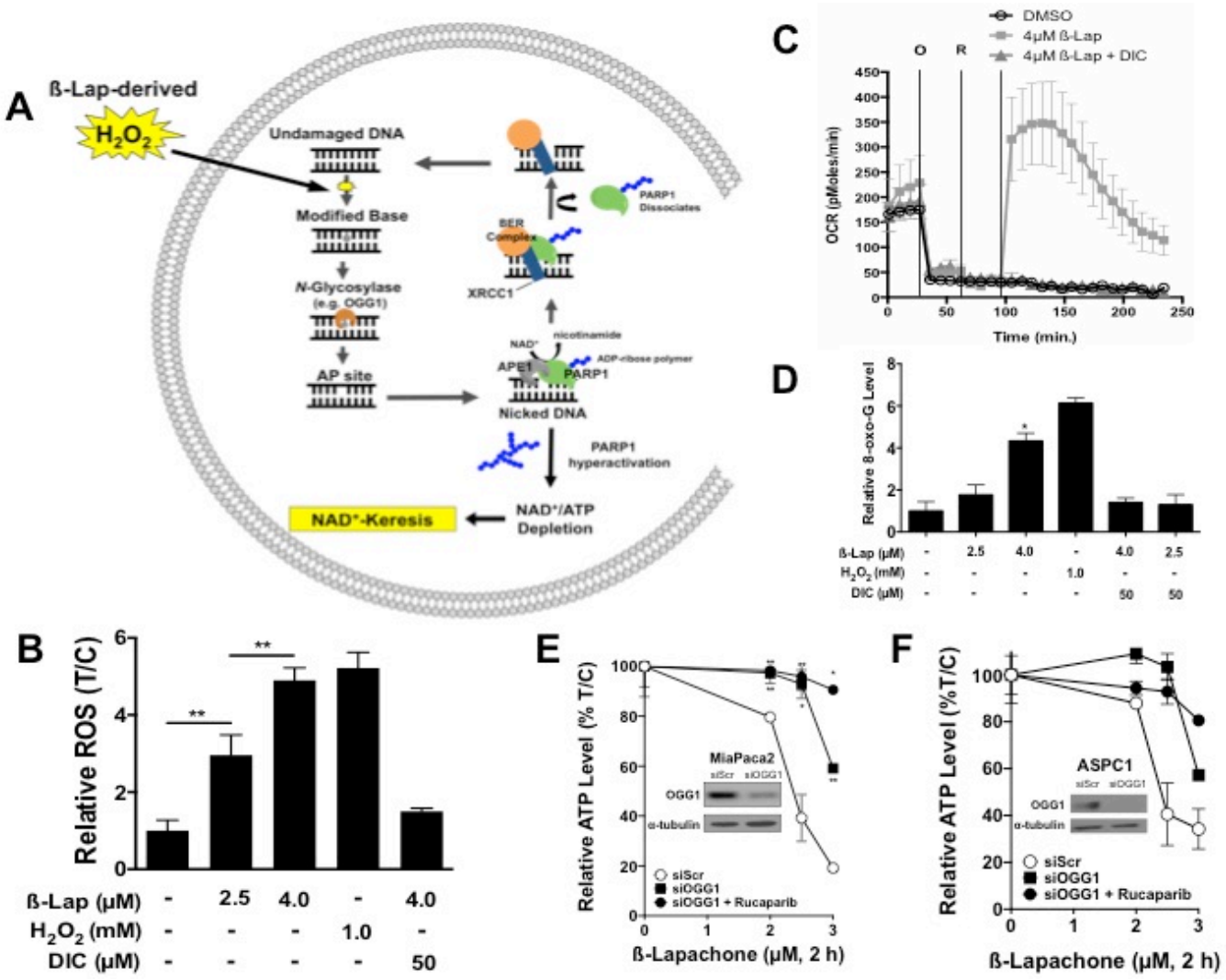

Figure 4.2. **OGG1 modulates cellular responses to ß-lap-induced DNA damage, PARP1 hyperactivation and lethality. (A)** ß-Lap-induced lethality is predicted to be caused by DNA base (8-oxo-G) and SSB formation, detection of base damage by N-glycosylases (e.g., 8-oxo-G by OGG1), and subsequent AP site detection and hyperactivation of PARP1, which results in dramatic NAD+ loss, metabolic catastrophe and a form of programmed necrotic cell death referred to as NAD+-Keresis. **(B)** ROS levels, resulting from NQO1-dependent futile redox cycling of ß-lap, were

monitored in MiaPaca2 cells after 30 min of treatment using CellRox-Glo. Values were normalized to DMSO-treated control cells. **(C)** Oxygen consumption rates (OCR) in MiaPaca2 cells treated with ß-lap ± DIC after mitochondrial inhibition with oligomycin (O) and rotenone (R). Data suggests that OCR and ROS are a distinct result of NQO1 activity. **(D)** 8-oxo-G levels were monitored after 30 min of ß-lap treatment using immunofluorescence in MiaPaca2 cells across various doses of ß-lap, normalized to DMSO-treated control cells. **(E,F)** OGG1 levels were depleted in 48 h by specific siRNA in MiaPaca2 or ASPC1 cells. Cells were then treated with ß-lap ± Rucaparib (25 μM) for 2 h and ATP levels monitored using CellTiter-Glo assays. Results were compared using Student's t-tests (+/- standard deviations). *$p<0.05$; **$p<0.01$; ***$p<0.001$.

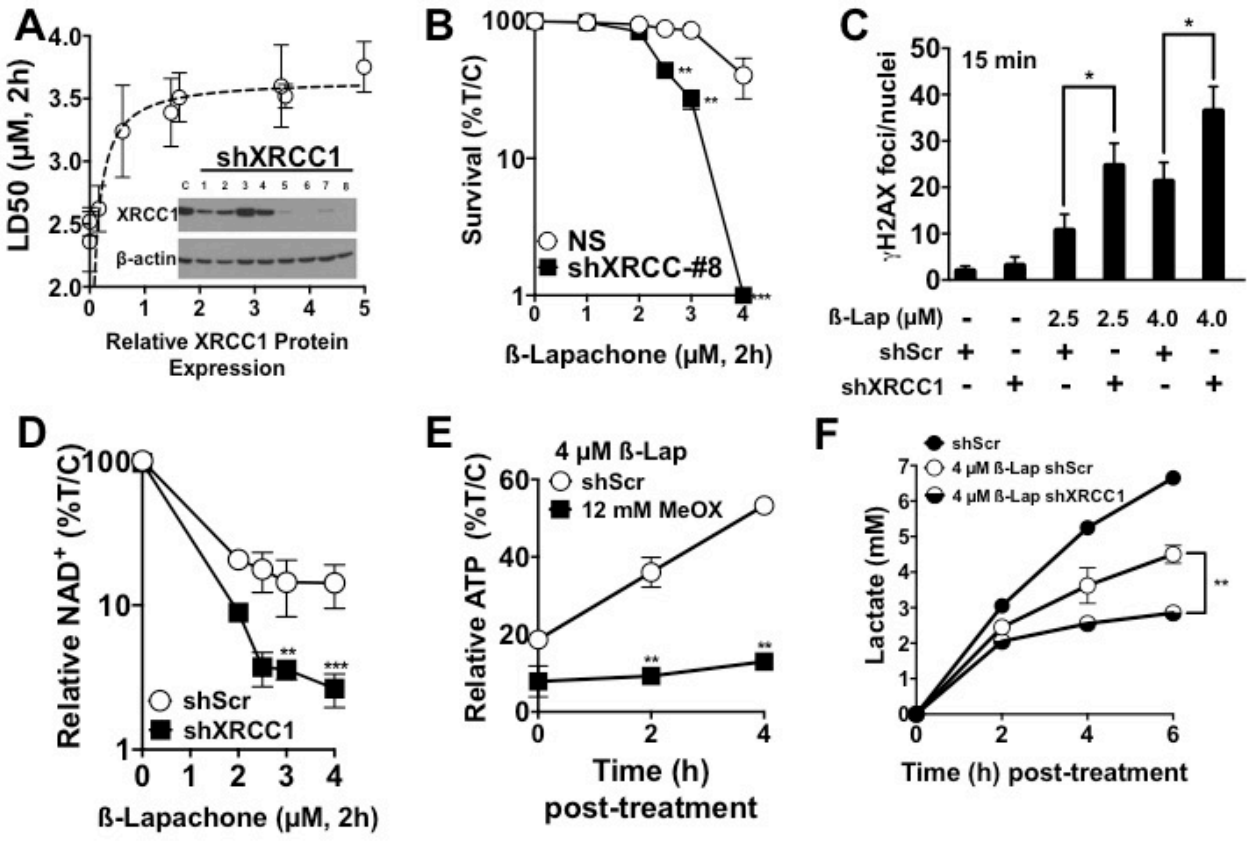

Figure 4.3. XRCC1 depletion enhances efficacy of ß-lap by increasing DNA damage and repressing metabolic recovery. (A) Stable shXRCC1 knockdown MiaPaca2 clones were generated as assessed by Western immunoblotting (inset). Clonogenic survival assays were used to determine LD_{50} values for each ß-lap-treated MiaPaca2-non-targeting (NS) or shXRCC1 clones in separate dose-response studies. Plating efficiencies were not altered by XRCC1 depletion. **(B)** ß-Lap dose-response of clone #8 assessed by clonogenic survival assays. **(C)** DSB formation (Average gH2AX foci/nuclei) in MiaPaca2 cells after sublethal (2.5 μM) or lethal (4.0 μM) ß-lap doses in stable shXRCC1 versus shScr MiaPaca2 cells. **(D)** Relative intracellular NAD^+ levels in stable shScr or

shXRCC1 knockdown MiaPaca2 cells after exposure with various doses of ß-lap (μM, 2h). **(E)** Cellular recovery (over a 4 h time-period) of ATP levels assessed in ß-lap-treated (4 μM, 2 h) stable shScr *versus* shXRCC1 knockdown MiaPaca2 cells monitored by CellTiter-Glo assays. **(F)** Lactate production normalized to cell number in media of ß-lap-treated (4 μM, 2 h) stable shScr or shXRCC1 knockdown MiaPaca2 cells over a 6 h period. All indicated results were compared with Student's t-test (+/- standard deviation). *$p<0.05$; **$p<0.01$; ***$p<0.001$.

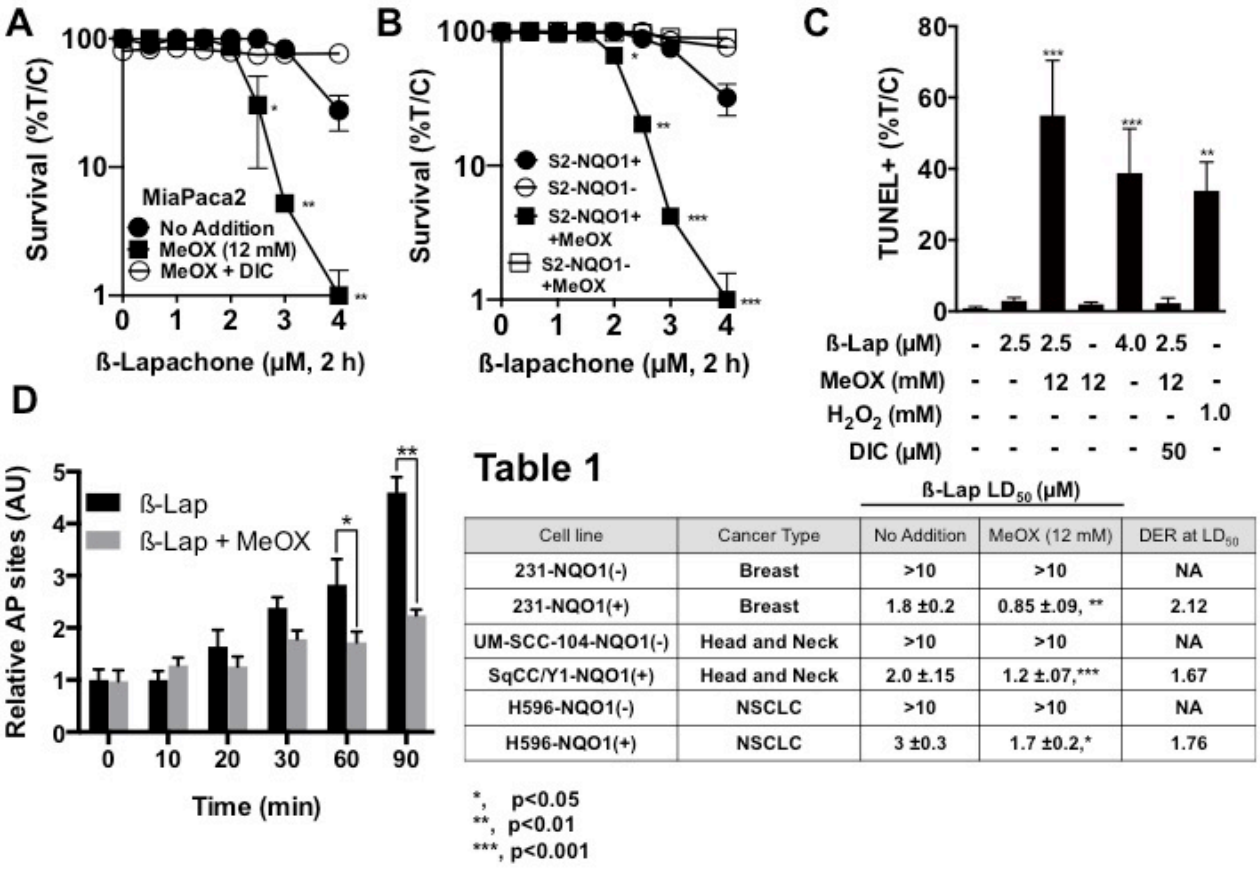

Table 1

		ß-Lap LD_{50} (µM)		
Cell line	Cancer Type	No Addition	MeOX (12 mM)	DER at LD_{50}
231-NQO1(-)	Breast	>10	>10	NA
231-NQO1(+)	Breast	1.8 ±0.2	0.85 ±.09, **	2.12
UM-SCC-104-NQO1(-)	Head and Neck	>10	>10	NA
SqCC/Y1-NQO1(+)	Head and Neck	2.0 ±.15	1.2 ±.07,***	1.67
H596-NQO1(-)	NSCLC	>10	>10	NA
H596-NQO1(+)	NSCLC	3 ±0.3	1.7 ±0.2,*	1.76

*, p<0.05
**, p<0.01
***, p<0.001

Figure 4.4. **The AP site modification factor, Methoxyamine (MeOX), sensitizes cancer cells to ß-lap in an NQO1-dependent manner. (A,B)** Clonogenic survival of MiaPaca2 or SUIT2-013-NQO1(+) *versus* SUIT2-013-NQO1(-) cells treated with ß-lap, ± 12 mM MeOX, and with or without 50 µM DIC for 2 h. Data represent survival means ± SE from sextuplicate samples. **(C)** Quantification of TUNEL+ MiaPaca2 cells after ß-lap ± 12 mM MeOX, with or without 50 µM DIC after 2 h. **(D)** AP sites monitored in MiaPaca2 cells exposed as in 'C' using a reactive aldehyde probe over time. Note that MeOX-modification of AP sites hides AP site measurements using the reactive aldehyde probe. **Table 1. MeOX enhances the lethality of ß-lap in a broad range of NQO1+ versus NQO1- cells.** Genetically matched NQO1-overexpressing (NQO1+) *versus* NQO1-

deficient (NQO1-) cancer cells were screened for sensitivity to ß-lap alone, MeOX alone or the ß-lap + MeOX combination. All results were compared using Student's t-tests (+/- SD). *$p<0.05$; **$p<0.01$; ***$p<0.001$.

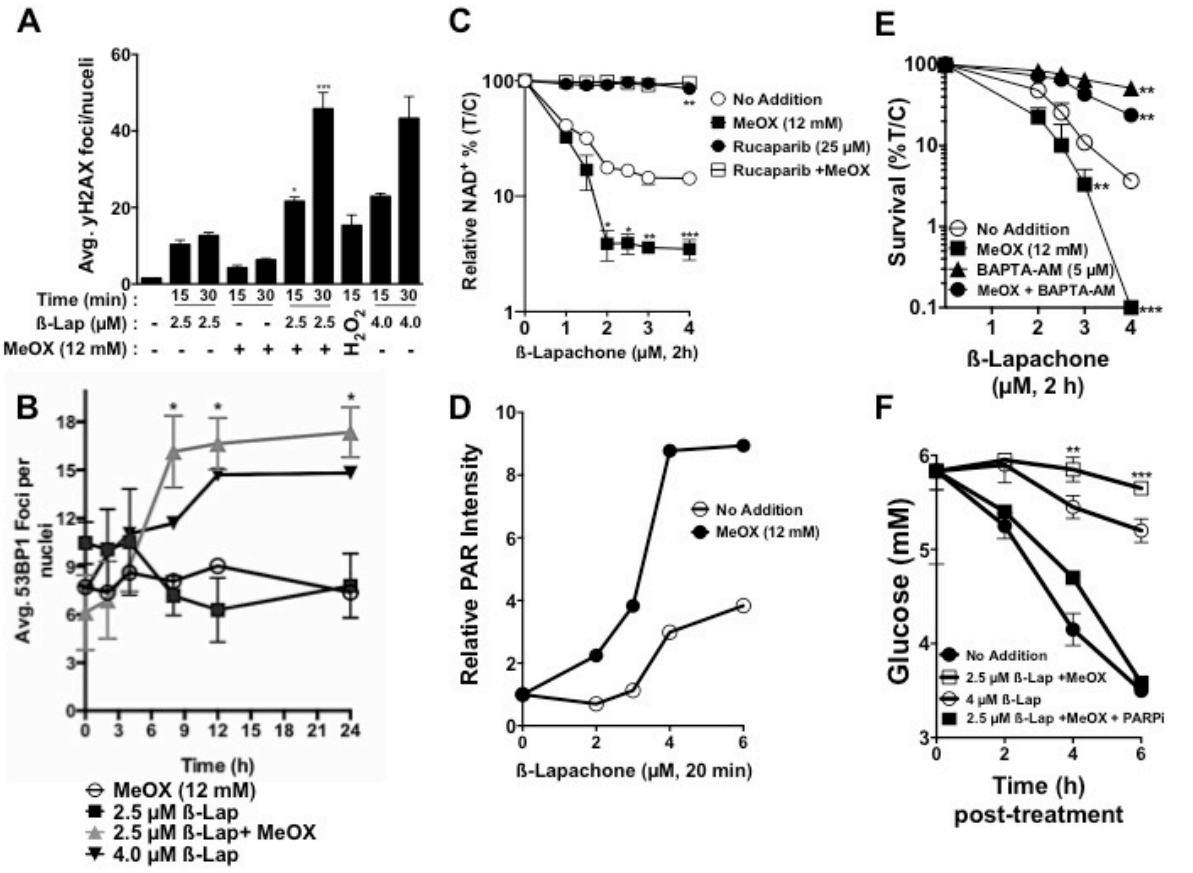

Figure 4.5. **MeOX sensitizes cells to ß-lap by potentiating DNA damage and PARP1 hyperactivation. (A)** MeOX enhances DSB formation in ß-lap-treated cells. Average gH2AX foci/nuclei were assessed in ß-lap-treated (μM, 2 h) MiaPaca2 cells, ± MeOX (12 mM) at 15 and 30 min during exposure. H_2O_2 (0.5 mM, 15 min) was used as a positive control. **(B)** Average 53BP1 foci/nuclei in ß-lap-treated (μM, 2 h) MiaPaca2 cells, ± 12 mM MeOX over time (h). Graph represents average foci of three separate experiments. **(C)** Relative NAD^+ levels in MiaPaca2 cells 2 h after treatment with ß-lap, ± 12 mM MeOX, and with or without Rucaparib (15 μM) in sextuplicate, means ± SEM. **(D)** Western blot quantification of relative PAR-PARP1 formation (using a-tubulin for loading) in MiaPaca2 cells 20 min after exposure to various doses of ß-lap ± 12

mM MeOX, with or without 50 μM dicoumarol (DIC). **(E)** Clonogenic survival of MiaPaca2 cells pre-treated with 5 μM BAPTA-AM (Ca^{2+} chelator) for 30 min followed by treatment with ß-lap (μM, 2 h), ± 12 mM MeOX. Data represent survival means ±SEM from quadruplicate samples. **(F)** Glucose consumption assessments from media of MiaPaca2 cells treated with Rucaparib (25 μM) for 2 h prior to 2 h exposure to ß-lap ± 12 mM MeOX. Data represent means ±SEM from triplicate samples. All results were compared using Student's t-tests (+/- standard deviation) unless otherwise stated. **p<0.05; **p<0.01; ***p<0.001.*

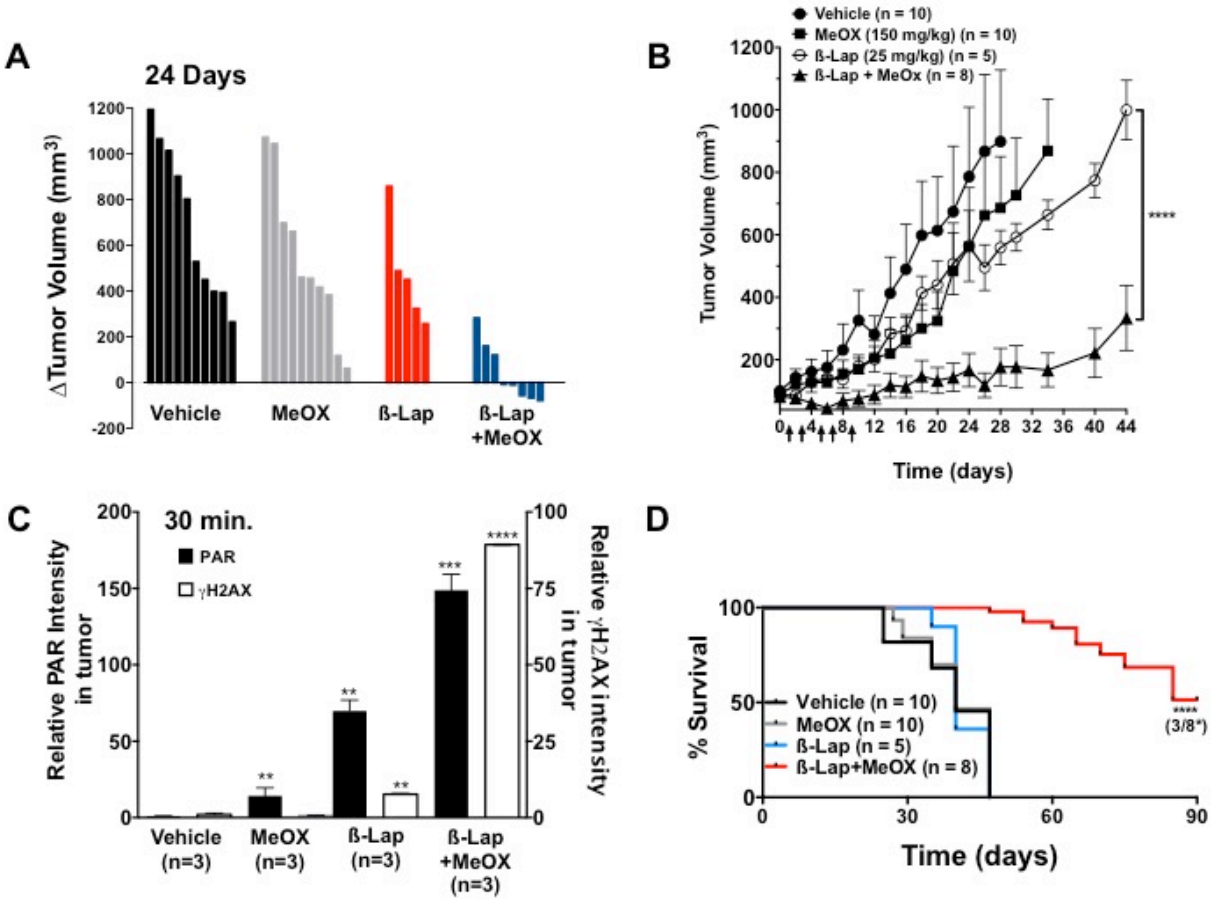

Figure 4.6. MeOX enhances the lethality of ß-lap against subcutaneous human pancreatic xenografts to ß-lap *in vivo*. (A,B) Subcutaneous xenograft tumors grown from MiaPaca2 cells in athymic nude mice were grown to 100 mm^3, after which mice were treated every other day with vehicle alone (HPßCD, n = 10), a nontoxic dose of MeOX (IP, 150 mg/kg in saline, n= 10), a sub-efficacious dose of ß-lap (IV, 25 mg/kg, n= 5) or a nontoxic dose of MeOX + ß-lap (IV, 25 mg/kg, n = 8) for a total of 5 doses over ten days (arrows). Tumor volumes were monitored by direct caliper measurements as described in 'Materials and Methods'. Note regression of tumors in three mice from the MeOX + ß-lap combination therapy. (**A**). Tumor growth was monitored until tumors reached 1,000 mm^3, where necrotic tissue, restricted movement and weight loss warranted sacrifice.

Error bars: means, ± SEM (**B**). **(C)** Immunoblot quantification of relative PAR and yH2AX levels (with respect to a-tubulin loading) from tumors harvested 30 min after treatment with HPßCD vehicle alone, ß-lap alone, MeOX alone or ß-lap + MeOX at doses indicated in '**B**'; n = tumors from 3 mice per group; Error bars: means, + SEM. **(E)** Kaplan-Meier survival plot of tumor–bearing mice treated with conditions described in A-C. Mice were sacrificed when tumors reached 1,000 mm^3 as per IACUC-approved animal protocol.

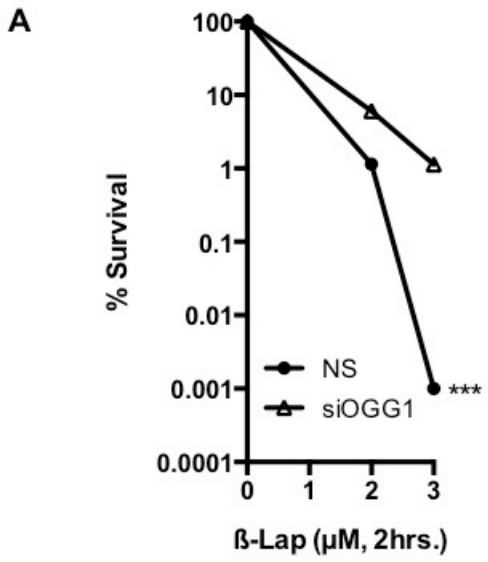

Figure SF4.1. **(A)** OGG1 depletion makes MiaPaca2 cells partially resistant to ß-lap-induced cytotoxicity.

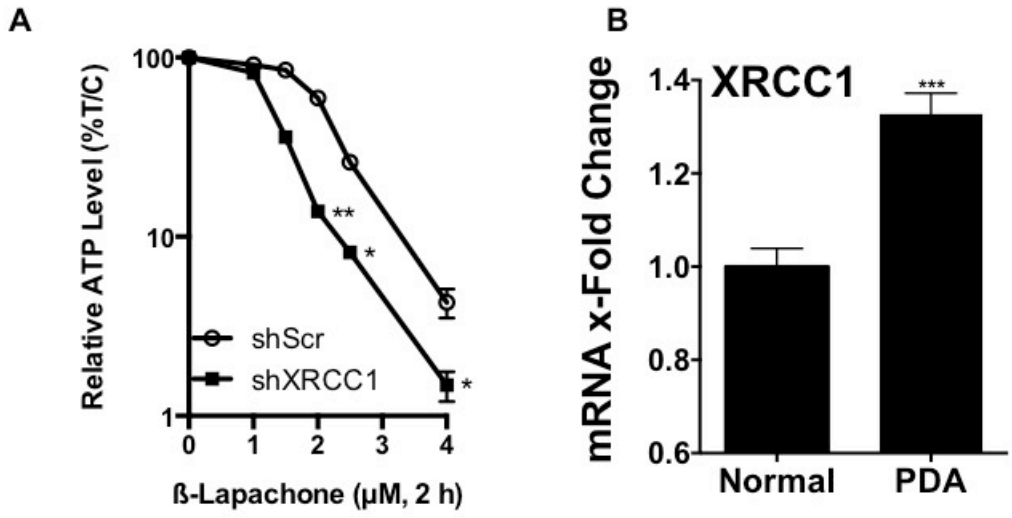

Figure SF4.2. **(A)** Relative intracellular ATP levels in stable shScr *versus* shXRCC1 MiaPaca2 cells treated with various doses of ß-lap for 2 h. **(B)** Relative XRCC1 mRNA expression in normal vs matched PDA tissue from 45 pancreatic cancer patients (GSE28735).

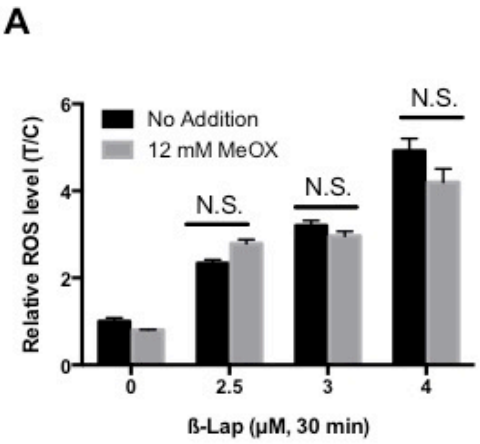

Figure SF4.3. **(A)** Relative ROS levels in MiaPca2 with ß-lap ± 12 mM MeOX cells determined by CellROX dye during 30 min. Data were from experiments performed in sextuplicate. Show are means, ± SEM.

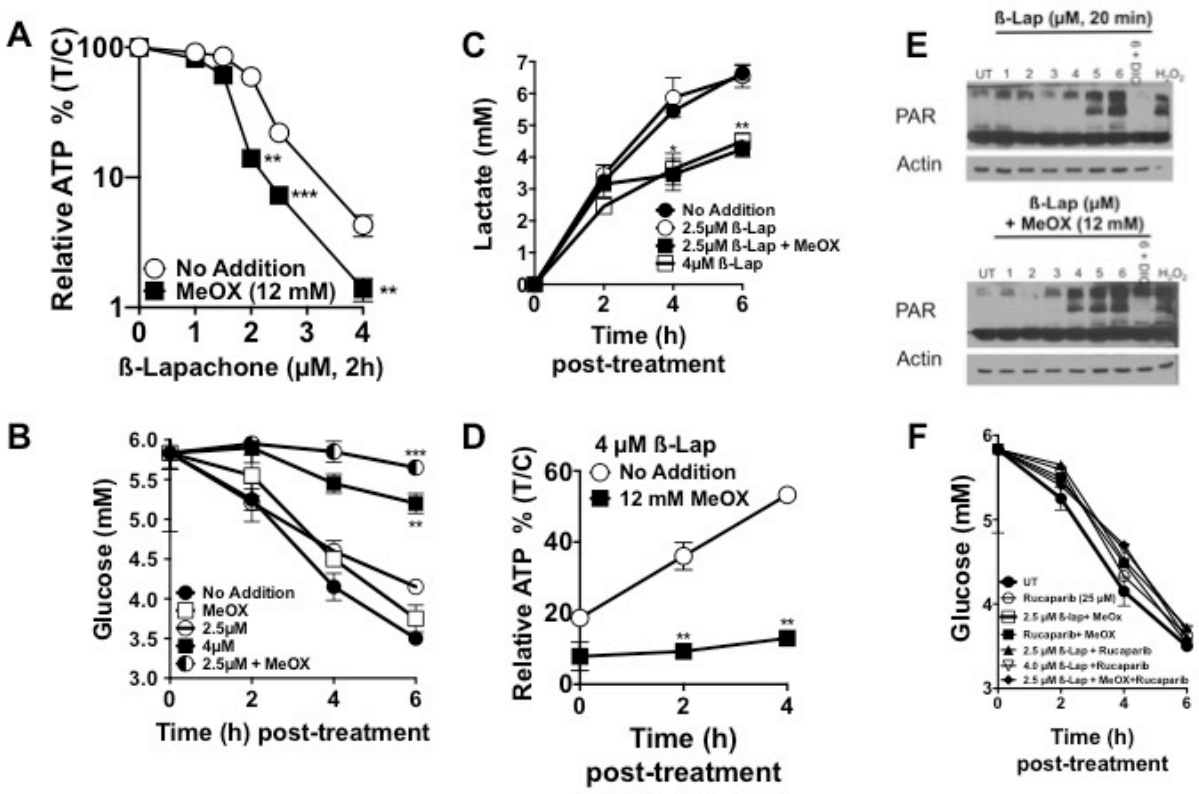

Figure SF4.4. **(A)** Relative intracellular ATP levels in MiaPaca2 cells after treatment with various doses of ß-lap (µM), ± 12 mM MeOX for 2 h. **(B,C)** Time-course of glucose consumption and lactate production over a 6 h period in media of MiaPaca2 cells after a 2 h treatment with ß-lap, ± 12 mM MeOX. **(D)** Relative ATP recovery assessed over a 4 h time period by CellTiter-Glo assay measured in MiaPaca2 cells after 2 h treatment with ß-lap, ± 12 mM MeOX. **(E)** Immunoblot image of relative PAR-PARP1 formation in MiaPaca2 cells after 20 min after treatment with various doses of ß-lap, ± 12 mM MeOX.

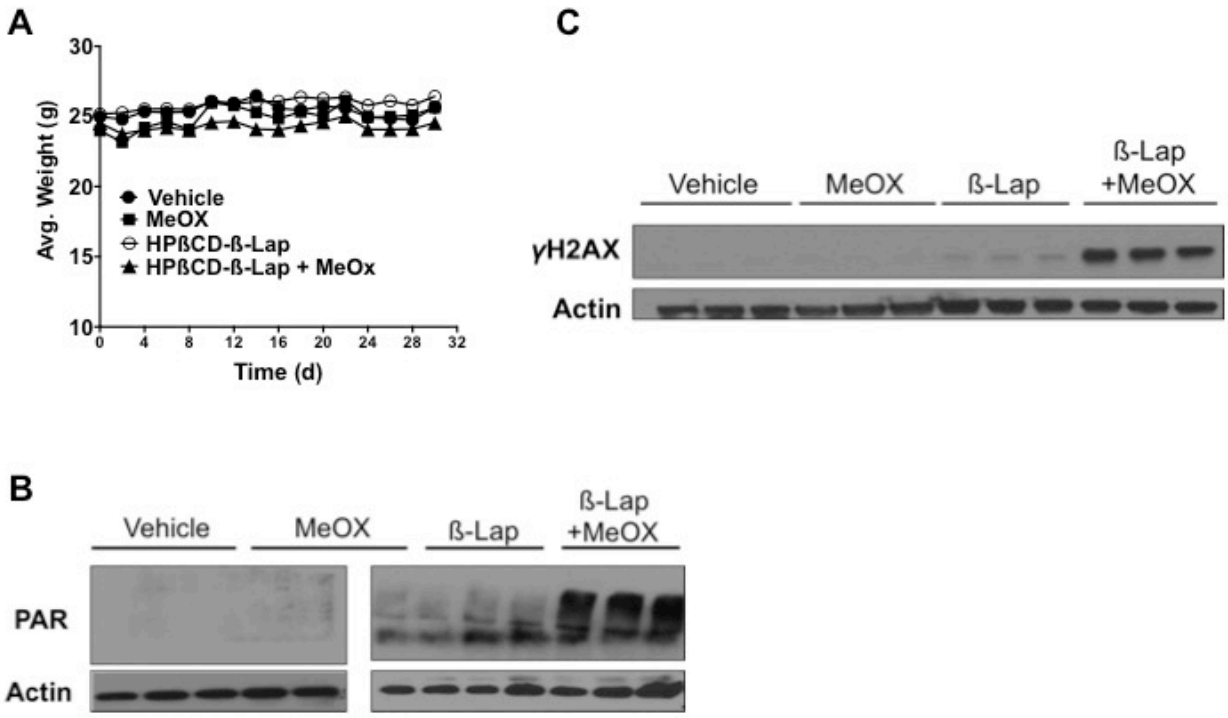

Figure SF4.5. **(A)** Mouse weights during treatment with ß-lap (IV, 25 mg/kg), MeOX (IP, 150 mg/kg) or vehicle treatment. **(B,C)** Immunoblot image of relative PAR-PARP1 and gH2AX formation in tumor tissue from animals treated as indicated.

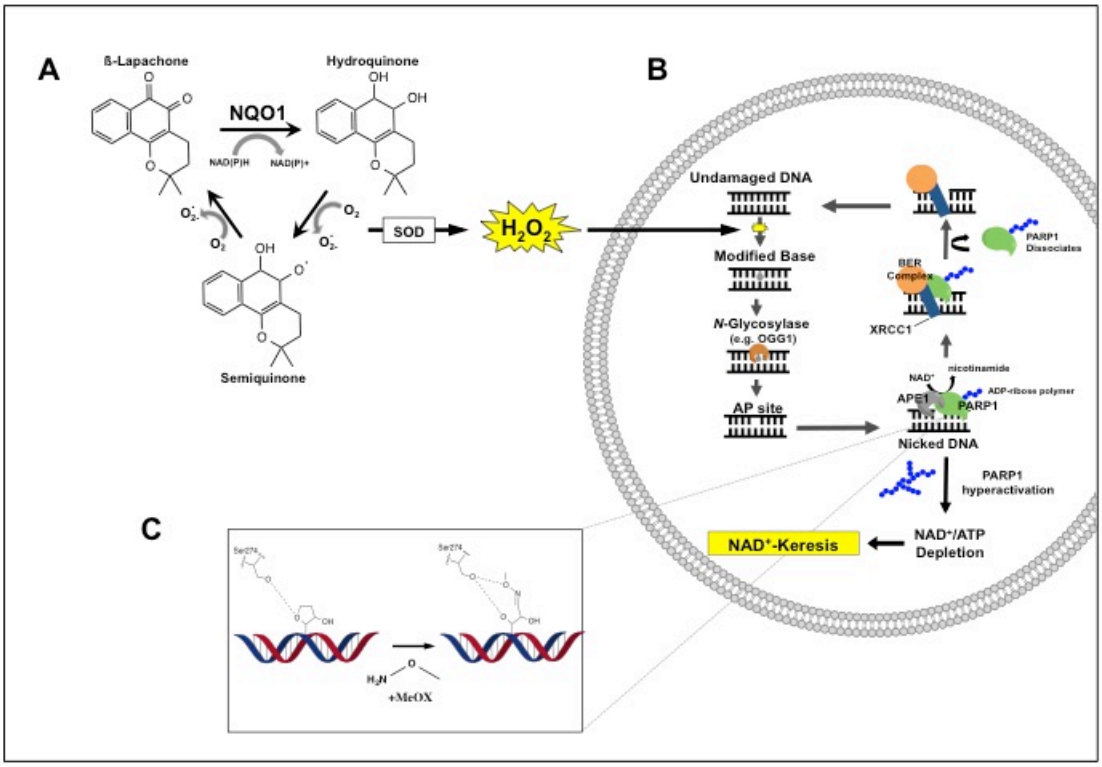

Figure SF4.6. **(A)** NQO1-dependent futile redox cycling of ß-lap demonstrating production of superoxide radical with NAD(P)H used as an electron donor. **(B)** Model of BER after oxidative DNA damage. **(C)** Interaction of MeOX with an AP site in DNA.

CHAPTER FIVE
Conclusions and Future Work

5.1 Conclusions

In summary, we found that the ROS generating agent ß-lap synergizes with two dramatically different therapeutic strategies, GLS1 inhibition (CB-839 and BPTES) and BER inhibition (MeOX), in pancreatic cancer through distinct mechanisms of action to induce PARP1 hyperactivation-dependent NAD^+ depletion. Importantly, the combinations did not affect associated NQO1-deficient, normal pancreas or liver, demonstrating that this synergism is selective for PDA. Inhibiting GLS1 genetically or pharmacologically in PDA resulted in tumors with decreased intracellular antioxidant defenses specifically in KRAS mutated cancer cells due to PDA's reliance on glutamine-dependent transamination reactions for cytoplasmic NADPH biogenesis and redox balance. Mechanistically, glutamine metabolism inhibition left cells hypersensitive to the ROS burst derived from ß-lap-induced NQO1-dependent futile redox cycling. Next, we demonstrated that ß-lap induced extensive oxidative DNA base damage that required the BER machinery for repair. Using the AP-site modifier MeOX in combination with ß-lap led to a lower threshold of PARP1 hyperactivation and NAD^+ depletion. Mechanistically, we believe that this may be due to increased affinity of PARP1 to MeOX-bound-AP sites, however further studies are needed to completely define the mechanism.

To further study biological pathways that attenuate ß-lap cytotoxicity in an unbiased manner, a genome wide RNAi screen in combination with ß-lap is warranted in NQO1 expressing cancer cells and NQO1 deficient normal cells. A gene will not be considered a potential "hit" if knockdown leads to cell death without ß-lap treatment or sensitizes normal, NQO1 deficient cells to off-target effects of ß-lap. Based on data from my dissertation, this screen would have "built-in" positive control genes such as GLS1, GOT1, GOT2, ME1 and XRCC1 that when knocked down sensitize cancer cells to ß-lap. This genetic screen will give mechanistic insight into pathways that attenuate ß-lap efficacy. Once a list of validated genes and their associated pathways are identified, a subsequent low-through put screen can be conducted with pharmacological agents that have been described to target these pathways. Once a series of compounds are proved to synergize *in vitro*, *in vivo* xenograft studies should immediately commence to determine the pharmacokinetic and pharmacodynamics profile of the novel combination. To increase the translational applicability of the secondary compound screen, the list of agents can be limited to drugs that are in late stage clinical trials or are already FDA approved. Overall, understanding the mechanism involved in these combinations will advance scientific knowledge of how the action of NQO1 bioactivatable drugs could be augmented in PDA and NSCLC models. Moreover, this information could be used for the development of effective clinical trials combining NQO1 bioactivatable drugs with other anticancer agents.

BIBLIOGRAPHY

2013. Cancer Facts & Figures.

Adjei, A. A. 2004. "Pemetrexed (ALIMTA), a novel multitargeted antineoplastic agent." *Clin Cancer Res* 10 (12 Pt 2):4276s-4280s. doi: 10.1158/1078-0432.CCR-040010.

Ahn, K. S., G. Sethi, A. K. Jain, A. K. Jaiswal, and B. B. Aggarwal. 2006. "Genetic deletion of NAD(P)H:quinone oxidoreductase 1 abrogates activation of nuclear factor-kappaB, IkappaBalpha kinase, c-Jun N-terminal kinase, Akt, p38, and p44/42 mitogen-activated protein kinases and potentiates apoptosis." *J Biol Chem* 281 (29):19798-808. doi: 10.1074/jbc.M601162200.

Almeida, K. H., and R. W. Sobol. 2007. "A unified view of base excision repair: lesion-dependent protein complexes regulated by post-translational modification." *DNA Repair (Amst)* 6 (6):695-711. doi: 10.1016/j.dnarep.2007.01.009.

Anastasiou, D., G. Poulogiannis, J. M. Asara, M. B. Boxer, J. K. Jiang, M. Shen, G. Bellinger, A. T. Sasaki, J. W. Locasale, D. S. Auld, C. J. Thomas, M. G. Vander Heiden, and L. C. Cantley. 2011. "Inhibition of pyruvate kinase M2 by reactive oxygen species contributes to cellular antioxidant responses." *Science* 334 (6060):1278-83. doi: 10.1126/science.1211485.

Anastasiou, D., Y. Yu, W. J. Israelsen, J. K. Jiang, M. B. Boxer, B. S. Hong, W. Tempel, S. Dimov, M. Shen, A. Jha, H. Yang, K. R. Mattaini, C. M. Metallo, B. P. Fiske, K. D. Courtney, S. Malstrom, T. M. Khan, C. Kung, A. P. Skoumbourdis, H. Veith, N. Southall, M. J. Walsh, K. R. Brimacombe, W. Leister, S. Y. Lunt, Z. R. Johnson, K. E. Yen, K. Kunii, S. M. Davidson, H. R. Christofk, C. P. Austin, J. Inglese, M. H. Harris, J. M. Asara, G. Stephanopoulos, F. G. Salituro, S. Jin, L. Dang, D. S. Auld, H. W. Park, L. C. Cantley, C. J. Thomas, and M. G. Vander Heiden. 2012. "Pyruvate kinase M2 activators promote tetramer formation and suppress tumorigenesis." *Nat Chem Biol* 8 (10):839-47. doi: 10.1038/nchembio.1060.

Atai, N. A., N. A. Renkema-Mills, J. Bosman, N. Schmidt, D. Rijkeboer, W. Tigchelaar, K. S. Bosch, D. Troost, A. Jonker, F. E. Bleeker, H. Miletic, R. Bjerkvig, P. C. De Witt Hamer, and C. J. Van Noorden. 2011. "Differential activity of NADPH-producing dehydrogenases renders rodents unsuitable models to study IDH1R132 mutation effects in human glioblastoma." *J Histochem Cytochem* 59 (5):489-503. doi: 10.1369/0022155411400606.

Awadallah, N. S., D. Dehn, R. J. Shah, S. Russell Nash, Y. K. Chen, D. Ross, J. S. Bentz, and K. R. Shroyer. 2008. "NQO1 expression in pancreatic cancer and its potential use as a biomarker." *Appl Immunohistochem Mol Morphol* 16 (1):24-31. doi: 10.1097/PAI.0b013e31802e91d0.

Baggetto, L. G. 1992. "Deviant energetic metabolism of glycolytic cancer cells." *Biochimie* 74 (11):959-74.

Balendiran, G. K., R. Dabur, and D. Fraser. 2004. "The role of glutathione in cancer." *Cell Biochem Funct* 22 (6):343-52. doi: 10.1002/cbf.1149.

Balss, J., J. Meyer, W. Mueller, A. Korshunov, C. Hartmann, and A. von Deimling. 2008. "Analysis of the IDH1 codon 132 mutation in brain tumors." *Acta Neuropathol* 116 (6):597-602. doi: 10.1007/s00401-008-0455-2.

Behrend, L., G. Henderson, and R. M. Zwacka. 2003. "Reactive oxygen species in oncogenic transformation." *Biochem Soc Trans* 31 (Pt 6):1441-4. doi: 10.1042/.

Belfi, C. A., S. Chatterjee, D. M. Gosky, S. J. Berger, and N. A. Berger. 1999. "Increased sensitivity of human colon cancer cells to DNA cross-linking agents after GRP78 up-regulation." *Biochem Biophys Res Commun* 257 (2):361-8. doi: 10.1006/bbrc.1999.0472.

Bensaad, K., A. Tsuruta, M. A. Selak, M. N. Vidal, K. Nakano, R. Bartrons, E. Gottlieb, and K. H. Vousden. 2006. "TIGAR, a p53-inducible regulator of glycolysis and apoptosis." *Cell* 126 (1):107-20. doi: 10.1016/j.cell.2006.05.036.

Bentle, M. S., K. E. Reinicke, E. A. Bey, D. R. Spitz, and D. A. Boothman. 2006. "Calcium-dependent modulation of poly(ADP-ribose) polymerase-1 alters cellular metabolism and DNA repair." *J Biol Chem* 281 (44):33684-96. doi: 10.1074/jbc.M603678200.

Bentle, M. S., K. E. Reinicke, Y. Dong, E. A. Bey, and D. A. Boothman. 2007. "Nonhomologous end joining is essential for cellular resistance to the novel antitumor agent, beta-lapachone." *Cancer Res* 67 (14):6936-45. doi: 10.1158/0008-5472.CAN-07-0935.

Bey, E. A., M. S. Bentle, K. E. Reinicke, Y. Dong, C. R. Yang, L. Girard, J. D. Minna, W. G. Bornmann, J. Gao, and D. A. Boothman. 2007. "An NQO1- and PARP-1-mediated cell death pathway induced in non-small-cell lung cancer cells by beta-lapachone." *Proc Natl Acad Sci U S A* 104 (28):11832-7. doi: 10.1073/pnas.0702176104.

Bey, E. A., K. E. Reinicke, M. C. Srougi, M. Varnes, V. E. Anderson, J. J. Pink, L. S. Li, M. Patel, L. Cao, Z. Moore, A. Rommel, M. Boatman, C. Lewis, D. M. Euhus, W. G. Bornmann, D. J. Buchsbaum, D. R. Spitz, J. Gao, and D. A. Boothman. 2013a. "Catalase abrogates beta-lapachone-induced PARP1 hyperactivation-directed programmed necrosis in NQO1-positive breast cancers." *Mol Cancer Ther* 12 (10):2110-20. doi: 10.1158/1535-7163.MCT-12-0962.

Bey, E. A., K. E. Reinicke, M. C. Srougi, M. Varnes, V. Anderson, J. J. Pink, L. S. Li, M. Patel, L. Cao, Z. Moore, A. Rommel, M. Boatman, C. Lewis, D. M. Euhus, W. G. Bornmann, D. J. Buchsbaum, D. R. Spitz, J. Gao, and D. A. Boothman. 2013b. "Catalase abrogates beta-lapachone-induced PARP1 hyperactivation-directed programmed necrosis in NQO1-positive breast cancers." *Mol Cancer Ther* In Press. doi: 10.1158/1535-7163.MCT-12-0962.

Bi, T. Q., X. M. Che, X. H. Liao, D. J. Zhang, H. L. Long, H. J. Li, and W. Zhao. 2011. "Overexpression of Nampt in gastric cancer and chemopotentiating effects of the Nampt inhibitor FK866 in combination with fluorouracil." *Oncol Rep* 26 (5):1251-7. doi: 10.3892/or.2011.1378.

Blanco, E., E. A. Bey, C. Khemtong, S. G. Yang, J. Setti-Guthi, H. Chen, C. W. Kessinger, K. A. Carnevale, W. G. Bornmann, D. A. Boothman, and J. Gao. 2010.

"Beta-lapachone micellar nanotherapeutics for non-small cell lung cancer therapy." *Cancer Res* 70 (10):3896-904. doi: 0008-5472.CAN-09-3995 [pii]
10.1158/0008-5472.CAN-09-3995.

Bleeker, F. E., N. A. Atai, S. Lamba, A. Jonker, D. Rijkeboer, K. S. Bosch, W. Tigchelaar, D. Troost, W. P. Vandertop, A. Bardelli, and C. J. Van Noorden. 2010. "The prognostic IDH1(R132) mutation is associated with reduced NADP+-dependent IDH activity in glioblastoma." *Acta Neuropathol* 119 (4):487-94. doi: 10.1007/s00401-010-0645-6.

Boiteux, S., and M. Guillet. 2004. "Abasic sites in DNA: repair and biological consequences in Saccharomyces cerevisiae." *DNA Repair (Amst)* 3 (1):1-12.

Boothman, D. A., S. Greer, and A. B. Pardee. 1987. "Potentiation of halogenated pyrimidine radiosensitizers in human carcinoma cells by beta-lapachone (3,4-dihydro-2,2-dimethyl-2H-naphtho[1,2-b]pyran- 5,6-dione), a novel DNA repair inhibitor." *Cancer Res* 47 (20):5361-6.

Boothman, D. A., D. K. Trask, and A. B. Pardee. 1989. "Inhibition of potentially lethal DNA damage repair in human tumor cells by beta-lapachone, an activator of topoisomerase I." *Cancer Res* 49 (3):605-12.

Brunelli, L., E. Caiola, M. Marabese, M. Broggini, and R. Pastorelli. 2014. "Capturing the metabolomic diversity of KRAS mutants in non-small-cell lung cancer cells." *Oncotarget* 5 (13):4722-31.

Bruner, S. D., D. P. Norman, and G. L. Verdine. 2000. "Structural basis for recognition and repair of the endogenous mutagen 8-oxoguanine in DNA." *Nature* 403 (6772):859-66. doi: 10.1038/35002510.

Bryant, K. L., J. D. Mancias, A. C. Kimmelman, and C. J. Der. 2014. "KRAS: feeding pancreatic cancer proliferation." *Trends Biochem Sci* 39 (2):91-100. doi: 10.1016/j.tibs.2013.12.004.

Campalans, A., T. Kortulewski, R. Amouroux, H. Menoni, W. Vermeulen, and J. P. Radicella. 2013. "Distinct spatiotemporal patterns and PARP dependence of XRCC1 recruitment to single-strand break and base excision repair." *Nucleic Acids Res* 41 (5):3115-29. doi: 10.1093/nar/gkt025.

Cao, H., D. Le, and L. X. Yang. 2013. "Current status in chemotherapy for advanced pancreatic adenocarcinoma." *Anticancer Res* 33 (5):1785-91.

Cao, L., L. S. Li, C. Spruell, L. Xiao, G. Chakrabarti, E. A. Bey, K. E. Reinicke, M. C. Srougi, Z. Moore, Y. Dong, P. Vo, W. Kabbani, C. R. Yang, X. Wang, F. Fattah, J. C. Morales, E. A. Motea, W. G. Bornmann, J. S. Yordy, and D. A. Boothman. 2014. "Tumor-selective, futile redox cycle-induced bystander effects elicited by NQO1 bioactivatable radiosensitizing drugs in triple-negative breast cancers." *Antioxid Redox Signal* 21 (2):237-50. doi: 10.1089/ars.2013.5462.

Cerna, D., H. Li, S. Flaherty, N. Takebe, C. N. Coleman, and S. S. Yoo. 2012. "Inhibition of nicotinamide phosphoribosyltransferase (NAMPT) activity by small molecule GMX1778 regulates reactive oxygen species (ROS)-mediated cytotoxicity in a p53- and nicotinic acid phosphoribosyltransferase1 (NAPRT1)-dependent manner." *J Biol Chem* 287 (26):22408-17. doi: 10.1074/jbc.M112.357301.

Cerwenka, H., R. Aigner, H. Bacher, G. Werkgartner, A. el-Shabrawi, F. Quehenberger, and H. J. Mischinger. 1999. "TUM2-PK (pyruvate kinase type tumor M2), CA19-9 and CEA in patients with benign, malignant and metastasizing pancreatic lesions." *Anticancer Res* 19 (1B):849-51.

Cheng, T., J. Sudderth, C. Yang, A. R. Mullen, E. S. Jin, J. M. Mates, and R. J. DeBerardinis. 2011. "Pyruvate carboxylase is required for glutamine-independent growth of tumor cells." *Proc Natl Acad Sci U S A* 108 (21):8674-9. doi: 10.1073/pnas.1016627108.

Cheong, H., C. Lu, T. Lindsten, and C. B. Thompson. 2012. "Therapeutic targets in cancer cell metabolism and autophagy." *Nat Biotechnol* 30 (7):671-8. doi: 10.1038/nbt.2285.

Cheung, E. C., D. Athineos, P. Lee, R. A. Ridgway, W. Lambie, C. Nixon, D. Strathdee, K. Blyth, O. J. Sansom, and K. H. Vousden. 2013. "TIGAR is required for efficient intestinal regeneration and tumorigenesis." *Dev Cell* 25 (5):463-77. doi: 10.1016/j.devcel.2013.05.001.

Chini, C. C., A. M. Guerrico, V. Nin, J. Camacho-Pereira, C. Escande, M. T. Barbosa, and E. N. Chini. 2014. "Targeting of NAD metabolism in pancreatic cancer cells: potential novel therapy for pancreatic tumors." *Clin Cancer Res* 20 (1):120-30. doi: 10.1158/1078-0432.CCR-13-0150.

Choi, E. K., K. Terai, I. M. Ji, Y. H. Kook, K. H. Park, E. T. Oh, R. J. Griffin, B. U. Lim, J. S. Kim, D. S. Lee, D. A. Boothman, M. Loren, C. W. Song, and H. J. Park. 2007. "Upregulation of NAD(P)H:quinone oxidoreductase by radiation potentiates the effect of bioreductive beta-lapachone on cancer cells." *Neoplasia* 9 (8):634-42.

Choo, A. Y., S. G. Kim, M. G. Vander Heiden, S. J. Mahoney, H. Vu, S. O. Yoon, L. C. Cantley, and J. Blenis. 2010. "Glucose addiction of TSC null cells is caused by failed mTORC1-dependent balancing of metabolic demand with supply." *Mol Cell* 38 (4):487-99. doi: 10.1016/j.molcel.2010.05.007.

Collins, M. A., and M. Pasca di Magliano. 2013. "Kras as a key oncogene and therapeutic target in pancreatic cancer." *Front Physiol* 4:407. doi: 10.3389/fphys.2013.00407.

D. Gerber, Y. Arriaga, M.S. Beg, J.E. Dowell, J.H. Schiller,, R. Leff A.E. Frankel, C. Meek, J. Bolluyt, O. Fatunde, R.T. Martinez,, F. Fattah P. Vo, V. Sarode, Y. Zhou, Y. Xie, M. McLeod,, and D.A. Boothman B. Schwartz. 2014. "Phase 1 correlative study of ARQ761, a b-lapachone analogue that promotes NQ01-mediated programmed cancer cell necrosis." *European Journal of Cancer* 50 (6).

DeBerardinis, R. J., J. J. Lum, G. Hatzivassiliou, and C. B. Thompson. 2008. "The biology of cancer: metabolic reprogramming fuels cell growth and proliferation." *Cell Metab* 7 (1):11-20. doi: 10.1016/j.cmet.2007.10.002.

Diehn, M., R. W. Cho, N. A. Lobo, T. Kalisky, M. J. Dorie, A. N. Kulp, D. Qian, J. S. Lam, L. E. Ailles, M. Wong, B. Joshua, M. J. Kaplan, I. Wapnir, F. M. Dirbas, G. Somlo, C. Garberoglio, B. Paz, J. Shen, S. K. Lau, S. R. Quake, J. M. Brown, I. L. Weissman, and M. F. Clarke. 2009. "Association of reactive oxygen species levels and radioresistance in cancer stem cells." *Nature* 458 (7239):780-3. doi: 10.1038/nature07733.

Dong, Y., E. A. Bey, L. S. Li, W. Kabbani, J. Yan, X. J. Xie, J. T. Hsieh, J. Gao, and D. A. Boothman. 2010. "Prostate cancer radiosensitization through poly(ADP-Ribose) polymerase-1 hyperactivation." *Cancer Res* 70 (20):8088-96. doi: 10.1158/0008-5472.CAN-10-1418.

El-Khamisy, S. F., M. Masutani, H. Suzuki, and K. W. Caldecott. 2003. "A requirement for PARP-1 for the assembly or stability of XRCC1 nuclear foci at sites of oxidative DNA damage." *Nucleic Acids Res* 31 (19):5526-33.

Elhammali, A., J. E. Ippolito, L. Collins, J. Crowley, J. Marasa, and D. Piwnica-Worms. 2014. "A high-throughput fluorimetric assay for 2-hydroxyglutarate identifies zaprinast as a glutaminase inhibitor." *Cancer Discov* 4 (7):828-39. doi: 10.1158/2159-8290.CD-13-0572.

Emadi, A., S. A. Jun, T. Tsukamoto, A. T. Fathi, M. D. Minden, and C. V. Dang. 2014. "Inhibition of glutaminase selectively suppresses the growth of primary acute myeloid leukemia cells with IDH mutations." *Exp Hematol* 42 (4):247-51. doi: 10.1016/j.exphem.2013.12.001.

Fan, J., J. Ye, J. J. Kamphorst, T. Shlomi, C. B. Thompson, and J. D. Rabinowitz. 2014. "Quantitative flux analysis reveals folate-dependent NADPH production." *Nature* 510 (7504):298-302. doi: 10.1038/nature13236.

Fedotcheva, N. I., A. P. Sokolov, and M. N. Kondrashova. 2006. "Nonezymatic formation of succinate in mitochondria under oxidative stress." *Free Radic Biol Med* 41 (1):56-64. doi: 10.1016/j.freeradbiomed.2006.02.012.

Fendt, S. M., E. L. Bell, M. A. Keibler, S. M. Davidson, G. J. Wirth, B. Fiske, J. R. Mayers, M. Schwab, G. Bellinger, A. Csibi, A. Patnaik, M. J. Blouin, L. C. Cantley, L. Guarente, J. Blenis, M. N. Pollak, A. F. Olumi, M. G. Vander Heiden, and G. Stephanopoulos. 2013. "Metformin decreases glucose oxidation and increases the dependency of prostate cancer cells on reductive glutamine metabolism." *Cancer Res* 73 (14):4429-38. doi: 10.1158/0008-5472.CAN-13-0080.

Fishel, M. L., Y. He, M. L. Smith, and M. R. Kelley. 2007. "Manipulation of base excision repair to sensitize ovarian cancer cells to alkylating agent temozolomide." *Clin Cancer Res* 13 (1):260-7. doi: 10.1158/1078-0432.CCR-06-1920.

Fisher, G. H., S. L. Wellen, D. Klimstra, J. M. Lenczowski, J. W. Tichelaar, M. J. Lizak, J. A. Whitsett, A. Koretsky, and H. E. Varmus. 2001. "Induction and apoptotic regression of lung adenocarcinomas by regulation of a K-Ras transgene in the presence and absence of tumor suppressor genes." *Genes Dev* 15 (24):3249-62. doi: 10.1101/gad.947701.

Fruehauf, J. P., and F. L. Meyskens, Jr. 2007. "Reactive oxygen species: a breath of life or death?" *Clin Cancer Res* 13 (3):789-94. doi: 10.1158/1078-0432.CCR-06-2082.

Garten, A., S. Petzold, A. Korner, S. Imai, and W. Kiess. 2009. "Nampt: linking NAD biology, metabolism and cancer." *Trends Endocrinol Metab* 20 (3):130-8. doi: 10.1016/j.tem.2008.10.004.

Gartner, E. M., A. M. Burger, and P. M. Lorusso. 2010. "Poly(adp-ribose) polymerase inhibitors: a novel drug class with a promising future." *Cancer J* 16 (2):83-90. doi: 10.1097/PPO.0b013e3181d78223.

Glen, V. L., P. R. Hutson, N. J. Kehrli, D. A. Boothman, and G. Wilding. 1997. "Quantitation of beta-lapachone and 3-hydroxy-beta-lapachone in human plasma samples by reversed-phase high-performance liquid chromatography." *J Chromatogr B Biomed Sci Appl* 692 (1):181-6.

Gorrini, C., I. S. Harris, and T. W. Mak. 2013. "Modulation of oxidative stress as an anticancer strategy." *Nat Rev Drug Discov* 12 (12):931-47. doi: 10.1038/nrd4002.

Gross, M. I., S. D. Demo, J. B. Dennison, L. Chen, T. Chernov-Rogan, B. Goyal, J. R. Janes, G. J. Laidig, E. R. Lewis, J. Li, A. L. Mackinnon, F. Parlati, M. L. Rodriguez, P. J. Shwonek, E. B. Sjogren, T. F. Stanton, T. Wang, J. Yang, F. Zhao, and M. K. Bennett. 2014. "Antitumor activity of the glutaminase inhibitor CB-839 in triple-negative breast cancer." *Mol Cancer Ther* 13 (4):890-901. doi: 10.1158/1535-7163.MCT-13-0870.

Guerreiro, P. S., A. S. Fernandes, J. G. Costa, M. Castro, J. P. Miranda, and N. G. Oliveira. 2013. "Differential effects of methoxyamine on doxorubicin cytotoxicity and genotoxicity in MDA-MB-231 human breast cancer cells." *Mutat Res* 757 (2):140-7. doi: 10.1016/j.mrgentox.2013.08.003.

Gyorffy, B., P. Surowiak, J. Budczies, and A. Lanczky. 2013. "Online survival analysis software to assess the prognostic value of biomarkers using transcriptomic data in non-small-cell lung cancer." *PLoS One* 8 (12):e82241. doi: 10.1371/journal.pone.0082241.

Hanahan, D., and R. A. Weinberg. 2011. "Hallmarks of cancer: the next generation." *Cell* 144 (5):646-74. doi: 10.1016/j.cell.2011.02.013.

Hidalgo, M. 2010. "Pancreatic cancer." *N Engl J Med* 362 (17):1605-17. doi: 10.1056/NEJMra0901557.

Horton, J. K., D. F. Stefanick, N. R. Gassman, J. G. Williams, S. A. Gabel, M. J. Cuneo, R. Prasad, P. S. Kedar, E. F. Derose, E. W. Hou, R. E. London, and S. H. Wilson. 2013. "Preventing oxidation of cellular XRCC1 affects PARP-mediated DNA damage responses." *DNA Repair (Amst)* 12 (9):774-85. doi: 10.1016/j.dnarep.2013.06.004.

Hou, J., J. Aerts, B. den Hamer, W. van Ijcken, M. den Bakker, P. Riegman, C. van der Leest, P. van der Spek, J. A. Foekens, H. C. Hoogsteden, F. Grosveld, and S. Philipsen. 2010. "Gene expression-based classification of non-small cell lung carcinomas and survival prediction." *PLoS One* 5 (4):e10312. doi: 10.1371/journal.pone.0010312.

Huang, X., Y. Dong, E. A. Bey, J. A. Kilgore, J. S. Bair, L. S. Li, M. Patel, E. I. Parkinson, Y. Wang, N. S. Williams, J. Gao, P. J. Hergenrother, and D. A. Boothman. 2013. "An NQO1 substrate with potent antitumor activity that selectively kills by PARP1-induced programmed necrosis." *Cancer Res* 72 (12):3038-47. doi: 0008-5472.CAN-11-3135 [pii]
10.1158/0008-5472.CAN-11-3135.

Hufton, S. E., P. T. Moerkerk, R. Brandwijk, A. P. de Bruine, J. W. Arends, and H. R. Hoogenboom. 1999. "A profile of differentially expressed genes in primary colorectal cancer using suppression subtractive hybridization." *FEBS Lett* 463 (1-2):77-82.

Ichimura, K., D. M. Pearson, S. Kocialkowski, L. M. Backlund, R. Chan, D. T. Jones, and V. P. Collins. 2009. "IDH1 mutations are present in the majority of common adult gliomas but rare in primary glioblastomas." *Neuro Oncol* 11 (4):341-7. doi: 10.1215/15228517-2009-025.

Izumi, T., L. R. Wiederhold, G. Roy, R. Roy, A. Jaiswal, K. K. Bhakat, S. Mitra, and T. K. Hazra. 2003. "Mammalian DNA base excision repair proteins: their interactions and role in repair of oxidative DNA damage." *Toxicology* 193 (1-2):43-65.

Jiang, P., W. Du, A. Mancuso, K. E. Wellen, and X. Yang. 2013. "Reciprocal regulation of p53 and malic enzymes modulates metabolism and senescence." *Nature* 493 (7434):689-93. doi: 10.1038/nature11776.

Kamphorst, J. J., M. Nofal, C. Commisso, S. R. Hackett, W. Lu, E. Grabocka, M. G. Vander Heiden, G. Miller, J. A. Drebin, D. Bar-Sagi, C. B. Thompson, and J. D. Rabinowitz. 2015. "Human pancreatic cancer tumors are nutrient poor and tumor cells actively scavenge extracellular protein." *Cancer Res* 75 (3):544-53. doi: 10.1158/0008-5472.CAN-14-2211.

Kato, H., E. Ito, W. Shi, N. M. Alajez, S. Yue, C. Lee, N. Chan, N. Bhogal, C. L. Coackley, D. Vines, D. Green, J. Waldron, P. Gullane, R. Bristow, and F. F. Liu. 2010. "Efficacy of combining GMX1777 with radiation therapy for human head and neck carcinoma." *Clin Cancer Res* 16 (3):898-911. doi: 10.1158/1078-0432.CCR-09-1945.

Khodyreva, S. N., R. Prasad, E. S. Ilina, M. V. Sukhanova, M. M. Kutuzov, Y. Liu, E. W. Hou, S. H. Wilson, and O. I. Lavrik. 2010. "Apurinic/apyrimidinic (AP) site recognition by the 5'-dRP/AP lyase in poly(ADP-ribose) polymerase-1 (PARP-1)." *Proc Natl Acad Sci U S A* 107 (51):22090-5. doi: 10.1073/pnas.1009182107.

Kong, B., C. Qia, M. Erkan, J. Kleeff, and C. W. Michalski. 2013. "Overview on how oncogenic Kras promotes pancreatic carcinogenesis by inducing low intracellular ROS levels." *Front Physiol* 4:246. doi: 10.3389/fphys.2013.00246.

Krokan, H. E., and M. Bjoras. 2013. "Base excision repair." *Cold Spring Harb Perspect Biol* 5 (4):a012583. doi: 10.1101/cshperspect.a012583.

Kruger, N. J., and A. von Schaewen. 2003. "The oxidative pentose phosphate pathway: structure and organisation." *Curr Opin Plant Biol* 6 (3):236-46.

L. P. Hartner LR, M. Hensley, D. Mendelson, A. P. Staddon, W. Chow, O. Kovalyov, W. Ruka, K. Skladowski, A. Jagiello-Gruszfeld, M. Byakhov. . 2007. "Phase 2 dose multi-center, open-label study of ARQ 501, a checkpoint activator, in adult patients with persistent, recurrent or metastatic leiomyosarcoma (LMS)." *Journal of Clinical Oncology*

Landi, M. T., T. Dracheva, M. Rotunno, J. D. Figueroa, H. Liu, A. Dasgupta, F. E. Mann, J. Fukuoka, M. Hames, A. W. Bergen, S. E. Murphy, P. Yang, A. C. Pesatori, D. Consonni, P. A. Bertazzi, S. Wacholder, J. H. Shih, N. E. Caporaso, and J. Jen.

2008. "Gene expression signature of cigarette smoking and its role in lung adenocarcinoma development and survival." *PLoS One* 3 (2):e1651. doi: 10.1371/journal.pone.0001651.

Le, A., A. N. Lane, M. Hamaker, S. Bose, A. Gouw, J. Barbi, T. Tsukamoto, C. J. Rojas, B. S. Slusher, H. Zhang, L. J. Zimmerman, D. C. Liebler, R. J. Slebos, P. K. Lorkiewicz, R. M. Higashi, T. W. Fan, and C. V. Dang. 2012. "Glucose-independent glutamine metabolism via TCA cycling for proliferation and survival in B cells." *Cell Metab* 15 (1):110-21. doi: 10.1016/j.cmet.2011.12.009.

Leonardi, R., C. Subramanian, S. Jackowski, and C. O. Rock. 2012. "Cancer-associated isocitrate dehydrogenase mutations inactivate NADPH-dependent reductive carboxylation." *J Biol Chem* 287 (18):14615-20. doi: 10.1074/jbc.C112.353946.

Lewis, A. M., M. Ough, M. M. Hinkhouse, M. S. Tsao, L. W. Oberley, and J. J. Cullen. 2005. "Targeting NAD(P)H:quinone oxidoreductase (NQO1) in pancreatic cancer." *Mol Carcinog* 43 (4):215-24. doi: 10.1002/mc.20107.

Li, L. S., E. A. Bey, Y. Dong, J. Meng, B. Patra, J. Yan, X. J. Xie, R. A. Brekken, C. C. Barnett, W. G. Bornmann, J. Gao, and D. A. Boothman. 2011. "Modulating endogenous NQO1 levels identifies key regulatory mechanisms of action of beta-lapachone for pancreatic cancer therapy." *Clin Cancer Res* 17 (2):275-85. doi: 1078-0432.CCR-10-1983 [pii]
10.1158/1078-0432.CCR-10-1983.

Li, S., A. P. Chou, W. Chen, R. Chen, Y. Deng, H. S. Phillips, J. Selfridge, M. Zurayk, J. J. Lou, R. G. Everson, K. C. Wu, K. F. Faull, T. Cloughesy, L. M. Liau, and A. Lai. 2013. "Overexpression of isocitrate dehydrogenase mutant proteins renders glioma cells more sensitive to radiation." *Neuro Oncol* 15 (1):57-68. doi: 10.1093/neuonc/nos261.

Liu, L., and S. L. Gerson. 2004. "Therapeutic impact of methoxyamine: blocking repair of abasic sites in the base excision repair pathway." *Curr Opin Investig Drugs* 5 (6):623-7.

Liu, L., Y. Nakatsuru, and S. L. Gerson. 2002. "Base excision repair as a therapeutic target in colon cancer." *Clin Cancer Res* 8 (9):2985-91.

Lyn-Cook, B. D., Y. Yan-Sanders, S. Moore, S. Taylor, B. Word, and G. J. Hammons. 2006. "Increased levels of NAD(P)H: quinone oxidoreductase 1 (NQO1) in pancreatic tissues from smokers and pancreatic adenocarcinomas: A potential biomarker of early damage in the pancreas." *Cell Biol Toxicol* 22 (2):73-80. doi: 10.1007/s10565-006-0156-3.

Lyssiotis, C. A., J. Son, L. C. Cantley, and A. C. Kimmelman. 2013. "Pancreatic cancers rely on a novel glutamine metabolism pathway to maintain redox balance." *Cell Cycle* 12 (13):1987-8. doi: 10.4161/cc.25307.

Maginn, E. N., C. H. de Sousa, H. S. Wasan, and E. A. Stronach. 2014. "Opportunities for translation: targeting DNA repair pathways in pancreatic cancer." *Biochim Biophys Acta* 1846 (1):45-54. doi: 10.1016/j.bbcan.2014.04.002.

Mahmood, D. F., A. Abderrazak, K. El Hadri, T. Simmet, and M. Rouis. 2013. "The thioredoxin system as a therapeutic target in human health and disease." *Antioxid Redox Signal* 19 (11):1266-303. doi: 10.1089/ars.2012.4757.

Mailloux, R. J., R. Singh, G. Brewer, C. Auger, J. Lemire, and V. D. Appanna. 2009. "Alpha-ketoglutarate dehydrogenase and glutamate dehydrogenase work in tandem to modulate the antioxidant alpha-ketoglutarate during oxidative stress in Pseudomonas fluorescens." *J Bacteriol* 191 (12):3804-10. doi: 10.1128/JB.00046-09.

Mardis, E. R., L. Ding, D. J. Dooling, D. E. Larson, M. D. McLellan, K. Chen, D. C. Koboldt, R. S. Fulton, K. D. Delehaunty, S. D. McGrath, L. A. Fulton, D. P. Locke, V. J. Magrini, R. M. Abbott, T. L. Vickery, J. S. Reed, J. S. Robinson, T. Wylie, S. M. Smith, L. Carmichael, J. M. Eldred, C. C. Harris, J. Walker, J. B. Peck, F. Du, A. F. Dukes, G. E. Sanderson, A. M. Brummett, E. Clark, J. F. McMichael, R. J. Meyer, J. K. Schindler, C. S. Pohl, J. W. Wallis, X. Shi, L. Lin, H. Schmidt, Y. Tang, C. Haipek, M. E. Wiechert, J. V. Ivy, J. Kalicki, G. Elliott, R. E. Ries, J. E. Payton, P. Westervelt, M. H. Tomasson, M. A. Watson, J. Baty, S. Heath, W. D. Shannon, R. Nagarajan, D. C. Link, M. J. Walter, T. A. Graubert, J. F. DiPersio, R. K. Wilson, and T. J. Ley. 2009. "Recurring mutations found by sequencing an acute myeloid leukemia genome." *N Engl J Med* 361 (11):1058-66. doi: 10.1056/NEJMoa0903840.

Montaldi, A. P., and E. T. Sakamoto-Hojo. 2013. "Methoxyamine sensitizes the resistant glioblastoma T98G cell line to the alkylating agent temozolomide." *Clin Exp Med* 13 (4):279-88. doi: 10.1007/s10238-012-0201-x.

Moore, Z., G. Chakrabarti, X. Luo, A. Ali, Z. Hu, F. J. Fattah, R. Vemireddy, R. J. DeBerardinis, R. A. Brekken, and D. A. Boothman. 2015. "NAMPT inhibition sensitizes pancreatic adenocarcinoma cells to tumor-selective, PAR-independent metabolic catastrophe and cell death induced by beta-lapachone." *Cell Death Dis* 6:e1599. doi: 10.1038/cddis.2014.564.

Nathan, C., and A. Ding. 2010. "SnapShot: Reactive Oxygen Intermediates (ROI)." *Cell* 140 (6):951-951 e2. doi: 10.1016/j.cell.2010.03.008.

Nekrutenko, A., D. M. Hillis, J. C. Patton, R. D. Bradley, and R. J. Baker. 1998. "Cytosolic isocitrate dehydrogenase in humans, mice, and voles and phylogenetic analysis of the enzyme family." *Mol Biol Evol* 15 (12):1674-84.

Okumura, S., T. Sasaki, Y. Minami, and Y. Ohsaki. 2012. "Nicotinamide phosphoribosyltransferase: a potent therapeutic target in non-small cell lung cancer with epidermal growth factor receptor-gene mutation." *J Thorac Oncol* 7 (1):49-56. doi: 10.1097/JTO.0b013e318233d686.

P. Caimi, B. Cooper, B.M. William, E.L. Campagnaro, R.J. Creger, M Afable, Y. Xu, J. Pink, A. Dowlati, H.M. Lazarus,M. Lima, and S.L. Gerson. 2014. "Phase I Trial of the Base – Excision Repair Blocker Methoxyamine (TRC-102) Combined with Fludarabine in Relapsed/Refractory Chronic Lymphocytic Leukemia (CLL) and Lymphoid Malignancies." *Blood* 124.

Parsons, D. W., S. Jones, X. Zhang, J. C. Lin, R. J. Leary, P. Angenendt, P. Mankoo, H. Carter, I. M. Siu, G. L. Gallia, A. Olivi, R. McLendon, B. A. Rasheed, S. Keir, T. Nikolskaya, Y. Nikolsky, D. A. Busam, H. Tekleab, L. A. Diaz, Jr., J. Hartigan, D. R. Smith, R. L. Strausberg, S. K. Marie, S. M. Shinjo, H. Yan, G. J. Riggins, D. D. Bigner, R. Karchin, N. Papadopoulos, G. Parmigiani, B. Vogelstein, V. E.

Velculescu, and K. W. Kinzler. 2008. "An integrated genomic analysis of human glioblastoma multiforme." *Science* 321 (5897):1807-12. doi: 10.1126/science.1164382.

Patra, K. C., and N. Hay. 2014. "The pentose phosphate pathway and cancer." *Trends Biochem Sci*. doi: 10.1016/j.tibs.2014.06.005.

Pena-Rico, M. A., M. N. Calvo-Vidal, R. Villalonga-Planells, F. Martinez-Soler, P. Gimenez-Bonafe, A. Navarro-Sabate, A. Tortosa, R. Bartrons, and A. Manzano. 2011. "TP53 induced glycolysis and apoptosis regulator (TIGAR) knockdown results in radiosensitization of glioma cells." *Radiother Oncol* 101 (1):132-9. doi: 10.1016/j.radonc.2011.07.002.

Phillips, D. C., K. J. Woollard, and H. R. Griffiths. 2003. "The anti-inflammatory actions of methotrexate are critically dependent upon the production of reactive oxygen species." *Br J Pharmacol* 138 (3):501-11. doi: 10.1038/sj.bjp.0705054.

Pink, J. J., S. M. Planchon, C. Tagliarino, M. E. Varnes, D. Siegel, and D. A. Boothman. 2000. "NAD(P)H:Quinone oxidoreductase activity is the principal determinant of beta-lapachone cytotoxicity." *J Biol Chem* 275 (8):5416-24.

Pink, J. J., S. Wuerzberger-Davis, C. Tagliarino, S. M. Planchon, X. Yang, C. J. Froelich, and D. A. Boothman. 2000. "Activation of a cysteine protease in MCF-7 and T47D breast cancer cells during beta-lapachone-mediated apoptosis." *Exp Cell Res* 255 (2):144-55. doi: 10.1006/excr.1999.4790.

Pongratz, R. L., R. G. Kibbey, G. I. Shulman, and G. W. Cline. 2007. "Cytosolic and mitochondrial malic enzyme isoforms differentially control insulin secretion." *J Biol Chem* 282 (1):200-7. doi: 10.1074/jbc.M602954200.

Prasad, R., J. K. Horton, P. D. Chastain, 2nd, N. R. Gassman, B. D. Freudenthal, E. W. Hou, and S. H. Wilson. 2014. "Suicidal cross-linking of PARP-1 to AP site intermediates in cells undergoing base excision repair." *Nucleic Acids Res* 42 (10):6337-51. doi: 10.1093/nar/gku288.

Ren, J. G., P. Seth, C. B. Clish, P. K. Lorkiewicz, R. M. Higashi, A. N. Lane, T. W. Fan, and V. P. Sukhatme. 2014. "Knockdown of Malic Enzyme 2 Suppresses Lung Tumor Growth, Induces Differentiation and Impacts PI3K/AKT Signaling." *Sci Rep* 4:5414. doi: 10.1038/srep05414.

Roberts, P. J., and T. E. Stinchcombe. 2013. "KRAS mutation: should we test for it, and does it matter?" *J Clin Oncol* 31 (8):1112-21. doi: 10.1200/JCO.2012.43.0454.

Saqcena, M., S. Mukhopadhyay, C. Hosny, A. Alhamed, A. Chatterjee, and D. A. Foster. 2014. "Blocking anaplerotic entry of glutamine into the TCA cycle sensitizes K-Ras mutant cancer cells to cytotoxic drugs." *Oncogene*. doi: 10.1038/onc.2014.207.

Savage, R. E., T. Hall, K. Bresciano, J. Bailey, M. Starace, and T. C. Chan. 2008. "Development and validation of a liquid chromatography-tandem mass spectrometry method for the determination of ARQ 501 (beta-lapachone) in plasma and tumors from nu/nu mouse xenografts." *J Chromatogr B Analyt Technol Biomed Life Sci* 872 (1-2):148-53. doi: 10.1016/j.jchromb.2008.07.031.

Schneider, J., K. Neu, H. Grimm, H. G. Velcovsky, G. Weisse, and E. Eigenbrodt. 2002. "Tumor M2-pyruvate kinase in lung cancer patients: immunohistochemical detection and disease monitoring." *Anticancer Res* 22 (1A):311-8.

Schumacker, P. T. 2006. "Reactive oxygen species in cancer cells: live by the sword, die by the sword." *Cancer Cell* 10 (3):175-6. doi: 10.1016/j.ccr.2006.08.015.

Seltzer, M. J., B. D. Bennett, A. D. Joshi, P. Gao, A. G. Thomas, D. V. Ferraris, T. Tsukamoto, C. J. Rojas, B. S. Slusher, J. D. Rabinowitz, C. V. Dang, and G. J. Riggins. 2010. "Inhibition of glutaminase preferentially slows growth of glioma cells with mutant IDH1." *Cancer Res* 70 (22):8981-7. doi: 10.1158/0008-5472.CAN-10-1666.

Shanware, N. P., A. R. Mullen, R. J. DeBerardinis, and R. T. Abraham. 2011. "Glutamine: pleiotropic roles in tumor growth and stress resistance." *J Mol Med (Berl)* 89 (3):229-36. doi: 10.1007/s00109-011-0731-9.

Shukla, K., D. V. Ferraris, A. G. Thomas, M. Stathis, B. Duvall, G. Delahanty, J. Alt, R. Rais, C. Rojas, P. Gao, Y. Xiang, C. V. Dang, B. S. Slusher, and T. Tsukamoto. 2012. "Design, synthesis, and pharmacological evaluation of bis-2-(5-phenylacetamido-1,2,4-thiadiazol-2-yl)ethyl sulfide 3 (BPTES) analogs as glutaminase inhibitors." *J Med Chem* 55 (23):10551-63. doi: 10.1021/jm301191p.

Sinha, S., R. Ghildiyal, V. S. Mehta, and E. Sen. 2013. "ATM-NFkappaB axis-driven TIGAR regulates sensitivity of glioma cells to radiomimetics in the presence of TNFalpha." *Cell Death Dis* 4:e615. doi: 10.1038/cddis.2013.128.

Son, J., C. A. Lyssiotis, H. Ying, X. Wang, S. Hua, M. Ligorio, R. M. Perera, C. R. Ferrone, E. Mullarky, N. Shyh-Chang, Y. Kang, J. B. Fleming, N. Bardeesy, J. M. Asara, M. C. Haigis, R. A. DePinho, L. C. Cantley, and A. C. Kimmelman. 2013. "Glutamine supports pancreatic cancer growth through a KRAS-regulated metabolic pathway." *Nature* 496 (7443):101-5. doi: 10.1038/nature12040.

Sousa, C. M., and A. C. Kimmelman. 2014a. "The complex landscape of pancreatic cancer metabolism." *Carcinogenesis* 35 (7):1441-50. doi: 10.1093/carcin/bgu097.

Sousa, C. M., and A. C. Kimmelman. 2014b. "The complex landscape of pancreatic cancer metabolism." *Carcinogenesis* 35 (7):1441-1450. doi: 10.1093/carcin/bgu097.

Srivastava, M., P. Khurana, and R. Sugadev. 2012. "Lung cancer signature biomarkers: tissue specific semantic similarity based clustering of digital differential display (DDD) data." *BMC Res Notes* 5:617. doi: 10.1186/1756-0500-5-617.

Stalnecker, C. A., S. M. Ulrich, Y. Li, S. Ramachandran, M. K. McBrayer, R. J. DeBerardinis, R. A. Cerione, and J. W. Erickson. 2015. "Mechanism by which a recently discovered allosteric inhibitor blocks glutamine metabolism in transformed cells." *Proc Natl Acad Sci U S A* 112 (2):394-9. doi: 10.1073/pnas.1414056112.

Sung, J. Y., J. H. Hong, H. S. Kang, I. Choi, S. D. Lim, J. K. Lee, J. H. Seok, J. H. Lee, and G. M. Hur. 2000. "Methotrexate suppresses the interleukin-6 induced generation of reactive oxygen species in the synoviocytes of rheumatoid arthritis." *Immunopharmacology* 47 (1):35-44.

Tagliarino, C., J. J. Pink, G. R. Dubyak, A. L. Nieminen, and D. A. Boothman. 2001. "Calcium is a key signaling molecule in beta-lapachone-mediated cell death." *J Biol Chem* 276 (22):19150-9. doi: 10.1074/jbc.M100730200.

Tagliarino, C., J. J. Pink, K. E. Reinicke, S. M. Simmers, S. M. Wuerzberger-Davis, and D. A. Boothman. 2003. "Mu-calpain activation in beta-lapachone-mediated apoptosis." *Cancer Biol Ther* 2 (2):141-52.

Talbot, S. G., C. Estilo, E. Maghami, I. S. Sarkaria, D. K. Pham, O. charoenrat P, N. D. Socci, I. Ngai, D. Carlson, R. Ghossein, A. Viale, B. J. Park, V. W. Rusch, and B. Singh. 2005. "Gene expression profiling allows distinction between primary and metastatic squamous cell carcinomas in the lung." *Cancer Res* 65 (8):3063-71. doi: 10.1158/0008-5472.CAN-04-1985.

Thapa, D., P. Meng, R. G. Bedolla, R. L. Reddick, A. P. Kumar, and R. Ghosh. 2014. "NQO1 suppresses NF-kappaB-p300 interaction to regulate inflammatory mediators associated with prostate tumorigenesis." *Cancer Res* 74 (19):5644-55. doi: 10.1158/0008-5472.CAN-14-0562.

Tian, W. N., L. D. Braunstein, J. Pang, K. M. Stuhlmeier, Q. C. Xi, X. Tian, and R. C. Stanton. 1998. "Importance of glucose-6-phosphate dehydrogenase activity for cell growth." *J Biol Chem* 273 (17):10609-17.

Trachootham, D., J. Alexandre, and P. Huang. 2009. "Targeting cancer cells by ROS-mediated mechanisms: a radical therapeutic approach?" *Nat Rev Drug Discov* 8 (7):579-91. doi: 10.1038/nrd2803.

Travelli, C., V. Drago, E. Maldi, N. Kaludercic, U. Galli, R. Boldorini, F. Di Lisa, G. C. Tron, P. L. Canonico, and A. A. Genazzani. 2011. "Reciprocal potentiation of the antitumoral activities of FK866, an inhibitor of nicotinamide phosphoribosyltransferase, and etoposide or cisplatin in neuroblastoma cells." *J Pharmacol Exp Ther* 338 (3):829-40. doi: 10.1124/jpet.111.184630.

Traverso, N., R. Ricciarelli, M. Nitti, B. Marengo, A. L. Furfaro, M. A. Pronzato, U. M. Marinari, and C. Domenicotti. 2013. "Role of glutathione in cancer progression and chemoresistance." *Oxid Med Cell Longev* 2013:972913. doi: 10.1155/2013/972913.

Vander Heiden, M. G., L. C. Cantley, and C. B. Thompson. 2009. "Understanding the Warburg effect: the metabolic requirements of cell proliferation." *Science* 324 (5930):1029-33. doi: 10.1126/science.1160809.

von Heideman, A., A. Berglund, R. Larsson, and P. Nygren. 2010. "Safety and efficacy of NAD depleting cancer drugs: results of a phase I clinical trial of CHS 828 and overview of published data." *Cancer Chemother Pharmacol* 65 (6):1165-72. doi: 10.1007/s00280-009-1125-3.

Walsh, M. J., K. R. Brimacombe, D. Anastasiou, Y. Yu, W. J. Israelsen, B. S. Hong, W. Tempel, S. Dimov, H. Veith, H. Yang, C. Kung, K. E. Yen, L. Dang, F. Salituro, D. S. Auld, H. W. Park, M. G. Vander Heiden, C. J. Thomas, M. Shen, and M. B. Boxer. 2010. "ML265: A potent PKM2 activator induces tetramerization and reduces tumor formation and size in a mouse xenograft model." In *Probe Reports from the NIH Molecular Libraries Program*. Bethesda (MD).

Wang, B., M. K. Hasan, E. Alvarado, H. Yuan, H. Wu, and W. Y. Chen. 2011. "NAMPT overexpression in prostate cancer and its contribution to tumor cell survival and stress response." *Oncogene* 30 (8):907-21. doi: 10.1038/onc.2010.468.

Wang, Y., C. E. Kaiser, B. Frett, and H. Y. Li. 2013. "Targeting mutant KRAS for anticancer therapeutics: a review of novel small molecule modulators." *J Med Chem* 56 (13):5219-30. doi: 10.1021/jm3017706.

Ward, P. S., J. Patel, D. R. Wise, O. Abdel-Wahab, B. D. Bennett, H. A. Coller, J. R. Cross, V. R. Fantin, C. V. Hedvat, A. E. Perl, J. D. Rabinowitz, M. Carroll, S. M. Su, K. A. Sharp, R. L. Levine, and C. B. Thompson. 2010. "The common feature of leukemia-associated IDH1 and IDH2 mutations is a neomorphic enzyme activity converting alpha-ketoglutarate to 2-hydroxyglutarate." *Cancer Cell* 17 (3):225-34. doi: 10.1016/j.ccr.2010.01.020.

Won, K. Y., S. J. Lim, G. Y. Kim, Y. W. Kim, S. A. Han, J. Y. Song, and D. K. Lee. 2012. "Regulatory role of p53 in cancer metabolism via SCO2 and TIGAR in human breast cancer." *Hum Pathol* 43 (2):221-8. doi: 10.1016/j.humpath.2011.04.021.

Wu, W. S. 2006. "The signaling mechanism of ROS in tumor progression." *Cancer Metastasis Rev* 25 (4):695-705. doi: 10.1007/s10555-006-9037-8.

Yan, H., D. W. Parsons, G. Jin, R. McLendon, B. A. Rasheed, W. Yuan, I. Kos, I. Batinic-Haberle, S. Jones, G. J. Riggins, H. Friedman, A. Friedman, D. Reardon, J. Herndon, K. W. Kinzler, V. E. Velculescu, B. Vogelstein, and D. D. Bigner. 2009. "IDH1 and IDH2 mutations in gliomas." *N Engl J Med* 360 (8):765-73. doi: 10.1056/NEJMoa0808710.

Yan, L., A. Bulgar, Y. Miao, V. Mahajan, J. R. Donze, S. L. Gerson, and L. Liu. 2007. "Combined treatment with temozolomide and methoxyamine: blocking apurininc/pyrimidinic site repair coupled with targeting topoisomerase IIalpha." *Clin Cancer Res* 13 (5):1532-9. doi: 10.1158/1078-0432.CCR-06-1595.

Ye, J., J. Fan, S. Venneti, Y. W. Wan, B. R. Pawel, J. Zhang, L. W. Finley, C. Lu, T. Lindsten, J. R. Cross, G. Qing, Z. Liu, M. C. Simon, J. D. Rabinowitz, and C. B. Thompson. 2014. "Serine catabolism regulates mitochondrial redox control during hypoxia." *Cancer Discov*. doi: 10.1158/2159-8290.CD-14-0250.

Ying, H., A. C. Kimmelman, C. A. Lyssiotis, S. Hua, G. C. Chu, E. Fletcher-Sananikone, J. W. Locasale, J. Son, H. Zhang, J. L. Coloff, H. Yan, W. Wang, S. Chen, A. Viale, H. Zheng, J. H. Paik, C. Lim, A. R. Guimaraes, E. S. Martin, J. Chang, A. F. Hezel, S. R. Perry, J. Hu, B. Gan, Y. Xiao, J. M. Asara, R. Weissleder, Y. A. Wang, L. Chin, L. C. Cantley, and R. A. DePinho. 2012. "Oncogenic Kras maintains pancreatic tumors through regulation of anabolic glucose metabolism." *Cell* 149 (3):656-70. doi: 10.1016/j.cell.2012.01.058.

Ying, W. 2008. "NAD+/NADH and NADP+/NADPH in cellular functions and cell death: regulation and biological consequences." *Antioxid Redox Signal* 10 (2):179-206. doi: 10.1089/ars.2007.1672.

Yu, S. W., H. Wang, M. F. Poitras, C. Coombs, W. J. Bowers, H. J. Federoff, G. G. Poirier, T. M. Dawson, and V. L. Dawson. 2002. "Mediation of poly(ADP-ribose)

polymerase-1-dependent cell death by apoptosis-inducing factor." *Science* 297 (5579):259-63. doi: 10.1126/science.1072221.

Zhang, G., A. Schetter, P. He, N. Funamizu, J. Gaedcke, B. M. Ghadimi, T. Ried, R. Hassan, H. G. Yfantis, D. H. Lee, C. Lacy, A. Maitra, N. Hanna, H. R. Alexander, and S. P. Hussain. 2012. "DPEP1 inhibits tumor cell invasiveness, enhances chemosensitivity and predicts clinical outcome in pancreatic ductal adenocarcinoma." *PLoS One* 7 (2):e31507. doi: 10.1371/journal.pone.0031507.

Zhdanov, A. V., A. H. Waters, A. V. Golubeva, R. I. Dmitriev, and D. B. Papkovsky. 2014. "Availability of the key metabolic substrates dictates the respiratory response of cancer cells to the mitochondrial uncoupling." *Biochim Biophys Acta* 1837 (1):51-62. doi: 10.1016/j.bbabio.2013.07.008.

Zong, W. X., D. Ditsworth, D. E. Bauer, Z. Q. Wang, and C. B. Thompson. 2004. "Alkylating DNA damage stimulates a regulated form of necrotic cell death." *Genes Dev* 18 (11):1272-82. doi: 10.1101/gad.1199904.

Zwerschke, W., S. Mazurek, P. Massimi, L. Banks, E. Eigenbrodt, and P. Jansen-Durr. 1999. "Modulation of type M2 pyruvate kinase activity by the human papillomavirus type 16 E7 oncoprotein." *Proc Natl Acad Sci U S A* 96 (4):1291-6.